UNIVERSITÀ DEGLI STUDI DI PADOVA

FRIEDRICH-ALEXANDER UNIVERSITÄT ERLANGEN-NÜRNBERG

UNIVERSITA' DEGLI STUDI DI PADOVA

Dipartimento di Ingegneria Industriale DII

Corso di Laurea Magistrale in Ingegneria Meccanica

Experimental investigations on hybrid parts made of 316L in stretch forming processes at different temperatures

Relatori:
Prof.ssa Stefania Bruschi
Prof.ssa Marion Merklein

Correlatore:
Jan Hafenecker, M.Sc.

Laureando:
Francesco Bacelle 1233974

Anno Accademico 2021/2022

Desidero porgere i miei più sentiti ringraziamenti alla Professoressa Stefania Bruschi, che mi ha dato la possibilità di redigere la mia tesi
presso la Friedrich-Alexander Universität.
È stata un'esperienza che mi ha fatto crescere
sia sul piano professionale che umano.
Un pensiero particolare va alla Professoressa Marion Merklein e a
M. Sc. Jan Hafenecker per avermi seguito e aiutato nei mesi di ricerca.
Da ultimo, ma non meno importante, ringrazio la mia famiglia per avermi sempre sostenuto e incoraggiato nel corso degli studi universitari.

Index

List of variables, symbols and abbreviations used

Symbol	Unit of measurement	Explanation
A	MPa	Strength coefficient, which combines the effects of C and S
A_f	mm^2	Final cross-sectional area
A_i	mm^2	Initial cross-sectional area
AISI	-	American Iron and Steel Institute
AOD	-	Argon Oxygen Decarburation
ASTM	-	American Society for Testing and Materials
BHF	N	Blank Holder Force
C	-	Carbon
c	MPa	Strength coefficient
CAD	-	Computer-Aided Design
Cr	-	Chromium
D	mm	Diameter of the additively manufactured elements
DD	mm	Drawing depth
D_0	mm	Diameter of the largest blank that can be successfully drawn
D_b	mm	Starting blank diameter
D_p	mm	Punch diameter
DED	-	Directed Energy Deposition
DMLM	-	Direct Metal Laser Melting
EBM	-	Electron Beam Melting
F	N	Stretching force
F_{die}	N	Force applied by the die
F_{max}	N	Maximum punch force required to perform a deep drawing process
FLD	-	Forming limit diagram
h	mm	Instantaneous height of the workpiece being deformed
h_s	mm	Hatch spacing
HIP	-	Hot Isostatic Pressing
K_f	MPa	Flow stress
$\overline{K}_f$	MPa	Average flow stress
L	mm	Distance between additively manufactured elements measured from centre.
L_p	mm	Length of the sheet in the direction perpendicular to stretching direction
l_z	mm	Layer thickness
LDR	-	Limiting Draw Ratio
m	-	Strain rate sensitivity exponent

Mn	-	Manganese
Mo	-	Molybdenum
n	-	Strain-hardening exponent
N	-	Nitrogen
Ni	-	Nickel
NP	-	Number of additively manufactured elements
P	-	Phosphorus
P_l	W	Laser power
PBF-LB/M	-	Laser-based powder bed fusion of metals
R	mm	Fillet radius in the transition area between sheet and the additively manufactured elements
R_{avg}	-	Average anisotropy
r_0	-	Anisotropy calculated along the rolling direction
r_{45}	-	Anisotropy calculated inclined of 45° with respect to the rolling direction
r_{90}	-	Anisotropy calculated perpendicular to the rolling direction
R_n	-	Normal anisotropy
Si	-	Silicon
SLM	-	Selective Laser Melting
STL	-	Stereolithography Tessellation Language
S	-	Sulphur
s	MPa	Strength constant, which is determined at a strain rate of 1.0 s^{-1}
T_m	°C	Melting point of the metal
T	°C	Forming temperature
T/T_m	-	Homologous temperature
t_0	mm	Original blank thickness
t	mm	True sheet thickness
UTS	MPa	Ultimate Tensile Strength
v	mm/s	Speed of deformation
v_s	mm/s	Scan speed
wt	%	Weight percent
ΔR	-	Planar anisotropy
φ	-	True strain
φ_f	-	Maximum strain value during the forming process
$\dot{\varphi}$	s^{-1}	True strain rate

Riassunto esteso

In questa tesi viene esaminata la combinazione della tecnologia di Additive Manufacturing e della tecnologia di formatura di lamiera per la realizzazione di componenti ibridi. Nello specifico, vengono considerate rispettivamente la tecnologia di fusione a letto di polvere di metallo basata su laser (PBF-LB/M) e il processo di stiratura. Lo scopo di questo lavoro è di esaminare l'influenza della temperatura di prova e dei parametri geometrici degli elementi prodotti in modo additivo sulla formabilità dei provini ibridi realizzati. La produzione additiva e la tecnologia di formatura offrono vantaggi significativi nei rispettivi campi di applicazione, ma presentano anche alcuni svantaggi.
L'approccio tool-less della tecnologia PBF-LB/M consente la realizzazione di componenti con un'elevata complessità geometrica e di strutture topologicamente ottimizzate in un unico processo di costruzione. Inoltre è possibile costruire strutture di riempimento, come ad esempio strutture a nido d'ape, per alleggerire il componente realizzato. Il materiale viene utilizzato in maniera più efficiente poiché è possibile riutilizzare la polvere non fusa rimanente per il successivo processo di costruzione, dopo che il componente è stato prodotto. Un altro rilevante vantaggio è la possibilità di utilizzare materiali caratterizzati da un'elevata resistenza, che richiedono tempo e costi elevati per essere lavorati con le tecnologie di produzione convenzionali. I principali svantaggi di questa tecnologia sono gli elevati tempi di produzione, l'alto costo dei materiali in polvere utilizzati e la bassa qualità superficiale dei componenti realizzati, i quali richiedono successive post-lavorazioni per ottenere la finitura superficiale richiesta.
Al contrario, le tecnologie di formatura della lamiera presentano bassi tempi di produzione, sono economicamente efficienti per lotti di grandi dimensioni e necessitano di pochi post-trattamenti. Le tecnologie di formatura della lamiera, tuttavia, non consentono la produzione di componenti con geometria complessa.
Combinando queste due tecnologie di produzione è possibile realizzare componenti ibridi, beneficiando dei vantaggi di entrambi i processi e compensando i loro svantaggi. In questo modo è possibile produrre componenti integrando la flessibilità progettuale e la personalizzazione delle tecnologie di produzione additiva con gli elevati ritmi di produzione del processo di formatura della lamiera. I potenziali campi di applicazione dei componenti ibridi sono i settori medico e aerospaziale, in particolare la produzione di protesi mediche e componenti funzionali ad elevata complessità geometrica.
Tuttavia, sono necessarie approfondite ricerche nel campo delle interazioni di processo. Infatti, gli elementi funzionali realizzati sui componenti ibridi utilizzando la tecnologia di PBF-LB/M interferiscono con il processo di stiratura e riducono la formabilità dei provini realizzati, il che potrebbe causare insorgenza di fratture e conseguente cedimento dei componenti.
Per analizzare come la formabilità dei componenti ibridi sia influenzata dalla presenza degli elementi funzionali prodotti in modo additivo, il processo di stiratura viene eseguito a diverse temperature di prova su vari provini che presentano valori differenti dei parametri geometrici degli elementi funzionali. Il materiale scelto per la realizzazione dei provini è l'acciaio inossidabile austenitico 316L. È stata scelta una geometria cilindrica

per gli elementi funzionali additivi. Per realizzare i provini ibridi, gli elementi funzionali prodotti in modo additivo vengono costruiti su un grezzo circolare di diametro 105 mm e spessore 1.5 mm. I campioni così ottenuti vengono successivamente formati a diverse temperature di prova. Per esaminare l'influenza della geometria degli elementi additivi e della temperatura di prova sulla formabilità dei componenti ibridi vengono scelti e variati i seguenti parametri geometrici: il diametro dei cilindri *D*, il numero dei cilindri *NP*, la distanza tra i cilindri misurata dal loro centro *L* e il raggio di raccordo *R* nell'area di transizione tra la lamiera e gli elementi additivi. Vengono selezionate tre diverse temperature di prova, ovvero 20°C, 250°C e 400°C. I componenti ibridi vengono successivamente misurati con un sistema di misura ottico per ottenere la distribuzione dello spessore della lamiera. Dai risultati delle misurazioni ottiche, è possibile determinare la posizione di massimo assottigliamento dei provini e quindi identificare le aree critiche. A una maggiore riduzione dello spessore consegue una ridotta formabilità dei componenti e quindi una possibile rottura prematura dei provini. Per prima cosa viene valutata l'influenza della temperatura di prova e dei singoli parametri geometrici degli elementi prodotti in modo additivo sulla formabilità dei componenti ibridi.

Successivamente, viene analizzata l'influenza della combinazione dei suddetti parametri sulla formabilità dei componenti ibridi. Da questa ultima analisi vengono realizzati grafici di interazione, per identificare quali parametri presentano una forte interazione tra di loro. Mediante i risultati così ottenuti è possibile raggiungere un trade-off tra i valori delle variabili esaminate al fine di ottenere la complessità geometrica e la formabilità desiderata del componente ibrido.

In conclusione, poiché gli elementi funzionali prodotti in modo additivo sono la parte dei componenti ibridi che deve rispondere alle esigenze dei consumatori, si renderà necessario condurre ulteriori analisi, esaminando differenti valori e combinazioni di parametri geometrici, in modo da realizzare geometrie più complesse dei componenti ibridi.

1 Introduction

Nowadays, mass customization, design complexity, sustainable production and short product life cycle have become increasingly important, especially in the manufacturing sector [1]. As a consequence, manufacturing industry has turned toward dynamic and flexible manufacturing processes [1], such as Additive Manufacturing technologies, which are no longer used only as a prototyping technology but have become a production technology [2]. Additive Manufacturing is a technique that uses a layer-by-layer process [3] to create a 3D physical object from a Computer-Aided-Design model [4] and it allows the manufacturing of products with a high geometrical complexity in small batch sizes, capable of satisfying consumers' demands for highly customized products [5]. A relevant advantage of Additive Manufacturing technologies is the possibility to use materials characterized by high strength [1], which are generally expensive and time consuming to process with conventional manufacturing technologies [6]. However, high production times [7], high process costs [5] and low geometrical accuracy [2] are among the main disadvantages of Additive Manufacturing technologies. On the contrary, sheet metal forming technologies have low production times, they are economically efficient for large batch sizes [8] and, furthermore, they require few post treatments, which are generally necessary for Additive Manufacturing technologies [9]. Sheet metal forming technologies, though, do not allow the manufacturing of components with complex geometry [8]. A strategy to overcome the limitations of Additive Manufacturing and sheet metal forming technologies is to combine them to manufacture hybrid components [8]. In this way, it is possible to manufacture parts integrating the design flexibility and customization of Additive Manufacturing technologies with the high production rates and profitability of sheet metal forming [5]. The potential fields of application of hybrid components are medical and aerospace sectors [10], in particular the manufacturing of medical prostheses [1] and functional components with high geometrical complexity [6]. The possibility of using biocompatible, high-strength and light-weight materials and the need for small series of customized products, allow hybrid components to find a field of use in these two sectors, obtaining high benefits [1].

The combination of different technologies to manufacture hybrid components involves many challenges, as interactions arise between the different processes [1]. These interactions can lead to the onset of defects in the manufactured components and to a decrease in formability [8]. In this thesis, hybrid components made of 316L stainless steel are analysed. The hybrid specimens are manufactured combining the technology of laser-based powder bed fusion of metals (PBF-LB/M) and sheet metal forming technology. To analyse how the formability of the manufactured parts is influenced by the combination of Additive Manufacturing and sheet metal forming technologies, hybrid components with different geometries of additively manufactured elements are built and formed at different testing temperatures.

2 State of the Art

In order to examine the properties of hybrid components it is necessary to analyse the technical principles of the two technologies involved in the manufacturing of the hybrid specimens: the laser-based powder bed fusion of metals and the sheet metal forming process. The aim of this thesis is to examine the influence of the testing temperature and the geometric parameters of the additively manufactured elements on the formability of the hybrid specimens. For further technical development, the current state of the art must be examined, as well as the basic properties of stainless steels and their suitability for these technologies.

2.1 Stainless steels

This chapter presents the main characteristics of stainless steels, their classification and their areas of use. In this thesis the material used to manufacture the hybrid components is 316L stainless steel, which will be subsequently described.

2.1.1 Properties and applications of stainless steels

Stainless steels are iron-based alloys containing a significant content of chromium [11]. In many cases, in addition to chromium, other alloying elements are added to modify their properties [11]. In Europe, the reference standard for stainless steels is EN-10088 [11], in which the various types of stainless steels, their chemical composition, mechanical properties, physical properties and heat treatments are listed [12]. In addition to European standardization, the AISI (American Iron and Steel Institute) handbook is widely used [13]. This handbook refers to a designation in which each stainless steel has its own progressive order number within a given series [13]. The series of the AISI were subsequently used by the ASTM (American Society for Testing and Materials) [14]. The AISI handbook divides stainless steels into distinct series. The most used are the following [13]:

- 200 series: chromium-nickel-manganese austenitic stainless steels
- 300 series: chromium-nickel austenitic stainless steels
- 400 series: martensitic and ferritic chromium stainless steels
- 600 series: precipitation hardening stainless steels

According to the European standard EN-10088, a steel is considered stainless when its chemical composition has a minimum chromium content of 10.5 % and a maximum carbon content of 1.2 % [12]. It should be noted that, in most stainless steels available in the market, the chromium content is much higher than the threshold indicated above, with values ranging between 11 % and 17 % [11]. Basically, a chromium content of at least 11 % is required to have a fair resistance to corrosion [11]. The presence of chromium in alloys grants the possibility of forming a very thin film on the surface of the steel, called

passive film, of the order of 1.0 to 2.0 nm [11]. It consists mainly of chromium oxides and hydroxides [15]. This film is insoluble [11], compact and continuous [16]. Besides, it adheres well to the substrate and protects the material on which it is formed [11]. All the properties described above are the consequence of the fast reaction of the chromium, present in the alloy, with the oxygen of the atmosphere [17]. The oxidation of stainless steel, also called passivation, occurs naturally and spontaneously in oxidizing environments, such as air [18]. The passive film has also another important quality, i.e. if it is scratched or mechanically damaged, it spontaneously re-forms itself on the surface of the component [17]. Finally, since chromium has the effect of increasing oxidation resistance at high temperatures, these steels can be used in high temperature environments, where degradation due to creep phenomena is prevalent [17]. In general terms, it can therefore be concluded that the greater the amount of chromium in the alloy, the greater is the resistance of the stainless steel to corrosion [11].
Typical areas of use of stainless steels are related to applications where particular resistance to corrosion is required to withstand aggressive environmental conditions [19]. The main fields of application are equipment for the oil and gas industry, equipment for the chemical process industry, food and beverage industry and aerospace industry [16]. Stainless steels are produced in many forms, such as in the form of cold rolled sheets, bars, hot rolled plates, tubes and castings [16]. In recent times, however, this type of materials has been used more and more in the Additive Manufacturing sector, in the form of powder [7]. Due to the wide use of this type of steels, a state of the art analysis is necessary.

2.1.2 Effects of alloying elements

The addition of alloying elements during steel production processes is common practice in the steel industry [11]. The variety of alloying elements used is considerable, as is the number of stainless steels available on the market today [13]. Each alloying element has a specific effect on the properties of the steel [16].
Since in this thesis hybrid components made of 316L are analysed, the main alloying elements of this type of steel are described below.

- **Chromium (Cr)**: Chromium is the main component of stainless steels. Chromium gives to stainless steels the ability to passivate and resist corrosive phenomena. The minimum chromium content needed to make a steel stainless is 10.5 %. If the chromium content is increased, the corrosion resistance increases. Chromium promotes a ferritic microstructure and increases the resistance to oxidation at high temperatures. [17]
- **Molybdenum (Mo):** Molybdenum increases the resistance to both general and localised corrosion and increases the mechanical strength. Molybdenum is used to promote a ferritic microstructure and also promotes the formation of secondary phases in ferritic, ferritic-austenitic and austenitic steels. [17]
- **Nickel (Ni):** Nickel increases ductility and toughness [17]. Nickel has no direct

influence on the passive layer [11] but reduces the corrosion rate [17]. For this reason, the presence of a certain percentage of nickel is useful for stainless steels that must be used in acid environments, such as sulphuric acid environments [11]. Nickel is used to promote an austenitic microstructure [17].

- **Carbon (C):** Carbon strongly promotes an austenitic microstructure [17]. Carbon is used to improve the mechanical strength of the steel [11]. Its presence reduces the resistance to intergranular corrosion [17], caused by the formation of carbides in the grain boundaries [16]. This type of corrosion causes substantial problems during the welding of austenitic stainless steels [16]. Furthermore, the weldability can be increased if the carbon content is reduced [16].
- **Silicon (Si):** Silicon is a ferrite stabiliser [11]. The presence of silicon allows the resistance to oxidation at high temperatures and in strongly oxidising solutions at lower temperature to be improved [17]. Silicon is also used to increase the mechanical strength of the steel [17].

In the next paragraph the different categories of existing stainless steels are analysed.

2.1.3 Classification of stainless steels

The high degree of technological development that the steel sector has had in recent decades, especially after the advent of AOD (Argon Oxygen Decarburation) converters in the 1970s, has made today's production of stainless steels increasingly diversified and specialized [17]. All the major steel companies currently possess different types of stainless steels with different compositions [17]. These can be grouped into four different classes, according to the microstructure of the metal, i.e., martensitic, ferritic, austenitic and biphasic (also called Duplex stainless steels) [13]. In this thesis hybrid specimens made of austenitic stainless steel 316L are analysed, therefore the main characteristics of this category of steels are described in the next paragraph.

2.1.4 Austenitic stainless steels

Austenitic types of steels represent the main group of stainless steels, in terms of variety of products, production and sales volumes [13]. They are characterised by a high corrosion resistance, high formability over a wide temperature range [19] and high weldability [17]. These types of steels are suitable for Additive Manufacturing technologies [20]. As before mentioned, they are widely used in various sectors, such as food, chemicals and pharmaceutical industries and, unlike all other stainless steels, they are non-magnetic [16].
Given the size of the group, it is possible to identify five subgroups [17]:

- **Cr-Ni grades:** This is the group of austenitic steels for general use in moderately corrosive environments, with a chromium and nickel content of approximately

18 % and 8 % respectively [17].

- **Cr-Ni-Mo grades:** These are an evolution of the steels of the previous group, to which molybdenum is added in percentages of 2-3 % to increase resistance to corrosion. These alloys have around 17 % chromium content and a nickel content of 10-13 %. [17]
- **Cr-Mn grades:** According to the American nomenclature, they are known as "200 series". They are a class of stainless steels where the nickel content is decreased and the austenitic microstructure is maintained by replacing some of the nickel with manganese and nitrogen. [17]
- **High performance grades:** This class of steels is used for the most demanding applications in terms of corrosion. The chromium content can vary between 17 and 25 % values, the nickel content between 14 and 25 %, while molybdenum between 3 and 7 %. [17]
- **Grades for high temperature applications:** The composition of these alloys is aimed at maximizing the resistance to oxidative phenomena at high temperatures. Therefore, chromium and nickel are present in abundant quantities of 17-25 % and 8-10 % respectively, while molybdenum is absent. [17]

316L steel belongs to the Cr-Ni-Mo steels category [21] and its main characteristics are analysed in the next paragraph.

2.1.5 Austenitic stainless steel AISI 316L

Out of all stainless steels, austenitic steels represent the most widely used and produced category [13]. In particular, the austenitic stainless steels of the 300 series exhibit an excellent ability to withstand aggressive environmental conditions combined with high formability over a wide temperature range [19]. An element that greatly influenced the evolution of this category of steel is carbon [16]. The first austenitic stainless steels contained, on average, a high carbon content, between 0.05 and 0.15 % [17]. As a result, they were extremely sensitive to intergranular corrosion (also called grain boundary attack [16]). This type of corrosion affects a narrow band of material along the grain boundaries [16]. When stainless steels are maintained at temperatures in the range of 450 °C to 815 °C, chromium carbides can be formed due to the presence of high amount of carbon [22]. The time required for these carbides to form is strictly dependent on temperature [22]. The phenomenon, according to which these carbides are created, is called sensitization [22]. This leads to difficulties when welding these steels [16]. To reduce or eliminate the occurrence of this phenomenon, modifications are made to the chemical composition, leading to the creation of austenitic stainless steels resistant to intergranular corrosion [16]. This is possible by adopting two strategies. First, the carbon content is lowered to reduce the risk of carbide precipitation [16]. Essentially, this reduces the level of free carbon to form the carbides [16]. Subsequently, alloying elements, such as titanium and niobium, are added [16]. Fundamentally, these elements form a more stable carbide than the one formed with chromium and have a greater tendency to react

with carbon [16]. This process is called stabilization [16]. Thus, stainless steels resistant to intergranular corrosion are obtained, which, for this reason, have a high weldability [16], a property which is beneficial for laser based Additive Manufacturing processes [23].
One of these steels is 316L [24]. Its carbon content is around 0.03 %, which is lower than the carbon content in 316 [25]. The “L” stands for "low carbon content” [25]. Hence, 316L has a higher weldability and, thus, is more suitable for Additive Manufacturing technologies, such as PBF-LB/M [23]. 316L is mainly used for parts that need a high resistance to corrosion at room and high temperatures [23].
The chemical compositions of 316 and 316L steel are given below in table 2.1.

Table 2.1: Chemical composition of stainless steel 316 and 316L in *wt%* according to [25].

Alloy	Cr	Ni	Mn	Mo	C	N	Si	Cu	P	Fe
316L	17-19	13-15	<2	2.25-3	<0.03	<0.1	<0.75	<0.5	<0.02	Bal.
316	17-19	13-15	<2	2.25-3	0.08	<0.1	<0.75	<0.5	<0.02	Bal.

The strength of the material is relatively low, but can be increased by strain hardening [23], as shown in the following table, where the mechanical properties of cold rolled 316L are reported. The percentage reduction of area $(A_i - A_f / A_i) \times 100$ determines the amount of cold-forming, where A_i is the initial cross-sectional area of the product and A_f is the final cross-sectional area [25].

Table 2.2: Mechanical properties of annealed [25] and cold rolled 316L steel [26].

Material condition	Yield Strength in MPa	Ultimate Tensile Strength in MPa
Annealed	240	550
15 % cold rolled	510	688
30 % cold rolled	592	854
45 % cold rolled	852	1057

Components made from 316L are typically produced using conventional manufacturing processes, such as casting, rolling, forging or extrusion [17]. However, complex geometries, such as those obtainable through Additive Manufacturing processes are difficult to achieve with conventional technologies [4]. Additive Manufacturing technologies and their advantages are analysed in the next chapter.

2.2 Additive Manufacturing

Additive Manufacturing, also named 3D printing, is an innovative production technology that transforms a computer aided-design model into a 3D physical object [4]. Unlike machining processes, in which the material is removed from a given volume, thus obtaining the final component, in Additive Manufacturing techniques, the material is added selectively to manufacture layer by layer the three-dimensional component [3]. As previously mentioned, Additive Manufacturing technologies allow the production of complex shapes and geometries, in some cases not achievable with conventional manufacturing technologies [4]. It is also possible to build components using high-strength materials, such as titanium alloys, that are expensive and time consuming to process with conventional manufacturing technologies [6]. Therefore, relevant advantages can be achieved by using Additive Manufacturing technologies [6]. The fields of application of these technologies are constantly increasing [6]. Some examples of industries in which Additive Manufacturing technologies are widely used are automotive industry, biomedical and pharmaceutical industry, aerospace industry and energy industry [6]. The reason of the wide use of these technologies is due to the fact that the market has changed compared to previous years [1]. Nowadays, customers prefer customized products rather than standard products [1]. Customization is achievable using Additive Manufacturing technologies [27]. Due to long process times, these technologies are suitable to produce small batch sizes of products with high geometrical complexity [6]. It is possible to obtain a high degree of customization of the product, adapting it to customers' requests [5]. Due to the increasing importance of Additive Manufacturing technologies in the industrial sector, it is important to conduct a more in-depth analysis.

2.2.1 Additive Manufacturing technologies

According to the ASTM, Additive Manufacturing techniques are grouped into seven categories, which includes different processes [28]. The categories are binder jetting, material jetting, direct energy deposition, sheet laminations, material extrusion, powder bed fusion and vat photo-polymerization [28]. The materials currently used to manufacture components using Additive Manufacturing techniques include polymers, metals, ceramics and composite materials [29].
This thesis focuses on Additive Manufacturing technologies related to metals. These technologies have seen a considerable development in recent years [27]. Examples of Additive Manufacturing technologies using metals are the following [29]:

- **Laser-based powder bed fusion of metals (PBF-LB/M):** PBF-LB/M is an Additive Manufacturing technology that produces metal components through the selective melting of a powder bed using a laser beam. [29]
- **Electron Beam Melting (EBM):** EBM is another Additive Manufacturing technology for metals that uses the principle of selectively melting a bed of

powder. It differs from PBF-LB/M because it does not use a laser beam to induce fusion between metal powder particles, but a high-energy electron beam. [29]

- **Directed Energy Deposition (DED):** DED is an Additive Manufacturing technology that does not use the principle of melting a powder bed [29]. In this technology, the material is brought directly into the affected area and it is melted with a focused energy source [30].

In the following paragraph, the potential of PBF-LB/M, which is the Additive manufacturing technology used to manufacture the hybrid components analysed in this thesis, is explained, highlighting its advantages and disadvantages.

2.2.2 Laser-based powder bed fusion of metals (PBF-LB/M)

Laser-based powder bed fusion of metals process (PBF-LB/M), also known as Selective Laser Melting (SLM) or direct metal laser melting (DMLM), is an Additive Manufacturing technology, which builds components layer by layer, through the selective melting of a metallic powder bed, using a high power laser [31]. In the past, laser radiation did not permit the complete fusion of the metal particles, leaving porosity inside the produced components [32]. Nowadays, PBF-LB/M, using adequate process parameters, can manufacture components with a density up to 100 % [32].

The process

The PBF-LB/M process consists of a certain number of consecutive steps to manufacture a component [29]. The first step is the creation of the 3D CAD model of the part [29]. Optimization methods can be used to create the CAD model of the components to be manufactured [29]. Through optimisation methods it is possible to improve the design of components by adjusting the values of design variables to fulfil an objective function, which is generally related to structural performance or weight, within certain constraints [29]. On the basis of the design variables analysed, it is possible to distinguish three types of optimization methods concerning the design of components in Additive Manufacturing, that are size optimization, shape optimization and topology optimization [9]. When designing the CAD models of the components, it is possible to use lattice structures, which allow to obtain structural lightening, thermal management, impact protection and vibration damping [9]. Another aspect to be considered when designing CAD models of components for Additive Manufacturing is the need to insert support structures, which provide mechanical fastening for the part during the building process and allow to reduce distortion of parts due to residual stresses caused by temperature gradients [9]. Unconnected regions, downward facing surfaces and large cantilevered regions require support structures to be built, which increase manufacturing costs because additional time is necessary to build and to remove them [9]. Besides, if it is needed, the component surface must be then polished [9].
The second step is the generation of the STL (Stereolithography Tessellation Language)

file, which consists of a list of triangular facets, uniquely identified by a unit normal vector and three vertices [29]. The language STL is used to describe mathematical models in Additive Manufacturing [29]. Thus, the 3D CAD model surface is approximated by triangles of different sizes, depending on the geometrical complexity and resolution required [29]. The STL file is then transferred to the Additive Manufacturing machine and edited, changing the orientation and position of the part and, if necessary, scaling the part [29]. Subsequently, the STL file is sliced in a certain number of layers with a fixed thickness [33]. After that, it is necessary to perform a setup of the Additive Manufacturing machine, before proceeding with the building process [29]. It is necessary to set the building parameters, such as the type of material used, the thickness of the layers etc. [29]. Afterwards, it is possible to start the building process [29]. The process of PBF-LB/M is illustrated in figure 2.1.

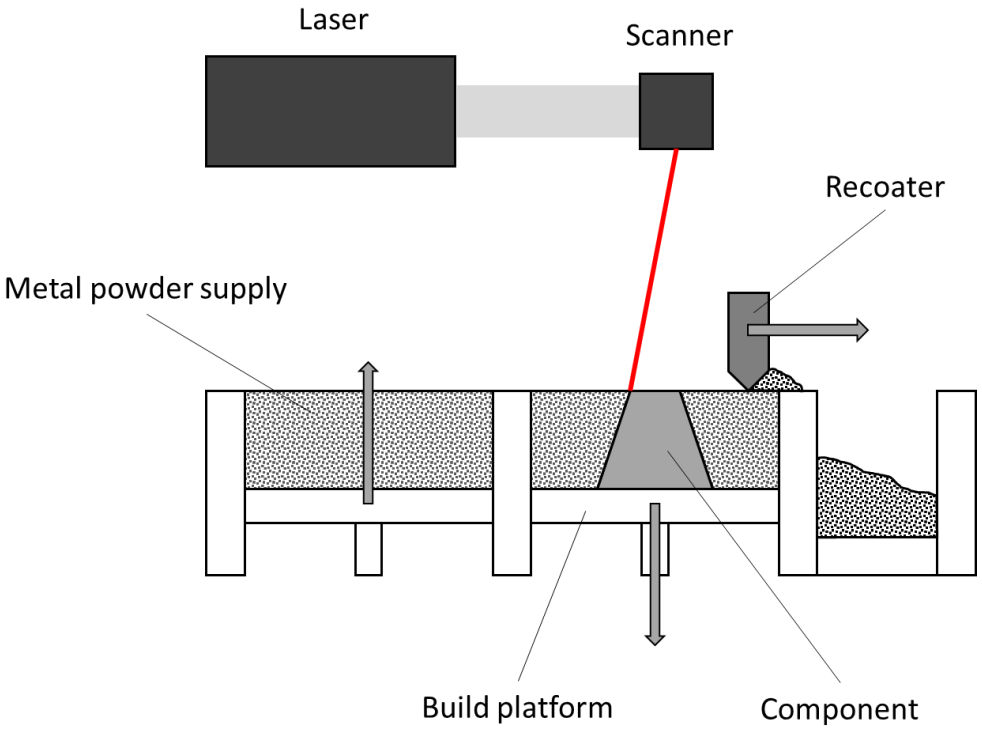

Figure 2.1: PBF-LB/M process diagram according to [34].

First and foremost, an inert atmosphere, with low oxygen content is needed inside the building chamber of the machine [29], in order to avoid oxidation caused by the reaction between oxygen and metal powder during processing, i.e., melting and solidification [9]. The inert atmosphere is created by a continuous flow of inert gas, like Argon or Nitrogen, that has also the function of blowing away the fumes created during the melting of powder [35]. The building process begins with the deposition of a thin layer of powder on the building platform, which is levelled by the motion of a suitable recoater [31]. Subsequently, a laser beam melts selective areas [31]. The cross-section area of the

component is built selectively, melting and re-solidifying metal powders in each layer [31]. The layer-by-layer building process is shown in figure 2.2.

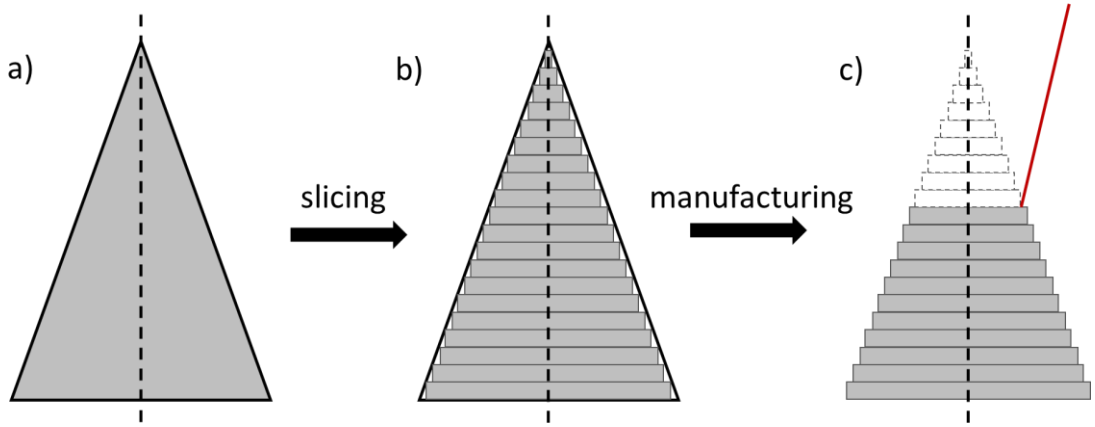

Figure 2.2: Layer-by-layer building process to manufacture a component with PBF-LB/M: a) designed model, b) sliced model, c) manufacturing of the component. According to [33].

Once the first layer is obtained, the building platform is lowered by an amount equal to the thickness of the next layer and the process can thus be repeated [31]. This procedure is repeated until the whole component is manufactured [33]. The thickness of the layer influences the building time and the roughness of the surface of the additively manufactured component [33]. The bigger the layer thickness is, the smaller the number of layers and the higher manufacturing speed are obtained for a given height of the component to be produced [33]. It has to be considered that the higher the layer thickness is, the more pronounced the stair-step effect will be [33]. The stair-step effect is shown in figure 2.3.

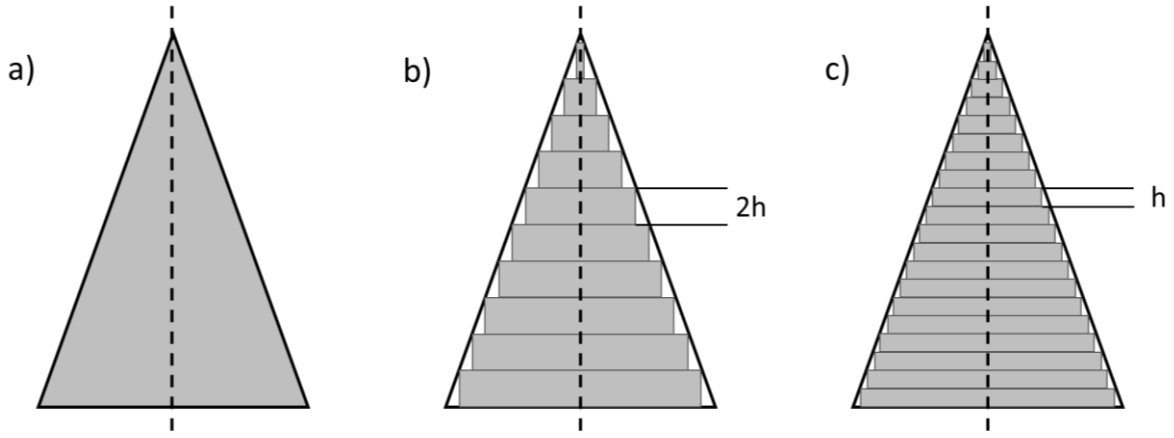

Figure 2.3: Schematic of the stair-step effect resulting from the layer-by-layer process. a) designed model, b) manufactured component with layer thickness 2h, c) manufactured component with layer thickness h. According to [33].

Once the process is finished, the component is taken out of the machine [29]. Subsequently the component is cleaned, to remove the particles not affected by the fusion [29]. Finally, it is necessary to remove the supports and post-process the part to obtain the required surface finish and mechanical properties [9]. Examples of post-processing techniques are mechanical machining, polishing and blasting, by which the surface roughness of the parts can be improved [9]. Moreover, due to the thermal gradient that occurs during the process, the parts are exposed to residual stresses which leads to their deformation [36]. Heat treatments are used to modify the microstructure of the manufactured component in order to obtain the required mechanical properties [9]. A typical process is hot isostatic pressing (HIP), which is used to reduce the porosity that could occur in the component and therefore improve the mechanical properties of the part [9].

It is possible to use a large number of metal powders in PBF-LB/M processes: aluminium, titanium, copper, chromium, cobalt chromium, stainless steel, tool steel and superalloys [31]. Most of the powders not affected by the melting process, which remain in the end, can be reused for subsequent production processes [31]. In some cases, however, some of these powders become non-recyclable, as they may have become contaminated or oxidized during the melting process [31]. Today, PBF-LB/M machines use metal powder particles of 20-50 µm in size, while the thicknesses of the layers produced are 20-100 µm [4]. Furthermore, the minimum feature size reported is in the range of 40-200 µm [4]. Powders are produced, for the most part, by inert gas atomization processes based on molten material [37]. Special attention must be paid to the quality and particle size of the powders used, as these characteristics heavily influence the quality of the manufactured part [37]. However, it is difficult to use powder particles with a size lower than 20-50 µm, since technical challenges can arise, such as inadequate spreadability of the powder [4].

Much research has been conducted to determine appropriate process parameters to be adopted in order to increase the resolution achievable [31] with Additive Manufacturing machines and to obtain components without porosity [9]. The process parameters depend on the Additive Manufacturing technology used, as well as the type of material and the machine used [9]. Examples of parameters that can influence the PBF-LB/M process are illustrated in Figure 2.4.

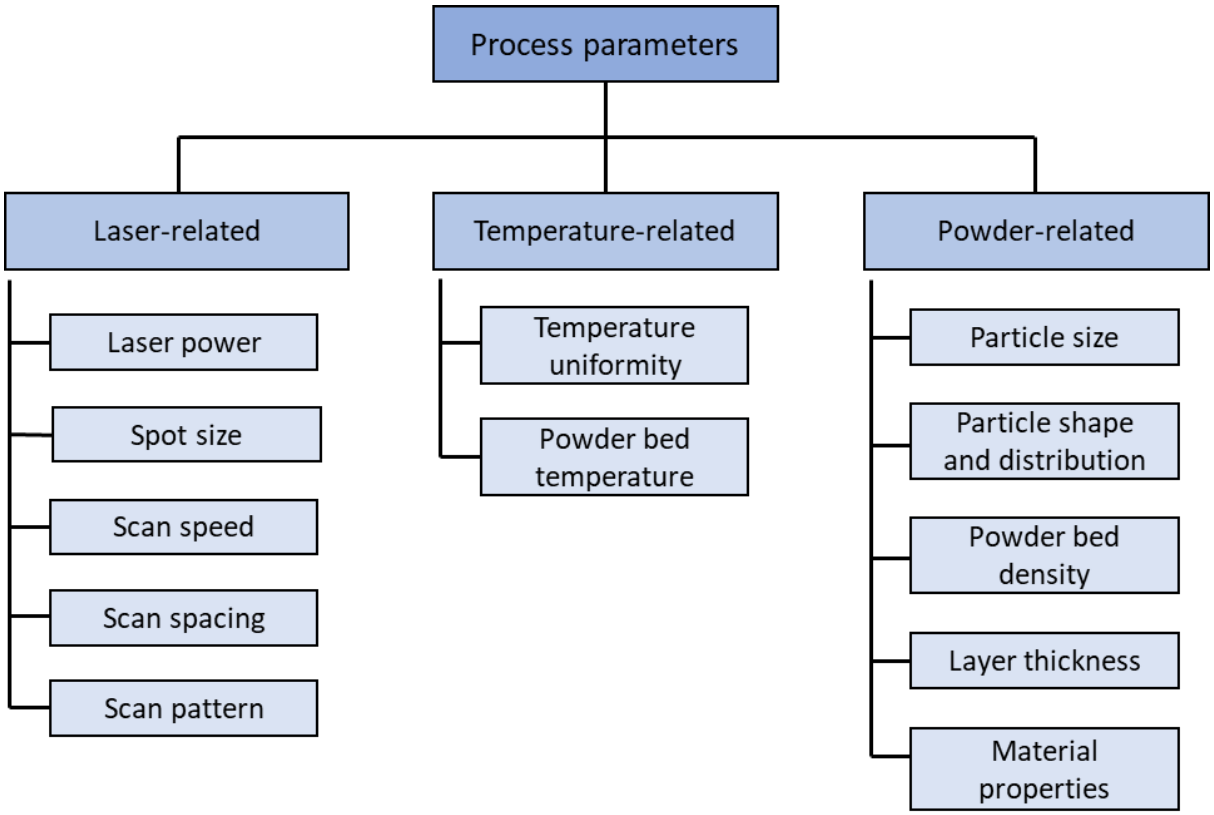

Figure 2.4: Process parameters of PBF-LB/M process having an influence on the quality of the manufactured component, according to [9].

In literature, the parameters considered to have a high influence on the process are the size of the powder particles, the diameter of the laser beam, the laser power, the thickness of the layer [31], the scan pattern, the scan strategy, the hatch spacing and the scan speed [9]. The scan pattern and the scan strategy are used in order to improve control over the microstructure of the manufactured component and to minimize defects during the building process [9]. The scan pattern defines the laser path within each layer [9]. Different patterns can be used, the most common being unidirectional, checkerboard and meander [9]. An example of these patterns is presented in figure 2.5.

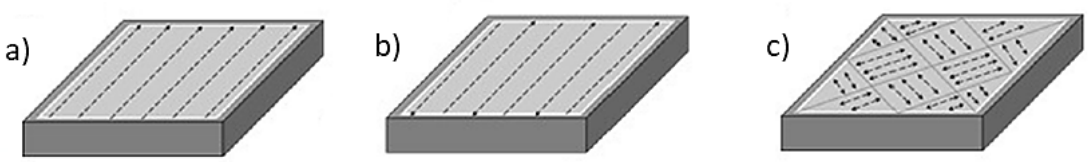

Figure 2.5: Examples of different scan patterns in PBF-LB/M: a) unidirectional, b) meander and c) checkerboard. According to [9].

In contrast, the scan strategy defines the difference in scan patterns between the different layers [9]. For example, it is possible to scan a layer multiple times, or to rotate the

orientation between layers, as shown in the figure 2.6.

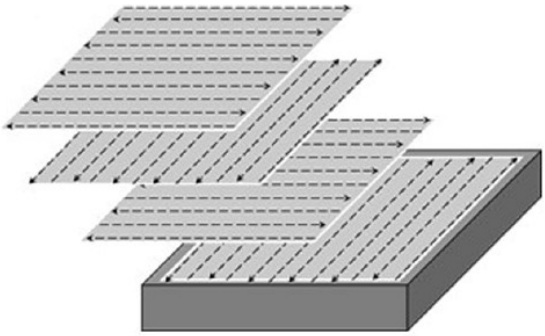

Figure 2.6: Example of scan strategy. According to [9].

The laser power is responsible for the amount of energy delivered into the material [9]. If the power is too low, defects, namely unmolten areas, emerge [9]. Scan speed, however, controls the melting of powders and solidification rate, which has a significant influence on the microstructure of the component obtained [9]. Finally, the layer thickness must be carefully determined, because if it is too high, defects may emerge, such as the incomplete melting of the powder layer or the loss in dimensional accuracy and tolerance [9].
A fundamental parameter used to find the suitable process parameters is the volumetric energy density E_v, calculated as follows [9]:

$$E_v = \frac{P_l}{v_s * h_s * l_z} \tag{2.1}$$

P_l is the laser power, v_s is the scan speed, h_s is the hatch spacing and l_z is the layer thickness. These quantities can be seen in figure 2.7, which illustrates the geometric parameters of PBF-LB/M process.

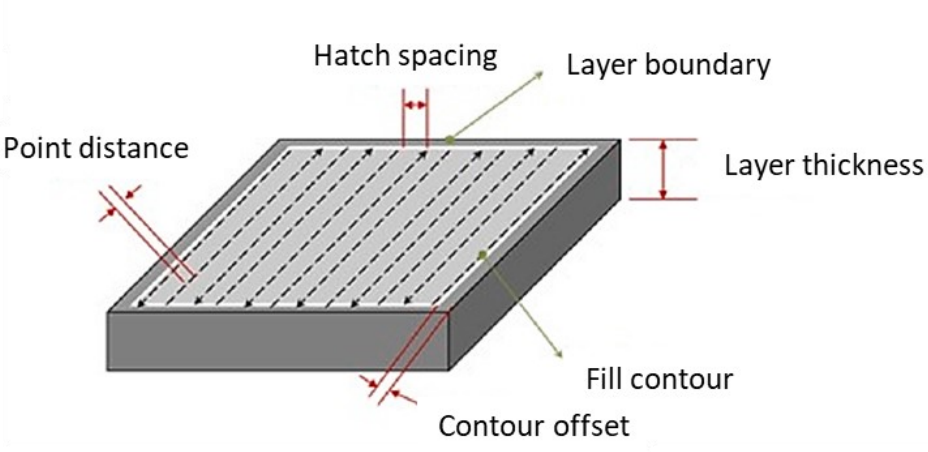

Figure 2.7: Geometric parameters of PBF-LB/M, according to [9].

The volumetric energy density is a relevant parameter regarding relative density [38]. In this thesis the used process parameters are according to previous investigations. Many studies have been performed with 316L components produced with PBF-LB/M [39]. 316L is an appropriate material to be processed with PBF-LB/M, due to its high weldability [38]. In [32] it is possible to see a comparison between the mechanical properties of components produced with the PBF-LB/M and 316L annealed bulk material. According to the results of this research, the tensile strength of the two tested specimens is similar, while the ductility of the additively manufactured component is reduced if compared to the one of the annealed bulk material [32]. Another important aspect to consider when manufacturing components with PBF-LB/M, is that anisotropic properties arise in the component, due to the layer-by-layer process [38]. Consequently, the yield strength and the tensile strength of components built using PBF-LB/M depend on the build direction [38].

Advantages and disadvantages

PBF-LB/M technology has several advantages, which make it a suitable technology to manufacture hybrid components. Through PBF-LB/M technology three-dimensional physical objects can be manufactured in a single production step, but it is also possible to add functional elements on previously made metal sheets [8].
Among the advantages, the following can be highlighted:

- **High geometrical complexity of the manufactured components:** The tool-less approach of PBF-LB/M enables the production of parts with high geometrical complexity in a single building process [6]. This overcomes a major limitation which is common for conventional manufacturing processes, where it is necessary to use different dies or moulds for each geometry to be obtained [6]. Free-form geometries and topologically optimized structures can be built [40]. Furthermore, it is possible to build infill structures, like honeycomb structures [40] and to integrate different functions in the same component [40].
- **Material efficiency:** In conventional subtractive manufacturing technologies, the process consists of removing material from a larger raw component to obtain a smaller element with the desired geometry. In PBF-LB/M the material is used more efficiently. After the component is built, it is possible to reuse the remaining unmolten powder for the next building process. [6]
- **Manufacturing of near-net shape components:** Parts built using PBF-LB/M have shape and size close to the finished product. For this reason the post-processing of the parts is minimized. [40]
- **Shorter times from design to part manufacturing**: The typical limitations of conventional manufacturing processes, such as tool accessibility and undercuts, become less limiting in the case of PBF-LB/M, thanks to the tool-less approach. For this reason, a reduced time to design the models of the components to be manufactured is needed and, consequently, a shorter time between the design of the part and the manufacturing is obtained [40].

However, there are still several characteristic limits of this innovative technology, which do not allow PBF-LB/M technology to fully compete with conventional manufacturing technologies.

- **High production times:** Processing speeds are lower than those of conventional manufacturing technologies [20].
- **Narrow range and high cost of powder materials:** Each machine can use a certain range of materials [27]. It is not possible to use every material, but the range of materials available on the market is increasing [6]. Besides, the cost of these powders is high [6].
- **Size limitation:** The dimensions of the components that can be produced with PBF-LB/M are related to the size of the working volumes. In addition, large parts are difficult to build in a short time, due to the high amount of time required to complete the layer-by-layer process. Another factor limiting the size of the component to be manufactured is the possibility of the occurrence of cracks and deformations, which are due to residual stresses. [40]
- **Need of support structures:** Support structures are used to dissipate heat, to compensate for distortions due to the thermal effects and to fix the component on the substrate plate [40]. As before mentioned, they are needed for unconnected regions, downward facing surfaces and large cantilevered regions [9]. The support structures increase manufacturing costs because additional time is necessary to build and to remove them [9].
- **Poor surface quality:** Components produced using PBF-LB/M processes have a rough surface finish. Hence, it is necessary to carry out subsequent post-processing, to obtain the required surface finish. [6]
- **Anisotropic properties of the manufactured component:** Due to the layered structure of the component manufactured using PBF-LB/M, parts have anisotropic properties. This can lead to the reduction of mechanical properties values, such as tensile strength and yield strength. However, the anisotropy of mechanical properties can be reduced by using heat treatments. [40]
- **Deformations, shrinkages and residual stresses:** Due to the high thermal gradients, deformations, shrinkages and residual stresses arise in the manufactured components, during the solidification phase [40].

The main disadvantage of the PBF-LB/M technology is the long process time [6]. For this reason, PBF-LB/M is used to produce small batch sizes of products with a high geometrical complexity [1], while metal forming technologies are used to manufacture components in large quantities, since they have shorter process times [8]. A strategy to overcome the limitations of PBF-LB/M is to manufacture hybrid components combining Additive Manufacturing technologies and sheet metal forming processes.

Future development

Today, Additive Manufacturing technologies are more and more widespread [2]. The availability of faster computers, more precise control systems and a growing range of materials will allow these technologies to become increasingly competitive in the world of manufacturing technologies [6]. Component accuracy and surface finish can be improved by using more accurate laser optics and machine controls [6]. Furthermore, the decrease in the prices of Additive Manufacturing machines and the reduction of the building time may lead to greater use of these technologies [6].

2.3 Forming technologies

Metal forming technologies are a large group of manufacturing processes [41]. These are generally processes performed immediately after the casting processes and before the finishing processes, like grinding, polishing, painting, and assembly [42]. In metal forming processes, plastic deformation is used to change the shape of the components to be manufactured [41]. The stresses applied to give the desired shape to the component, therefore, exceed the yield strength of the material used [41]. In these processes the material can be compressed, stretched, bent or a shear stress can be applied to it [41]. It is possible to classify these technologies based on different parameters: type of product to be made, material used, forming temperature and nature of deformation [42]. As can be seen in figure 2.8, metal forming processes are numerous and are divided into two categories, that are bulk deformation processes and sheet metal forming processes [41].

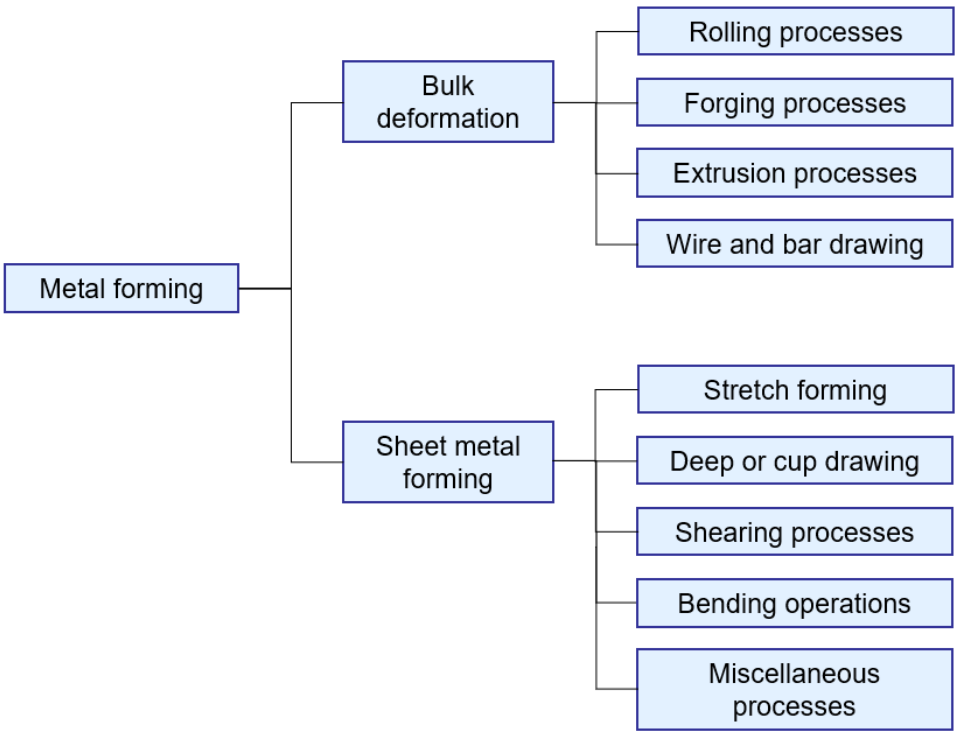

Figure 2.8: Classification of metal forming processes according to [41].

A material is easily formable through metal forming technologies if it has a high ductility and a low yield strength [41]. Ductility and yield strength are influenced by temperature [41]. As the temperature increases, the yield strength decreases and the ductility increases [41]. Therefore, the influence of the temperature is important because lower forces during forming are needed and larger plastic deformations can be applied to the material without failure [41]. Consequently, higher temperatures are used to soften the material and make it more formable. Accordingly, it is possible to divide the metal forming technologies into three categories, based on the ratio T/T_m, known as homologous temperature, where T is the forming temperature and T_m is the melting point of the metal [43]. The temperature ranges of these three forming categories are listed in table 2.3.

Table 2.3: Temperature ranges of the three different type of forming categories, according to [43].

Process	T/T_m
Cold forming	< 0.3
Warm forming	$0.3\ to\ 0.5$
Hot forming	> 0.5

The main advantages of cold forming, when compared to warm and hot forming, are better surface finish, greater accuracy, higher hardness and strength of the part due to strain hardening. Furthermore, no heating is required, which enables higher production rates and fewer heating costs. The main disadvantage of cold forming is that higher loads on tools are needed. Moreover, the ductility and strain hardening of the material limit the amount of deformation that can be applied to the component.
Regarding warm forming, its main advantage is that lower forces are needed in the forming process. Therefore, it is possible to reach a higher degree of deformation of the material and decrease the amount of the process steps needed to manufacture the component. Furthermore, the need for annealing is reduced or eliminated.
Hot forming processes are carried out at temperatures higher than the recrystallization temperature. This has both advantages and disadvantages. Among the main advantages there is the possibility of applying high plastic deformations to the component, obtaining complex geometries and using lower forces, which are required to deform the component. For this reason, it is possible to process materials that are difficult to work with cold forming. Moreover, components that have isotropic strength properties can be obtained, due to the absence of the oriented grain structure, which generally arise when the component is processed in cold forming. Finally, there is no strengthening of the component from work hardening. Among the disadvantages are the surface oxidation, the lower dimensional accuracy, the inadequate surface finish and the short lifespan of the tool used

to deform the component. Furthermore, a higher total energy is required, due to the thermal energy required to heat the component. [41]

Behaviour of metals during forming processes

The behaviour of the material during forming processes can be inferred from the analysis of stress-strain curves and depends on strain, strain rate and temperature [44]. Stress-strain curves are generally divided into an elastic and a plastic region [41]. Below the yield point the material exhibits elasticity, while above it shows plasticity [41]. At room temperature, as the amount of deformation applied to the metal increases, its strength increases due to strain hardening [41]. Consequently, in order to continue with the forming process, the stress must be increased to match this increase in strength [41]. Since it is necessary to change the shape of the processed material by applying a plastic deformation in these processes, the plastic region of the curve is the one of greatest interest [41]. In this region, the behaviour of the metal is expressed using the flow curve [41]:

$$K_f = c * \varphi^n \tag{2.2}$$

where K_f is the flow stress, c is the strength coefficient, φ is the true strain and n is the strain-hardening exponent. For metals, the values of c and n depend on temperature [41]. The forces necessary to obtain a correct forming process can be estimated by using the flow curve [41]. Flow stress K_f represents the instantaneous value of stress required to continue to deform the material [41]. It is the yield strength of the metal as a function of strain [41]. This relationship is, however, an instantaneous relationship [41]. To analyse a forming process, it is more convenient to use another parameter, the average flow stress during deformation $\overline{K}_f$, which is defined as the average value of stress over the stress-strain curve, starting from the beginning of strain to the maximum value that takes place during deformation [41]. The average flow stress can be calculated using the following relationship, obtained by integrating the flow curve equation in the range of interest, which starts from zero and reaches the final strain value [41]:

$$\overline{K}_f = \frac{c * {\varphi_f}^n}{1 + n} \tag{2.3}$$

$\overline{K}_f$ represents the average flow stress and φ_f represents the maximum strain value during the deformation process. A representation of these quantities can be found in figure 2.9.

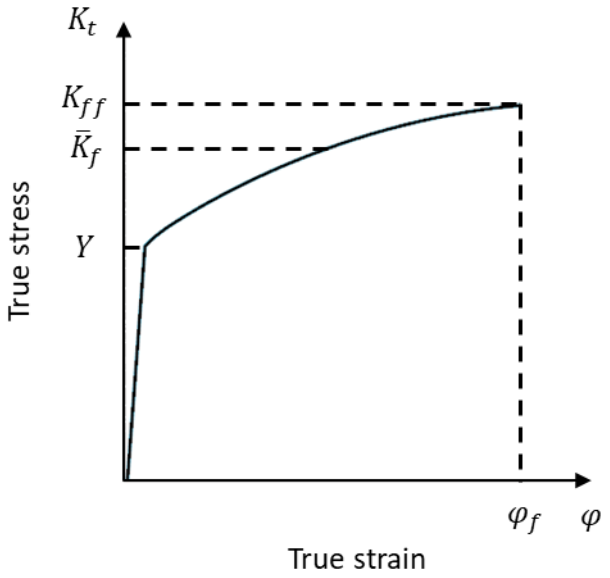

Figure 2.9: Stress-strain curve showing the average flow stress $\bar{K}_f$ in relation to yield strength *Y* and final flow stress K_{ff} according to [41].

Another parameter to consider is strain rate sensitivity, as flow stress depends on strain rate in forming processes [41]. The speed of deformation *v* is directly related to the rate at which the metal is strained in a forming process and it is generally equal to the velocity of the ram [41]. The strain rate is calculated with the equation number 2.4 [41]:

$$\dot{\varphi} = \frac{v}{h} \tag{2.4}$$

where $\dot{\varphi}$ is the true strain rate and *h* is the instantaneous height of the component being deformed. The resistance to deformation increases if the strain rate is increased [41]. This relationship can be expressed through the following equation [41]:

$$K_f = s * \dot{\varphi}^m \tag{2.4}$$

where *s* is the strength constant, which is determined at a strain rate of 1.0 s^{-1}, $\dot{\varphi}$ is the strain rate and *m* is the strain rate sensitivity exponent. The effect of the strain rate becomes relevant if the temperature increases, as this leads to an increase in the value of *m* and a decrease in the value of *s* [41]. A more complete expression of flow stress as a function of strain and strain rate can be obtained by combining all the previous equations [41]:

$$K_f = A * \varphi^n * \dot{\varphi}^m \tag{2.5}$$

where *A* represents a strength coefficient, which combines the effects of the previous *c* and *s* values. The values of *A*, *n*, and *m* are all functions of the temperature [41].

2.3.1 Sheet metal forming

Sheet metal forming technologies are grouped into cutting and forming operations performed on metal sheets, which are manufactured by rolling [41]. The metal sheets used generally have thicknesses between 0.4 mm and 6 mm [41]. If the thickness of the sheet exceeds 6 mm, the sheet is called plate [41]. Sheet metal forming processes are widely used in several industrial sectors, such as the automotive industry, aerospace industry, and in the manufacturing of household items [41].
Most sheet metal forming processes are performed at room temperature [43]. The components thus obtained have high strength, high-grade surface finish and high dimensional accuracy [41]. It is possible to use warm or hot sheet metal forming processes to increase the formability of materials characterized by high strength and to decrease loads on tools [43]. Sheet metal forming processes are economically efficient for large batch sizes [41] and have low production times [8].
Among the sheet metal forming processes it is possible to mention the drawing, deep drawing, stretch forming, shearing and bending processes [43]. The processes of deep drawing and stretch forming are two technologies that are of interest for this thesis and will be described in the following sections.

2.3.2 Deep drawing

Deep drawing is a process through which a metal sheet is plastically deformed, obtaining cup-shaped, box-shaped or other complex-curved and concave metal sheet parts [41]. A diagram of this process is depicted in figure 2.10.

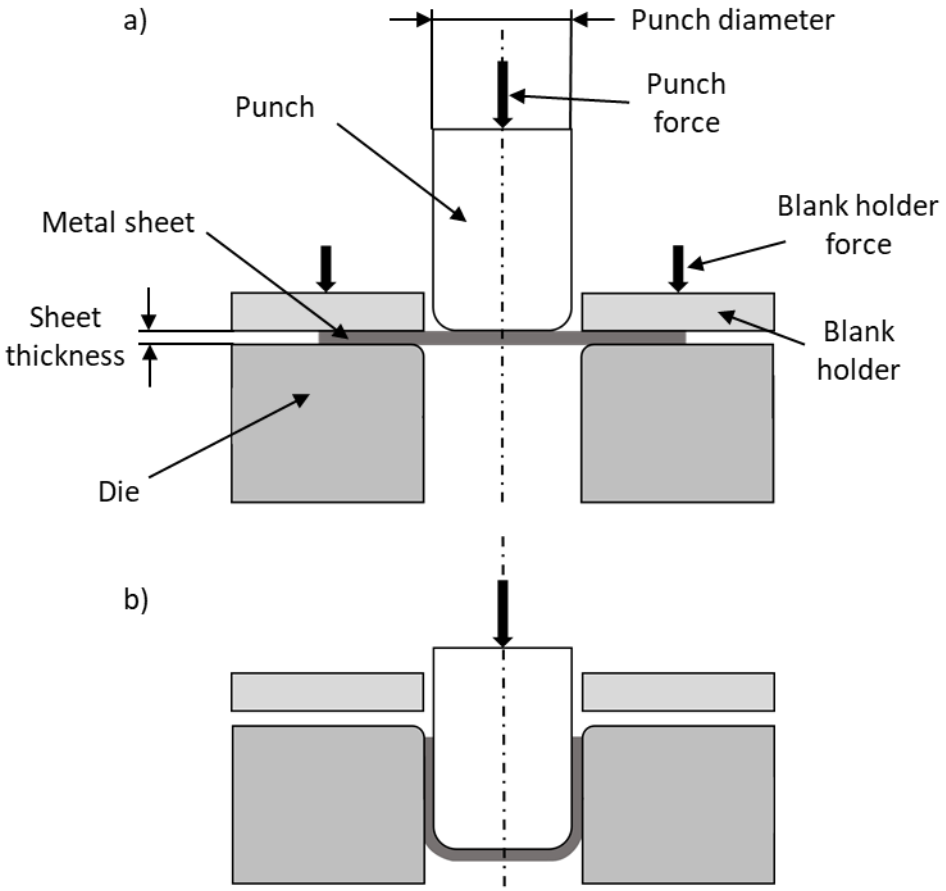

Figure 2.10: a) Starting step and b) final step of a deep drawing process. According to [43].

During the process of deep drawing, the sheet metal blank is subjected to the pressure of the punch, which pushes the sheet through the die cavity [43]. The blank is held down against the die using a blankholder [43].
The maximum punch force F_{max} required to perform a deep drawing process can be roughly estimated using the following equation [43]:

$$F_{max} = \pi * D_p * t_0 * UTS * \left[\left(\frac{D_b}{D_p}\right) - 0.7\right] \tag{2.6}$$

where F_{max} is the maximum punch force, D_p is the punch diameter, t_0 is the blank thickness, *UTS* is the ultimate tensile strength, D_b is the starting blank diameter and the constant *0.7* is a correction factor to take into account the friction.
The blank holder exerts a force that maintains the metal sheet always tensed during the lowering phase of the punch [45]. The force exerted by the blank holder is known as *BHF* (blank holder force) [45]. To obtain an appropriate deep drawing process, the *BHF* and the clearance between the punch and the die must be carefully chosen [45]. These parameters are important, as they can cause defects in the manufactured

component [45]. If the force exerted by the blank holder is too low, wrinkling can occur, while if it is too high, tearing arises [45]. Additionally, if the clearance is too small, the phenomenon of ironing appears [45]. The most used clearance values are 7 % to 14 % greater than sheet thickness [43].
During the deep drawing process different stress conditions coexist [46], as shown in figure 2.11. Three different areas can be distinguished in the produced component [46]:

- flange: the stress condition in this area is a tensile load in radial direction and compression load in tangential direction
- side wall (cup wall): this zone is characterized by a plane strain load
- bottom: there is a biaxial tensile stress load in this area

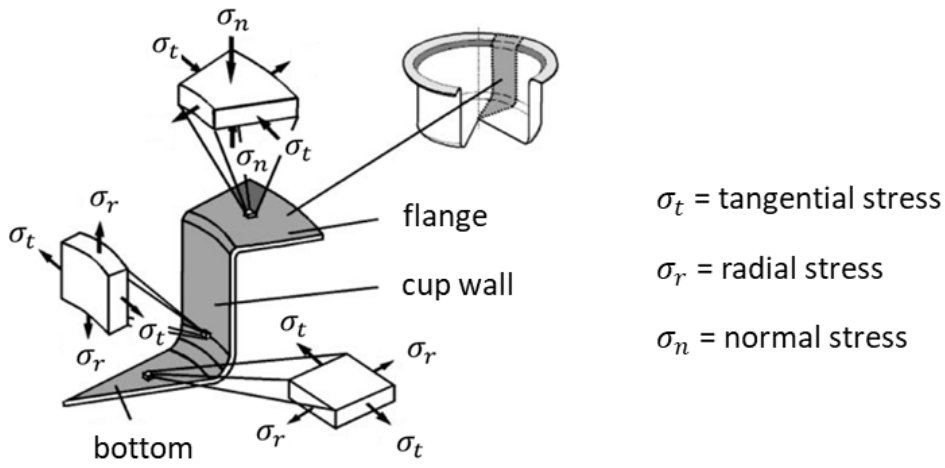

Figure 2.11: Stress conditions in a deep drawn component according to [46].

The stress conditions present during the deep drawing process determine the success or failure of the manufacturing process [46]. If the elongation, due to the state of stress, which occurs on the cup wall is excessive, there will be a high reduction of the thickness of the sheet, which can lead to the tearing of the cup [43]. Another common defect is the orange peeling [45]. In these cases, a high surface roughness is created in the region of the sheet, which has been subjected to a high deformation [45]. Nevertheless, this defect can be avoided using ironing [45].
Finally, surface scratches are another defect [41]. These can occur on the manufactured component if there is insufficient lubrication or if the punch and the die have a too high surface roughness [41]. Figure 2.12 illustrates the different defects.

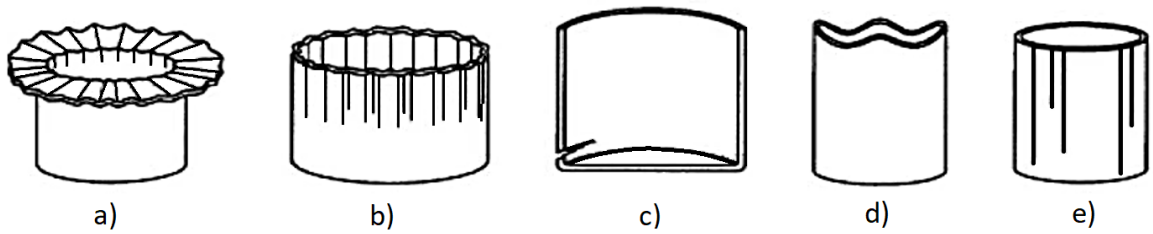

Figure 2.12: Common defects in deep drawn components: a) wrinkling at the flange, b) wrinkling in the wall, c) tearing, d) earing, and e) surface scratches. According to [41].

The quality of the material used, the die, the blank holder and the lubrification between the die and the metal sheet must all be chosen carefully in order to obtain a drawing process that does not result in defects [43].
The anisotropy of the sheet is an additional feature to be considered [45]. This greatly affects the deep drawing ability of the sheet [45]. In particular, planar anisotropy can be the cause of the presence of earing defects [45].
The capability of a deep drawing process to manufacture defect-free components is a function of the normal anisotropy R_n of the metal sheet (also called plastic anisotropy) [45]. It has been established in literature that there is a close relationship between the value of the anisotropy and the Limiting Draw Ratio (*LDR*) [25]. *LDR* is used to measure the formability of the sheet to be formed [45]. *LDR* is calculated with the equation number 2.7:

$$LDR = \frac{D_0}{D_p} \tag{2.7}$$

LDR is the ratio between the diameter D_0 of the largest blank that can be successfully drawn and the diameter of the punch D_p [45]. The theoretical limit value is 2.7 [45]. This value depends on the different process conditions that occur during the deep drawing process [41]. These conditions include the friction conditions, drawing depth, the punch and die corner radii, and mechanical characteristics of the metal sheet [41]. To understand if a metal sheet can be successfully processed in a deep drawing process, it is necessary to analyse the anisotropy of the sheet, especially the normal anisotropy *R* of the sheet [43]. Cold-rolled sheets generally show anisotropy in their planar direction [43]. For this reason, the *R* value of the metal sheet depends on its orientation with respect to its rolling direction [43]. Taking this fact into account, the average parameter R_{avg} is used to describe the anisotropy of a metal sheet [43]:

$$R_{avg} = \frac{r_0 + 2 * r_{45} + r_{90}}{4} \tag{2.8}$$

The subscripts represent the angles with respect to the rolling direction of the sheet.

Another parameter relating to the anisotropy of a metal sheet, is the planar anisotropy *ΔR* [43], which can be calculated using the following formula:

$$\Delta R = \frac{r_0 - 2 * r_{45} + r_{90}}{2} \tag{2.9}$$

This parameter is relevant in terms of earing defect [43]. Due to this phenomenon, it is possible to find edges in the final component that can be curved [43]. These must then be trimmed off, thus generating scrap [43].
When the value of the planar anisotropy is 0, no ears will form [43]. When the planar anisotropy is different from 0, higher ears will start to form, as the *ΔR* value increases [43]. For this reason, in a deep drawing process, it is advisable to use sheets with a high R_{avg} value and a low *ΔR* value [43].

2.3.3 Stretch forming

The stretch forming process differs from the deep drawing process in some features. Stretch forming is a tensile forming process, in which a metal sheet is simultaneously stretched and bent over a convex die, called form block or form die [43], to create a contoured part [41]. The widening of the sheet is due to the decrease in thickness that occurs [47]. Consequently, unlike in deep drawing processes, there will be a reduction of sheet thickness [46]. In figure 2.13 a diagram of the stretch forming process is shown.

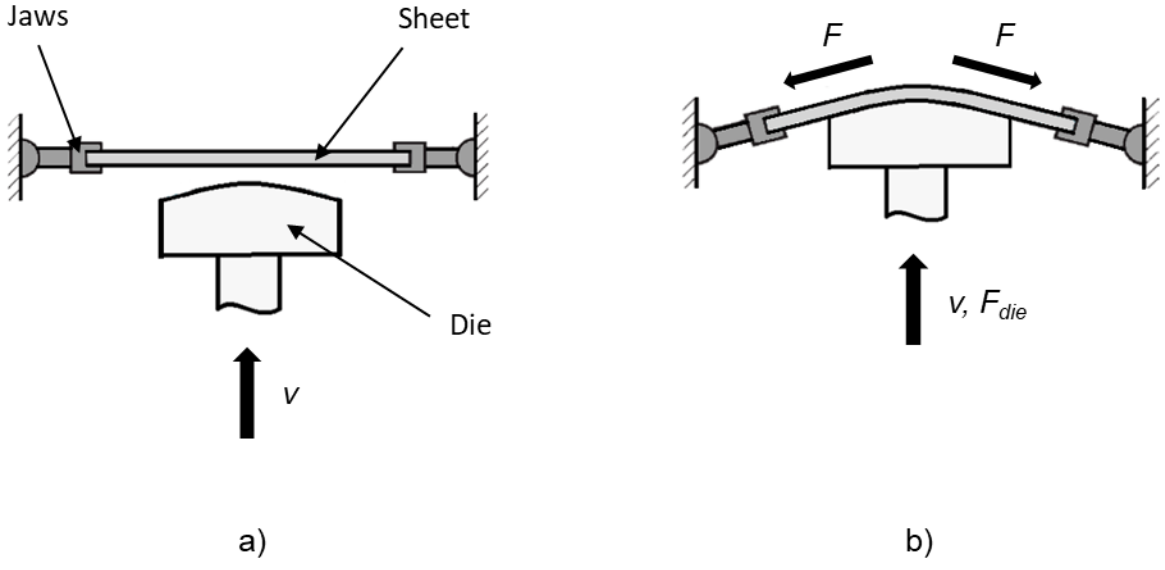

Figure 2.13: Illustration of stretch forming process: a) situation before starting the process; b) situation during the process. *v* is the speed of the die, *F* is the stretching force and F_{die} is the force applied by the die. According to [41].

In the stretch forming process, the metal sheet is gripped by one or more jaws at the ends, which hold it in position [41]. Subsequently, the sheet is stretched and bent over a convex die, which contains the required shape of the component [41]. To make the die plastically deform the sheet into a new shape, the stress applied to the sheet is greater than the yield stress of the material [41]. It is to be considered the effect of the springback that occurs once the force is removed [41].
It is possible to estimate the force required in a stretch forming process with the equation number 2.10, i.e., by multiplying the cross-sectional area of the sheet in the direction of pulling by the flow stress of the metal [41]:

$$F = L_p * t * K_f \tag{2.10}$$

where F represents the stretching force, L_p represents the length of the sheet in the direction perpendicular to stretching direction, t represents true sheet thickness and K_f represents the flow stress.
The process parameters that most influence the stretch forming process are the thickness of the sheet, the radius of the punch and its stroke, the friction and the mechanical properties of the material [47]. In particular, the mechanical properties of the sheet material, such as the yield stress, strain hardening exponent and Young's modulus, play a fundamental role in springback [47]. As yield stress and strain hardening exponent increase, springback becomes more relevant, due to lower overall plasticity [47]. If the thickness of the sheet is bigger [47] or the Young's modulus is higher [43], the springback decreases. The springback that occurs in the component is also affected by the forming temperature, since, if the forming temperature increases, the springback decreases [48]. Other types of defects that can occur are wrinkles, uneven deformation, or material failure [49]. Monitoring the amount of stretching, in order to prevent tearing, is essential [43]. Furthermore, in this process it is not necessary to have a good lubrication [43].
The forming limit diagram (FLD) is a useful tool for the analysis of this type of process, as it defines failure criteria [47]. The stretch forming process is versatile and economical, even if it is generally used for low volume production [43], and it is used in almost all sectors of industrial production, for example in the automotive, aeronautics, household appliances and food industries [43].
The sheet metal forming process employed to manufacture the hybrid components analysed in this thesis is a combination of deep drawing and stretch forming, as it presents characteristics of both. In the process used, the shape of the punch is hemispherical, different from those used in deep drawing processes and more similar to the ones used in stretch forming processes. Therefore, the stresses to which the component is subjected during the forming process are different from those obtained in the case of pure deep drawing and pure stretch forming process. Furthermore, a reduced material flow occurs due to the presence of the blank holder, if compared to a pure deep drawing process. As a consequence, a higher reduction in thickness arises.

2.4 Manufacturing of hybrid components combining Additive Manufacturing and sheet metal forming technologies

Hybrid components are manufactured by combining two or more manufacturing processes [50]. In [50] a process is defined as hybrid if the combination of the involved processes allows to reduce the disadvantages of the individual technologies and merge their advantages. There are several ways to manufacture hybrid components, depending on the chosen technologies [50]. A recently developed approach for manufacturing hybrid components is to combine Additive Manufacturing with forming technologies [50]. In literature it is possible to find examples of hybrid components manufactured combining Additive Manufacturing with either bulk metal forming technologies or sheet metal forming technologies [50]. Today, the objectives of production are oriented towards the complexity of design, mass customization and sustainable production [5]. Therefore, flexible and dynamic production processes are needed, such as those provided by Additive Manufacturing technologies [5]. In this way it is possible to manufacture highly customized components, which can adapt to customers' demands [7]. Additive Manufacturing, however, has low productivity and high energy consumption [3]. For this reason the costs of the process are high [3]. On the contrary, conventional forming processes have much shorter production times [50], but can only produce components with simple shapes, compared to those produced with Additive Manufacturing technologies [8]. Hence, the combination of Additive Manufacturing and metal forming technologies can significantly reduce production times and costs, and enables the manufacturing of components with complex geometries [1].

An example of combination of Additive Manufacturing and bulk metal forming technologies is the manufacturing of turbine blades made of Ti-6Al-4V by means of a combination of wire arc additive manufacturing with hot forging [50]. In such way a smaller number of forging steps are needed to manufacture the final component, reducing, at the same time, the loads on the tools and their wear [50]. Regarding the combination of Additive Manufacturing and sheet metal forming technologies, in literature there are some examples of areas of use of this type of hybrid components, e.g., the medical and aerospace sectors. As previously mentioned, hybrid components can be used to manufacture medical prostheses [5] and functional components with high geometrical complexity [6]. According to [50], the most suitable Additive Manufacturing techniques for the production of hybrid components consisting of metal sheet and additively manufactured elements are the powder bed fusion of metals processes, specifically PBF-LB/M and EBM. Using these techniques, there are more advantageous process conditions, i.e. the high process temperature and the presence of an inert atmosphere in the building chamber [50]. The high temperature that occurs during the building process reduces the thermal gradients and, consequently, allows to reduce the residual stresses that arise in the manufactured hybrid components, while the inert atmosphere reduces the risk of oxidation of the metal powders [50]. The major disadvantages of these techniques are the high surface roughness that arises from the layer-by-layer process and the long production times due to the times needed to heat

and cool the building chamber [50]. An example of hybrid component manufactured using a combination of PBF-LB/M and sheet metal forming is shown in figure 2.14.

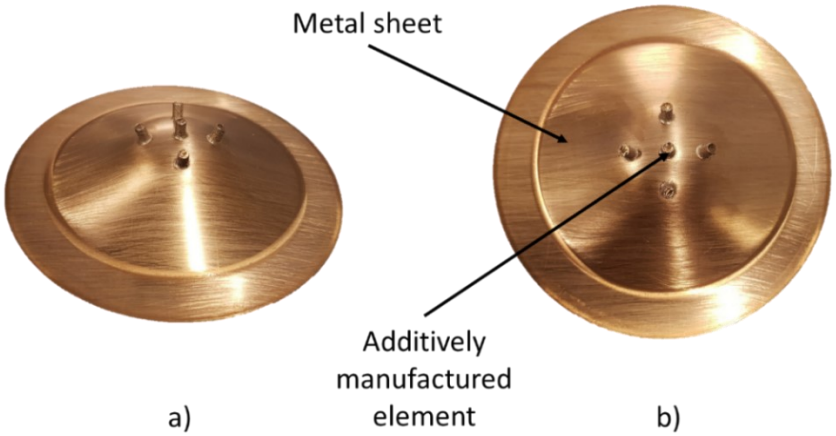

Figure 2.14: Example of a hybrid component analysed in this thesis: a) front view, b) upper view.

It is possible to use different forming processes and different strategies to manufacture hybrid components consisting of metal sheet and additively manufactured elements [50]. In [8] two different strategies to manufacture hybrid specimens combining Additive Manufacturing and sheet metal forming technologies are described. Figure 2.15 shows the two different strategies to manufacture hybrid specimens, that are:

- first, the sheet is formed and then the additively manufactured element is built
- first, the additively manufactured element is built on the sheet and then the sheet is formed

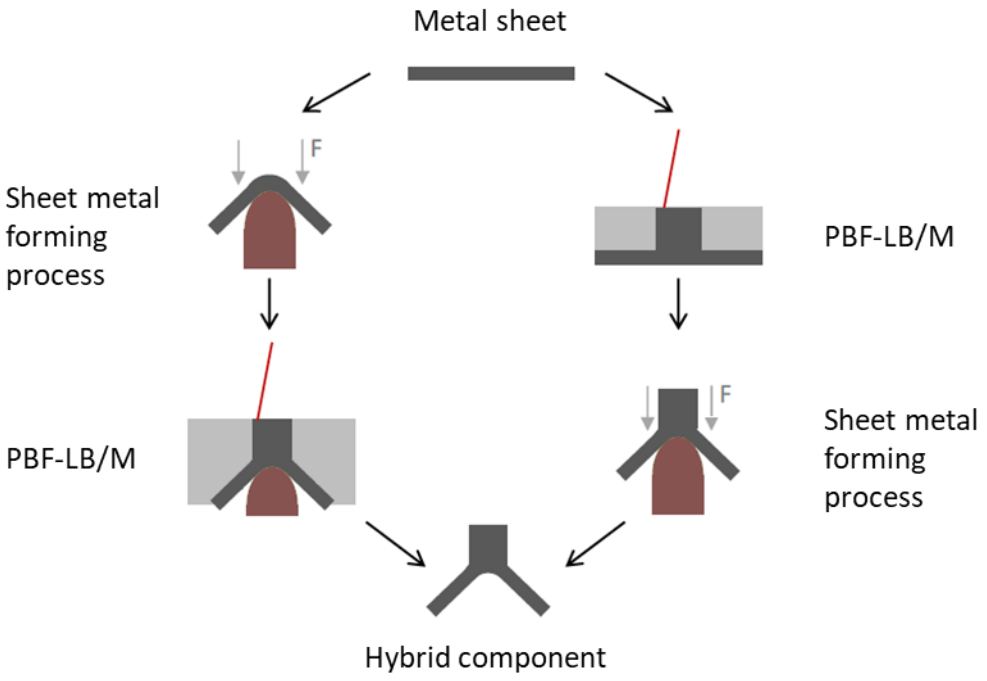

Figure 2.15: Different strategies to manufacture hybrid components combining sheet metal forming and PBF-LB/M. According to [8].

According to the sequence of the technologies used for the manufacturing of the hybrid specimens, interactions arise between the processes, since the first process performed influences the next [8]. If the Additive Manufacturing process is performed first, the presence of the additively manufactured element leads to a decrease of the formability and to a possible premature failure of components, which must be subsequently formed [8]. This is due to the stiffening effect of the additively manufactured element [8]. If the Additive Manufacturing process is performed as second, the main difficulty is to build the additively manufactured element on the previously formed metal sheet, since the surface on which the pin will be built is a curved surface [8]. To solve this problem, an elastic silicon lip is used [8], allowing the powder to be distributed even below the highest point, as shown in figure 2.16.

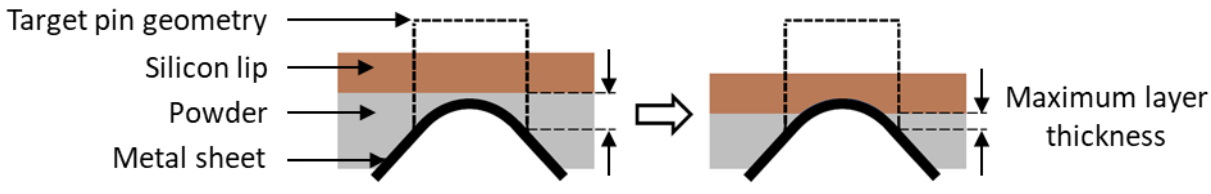

Figure 2.16: Scheme of the strategy to build the additively manufactured element on the formed metal sheet using a silicon lip. According to [8].

In this thesis, as previously mentioned, 316L hybrid components manufactured with the second strategy are analysed, that is, first, the additively manufactured elements are built on the metal sheet using PBF-LB/M and then the specimens are formed.
Different sheet metal forming technologies can be used to manufacture hybrid components, i.e. bending, stretch forming and deep drawing [50]. In [50] different types of hybrid components, manufactured combining Additive Manufacturing and the before mentioned sheet metal forming technologies, are analysed [50]. From the analysis of the stress states that arise due to the forming processes used for the manufacturing of the hybrid components, it was found that additively manufactured elements built on the metal sheet have a stress concentrating effect and, thus, increasing necking, which can lead to an earlier failure of the hybrid specimens [50]. According to the authors, this is the reason for the lower formability of the hybrid components compared to conventional sheet metal specimens [50]. Although in the literature it is possible to find many studies regarding the manufacturing of hybrid components by combining Additive Manufacturing with metal forming technologies, further research must be done to analyse the interactions that arise between the different processes used [50]. The manufacturing of hybrid components, in fact, leads to interactions between the processes involved, which have the effect of decreasing the formability of the hybrid components and cause the possible premature failure of the components [50]. Some studies have been carried on using Ti-6Al-4V titanium alloy, while studies involving hybrid components in 316L stainless steel are scarce. An example of research regarding the investigation of the interactions between

the technologies involved in the manufacturing of the hybrid specimens can be found in [51]. In this research the influence of the additively manufactured elements on the formability of hybrid components made of Ti-6Al-4V is analysed through numerical simulations [51]. Several geometric parameters of the additive manufactured elements are analysed to determine how these affect the formability of the obtained hybrid components [51]. The analysed parameters are geometry, diameter, fillet radius, number and distance of additively manufactured elements [51]. As additively manufactured elements are the part of hybrid components that adapts to the needs of consumers, it is necessary to investigate different combinations and values of the geometric parameters, as these have a strong influence on formability [51].

3 Thesis task

Stainless steels, nowadays, are used in many industrial sectors [13], because of their high corrosion resistance properties, high weldability [17] and high formability over a wide temperature range [19]. The products made of stainless steels are manufactured, for the most part, using conventional production processes, such as bulk forming and sheet metal forming technologies [17]. Conventional manufacturing processes are economically efficient for large batch sizes, due to their low production times, but they do not permit to manufacture components with high geometrical complexity [8]. In the last few decades, however, the use of Additive Manufacturing technologies has become increasingly popular [2]. These technologies allow the manufacturing of components with complex geometries [5] in a single production step [6]. The main disadvantages of Additive Manufacturing technologies are the high production time and the high process costs [7]. Since stainless steel is widely used in Additive Manufacturing as well, due to the high weldability, it can be used in both processes [7]. A strategy to overcome the limitations of Additive Manufacturing and sheet metal forming technologies is to combine them to manufacture highly customized hybrid components [8], capable of adapting to specific customers' requests [2]. The main disadvantage of the combination of the above mentioned technologies are the interactions between them [5]. Regardless of the sequence of the technologies chosen for the manufacturing of hybrid components, the first process to be performed has a negative influence on the second one [50] and, consequently, a lower formability of the hybrid components is achieved [8]. As above mentioned, the potential fields of application of hybrid components are medical and aerospace sectors [10]. In particular, hybrids components can be used for the manufacturing of medical prostheses [5] and of functional components made of high-strength and light-weight materials with high geometrical complexity [6]

The hybrid components analysed in this thesis are made from a 316L metal sheet, on which additively manufactured elements are built using PBF-LB/M technology. Subsequently, the specimens thus obtained are formed at different testing temperatures. The aim of this thesis is the analysis of the influence of the geometry of the additively manufactured elements and of the testing temperature on the formability of hybrid components. The geometric parameters examined are the diameter of the pins D, the distance between the pins measured from the centre L, the number of pins NP and fillet radius R in the transition area between the sheet and the pins. The chosen testing temperatures are 20 °C, 250 °C and 400 °C. The manufactured specimens are analysed to determine the position and value of the minimum thickness, which is used to compare the different components and determine the influence of the different variables on formability. First, the influence of the individual parameters on the formability of the hybrid parts is determined, then the influence of the combination of parameters is considered.

4 Experimental setup and procedure

This chapter describes the machines, the tools, the software and the experimental procedure used in this thesis to manufacture and analyse the specimens. The material used for the manufacturing of the hybrid components is described as well.

4.1 Stainless steel 316L

The hybrid components consist of a 1.5 mm thick sheet on which one or more additively manufactured elements are built. The sheet is made of 316L stainless steel. The chemical composition is shown in the table 4.1.

Table 4.1: Chemical composition of 316L stainless steel (weight percent). According to [25].

Cr	Ni	Mn	Mo	C	N	Si	P	S	Fe
17-19	13-15	<2	2.25-3	<0.03	<0.1	<0.75	<0.025	<0.01	Bal.

316L is also used for the additively manufactured elements that are built using PBF-LB/M. The powder used for this process has a size distribution of 10 - 45 µm, and is made by atomization process [52]. The chemical composition of the powder is shown in table 4.2.

Table 4.2: Chemical composition of 316L stainless steel powder for PBF-LB/M, distributed by the company DMG MORI. According to [52].

Cr	Ni	Mn	Mo	C	N	Si	P	S	Fe
16-18	10-14	Max.2	2-3	Max. 0.03	Max 0.1	Max. 1	Max 0.045	Max. 0.015	Bal.

The mechanical properties of 316L components, built using Additive manufacturing, vary according to the machine used and the building parameters [52].

4.2 Machines used to manufacture and analyse hybrid components

The systems used to manufacture the hybrid components are the additive manufacturing machine LaserTec 30 SLM from the company DMG Mori and the Lasco TSP 100 S0 hydraulic press. The optical measurement system ATOS is used to analyse the thickness distribution of the hybrid specimens. In this chapter the characteristics of these machines are described.

4.2.1 Additive Manufacturing machine: LaserTec 30 SLM

The Additive Manufacturing LaserTec 30 SLM machine is used to build the additively manufactured elements on the metal sheet. The technical features of this machine are shown in the following table 4.3.

Table 4.3: Technical features of LaserTec 30 SLM machine from the company DMG Mori. According to [53].

Technical feature	Value
Build volume X	300 mm
Build volume Y	300 mm
Build volume Z	300 mm
Layer thickness	20 - 50 µm
Focus diameter	50 - 300 µm
Laser power standard	1000 W
Inert gas	Argon

This machine is provided with a high-precision optic module with dynamically adjustable focus diameter, which can range from 50 µm to 300 µm [53].

4.2.2 Forming press: Lasco TSP 100 S0

The hydraulic forming press of Lasco Umformtechnik GmbH, type TSP 100 S0, is used to carry out the sheet metal forming process. The technical parameters of the forming press are shown in table 4.4.

Table 4.4: Technical parameters of the Lasco forming press type TSP 100 S0 [54].

Technical parameters	Value
Maximum nominal pressure force in kN	1000
Maximum cushion force in kN	250
Maximum slide stroke in mm	600
Maximum piston speed in the working stroke in mm/s	8

A heatable forming tool, which can reach testing temperatures up to 550 °C using heating

elements, is utilized to carry out the forming experiments. A method used to prevent thermally induced expansion of the entire tool is water cooling. Cooling plates are installed between the heated elements and the base plate. The forming tool is shown in figure 4.1.

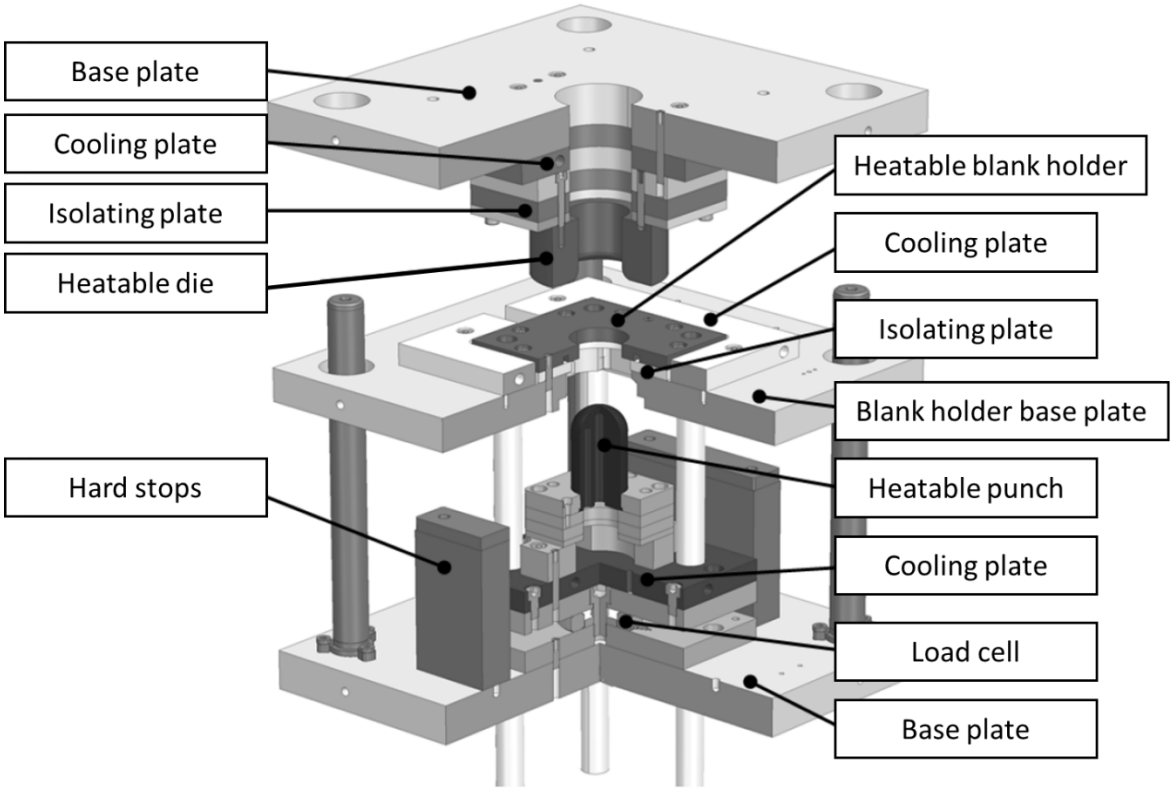

Figure 4.1: Drawing tool for forming metal sheet up to 550 ° C. According to [55].

The punch used has a diameter of 60 mm, while the internal diameter of the die is 63.4 mm. As a result, a drawing gap of 1.7 mm is obtained.

4.2.3 Optical measurement system: ATOS

The optical measuring system ATOS Professional V8 SR1 by GOM GmbH Braunschweig is used for the three-dimensional measurement of the components. This instrument is a non-contact measurement system, which can perform high-speed and high resolution scans of parts using structured blue light projection [56].
Several measurements are made from multiple angles using the scanner, to obtain the three-dimensional measurement of the component. The scanner creates precise fringe patterns onto the component surface, which are captured by two cameras [56]. Therefore, the surfaces must not be reflective. For this reason, the analysed components must be covered with a thin layer of coating to make the surface opaque.

4.3 Software

The software used to create the CAD geometries, to manufacture and to analyse the specimens is PTC Creo Parametric CAD software, RDesigner, CELOS and GOM Inspect Suite 2020. They are described below.

4.3.1 PTC Creo Parametric CAD

PTC's Creo Parametric 7.0.2.0 Computer-Aided Design (CAD) software is used to create digital models [57]. The geometries of the different specimens are created and saved in .stl format. This file is subsequently imported into RDesigner.

4.3.2 RDesigner

RDesigner is a software from the company DMG MORI. It allows the subdivision of the created geometries into layers, which are the sections of the additively manufactured elements that will be built using PBF-LB/M. The resulting file is in .rea format. This file is used in the additive manufacturing machine.

4.3.3 CELOS

CELOS is the controlling software of the Additive Manufacturing machine [58]. The .rea files are imported into this software and then the laser hatches on each layer are defined. The process parameters are then set, such as laser power, focus diameter, building temperature, oxygen level, etc. Once all the different parameters have been set, the building process can be saved in .rdx format and subsequently be performed.

4.3.4 GOM Inspect Suite 2020

GOM Inspect Suite 2020 software by the company GOM GmbH Braunschweig [59] is used to analyse the results obtained from the optical measuring system ATOS. Through this software it is possible to measure the thickness distribution of the hybrid components and analyse the data thus obtained.

4.4 Experimental procedure

Different geometries of specimens are built to analyse how the presence of additively manufactured elements influences the formability of hybrid components in 316L stainless steel during the sheet metal forming process. The additively manufactured elements, in fact, interfere with the sheet metal forming process, reducing the maximum achievable drawing depth and causing an earlier failure of the specimens [50].

4.4.1 Geometries of specimens

The hybrid components are manufactured from 316L round blanks with a thickness of s_0 = 1.5 mm and diameter D_0 = 105 mm, on which the additively manufactured elements are built using PBF-LB/M. In figure 4.2 it is possible to see a representation of these quantities and the manufacturing process sequence used to produce the hybrid components.

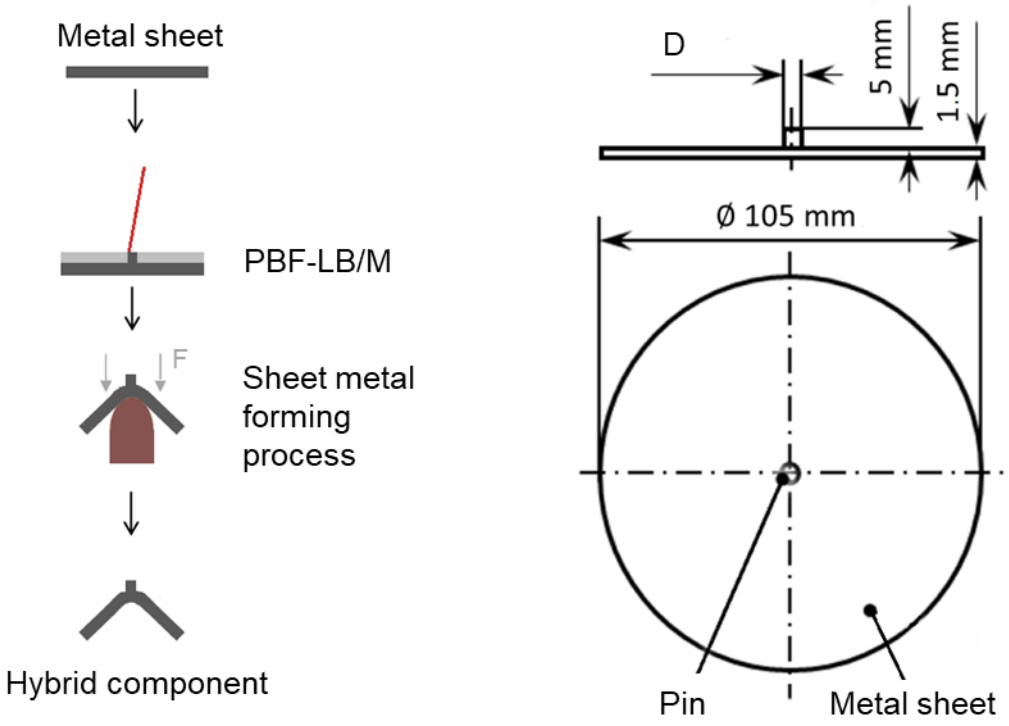

Figure 4.2: Manufacturing process sequence of hybrid components (left) according to [8] and round blank with an additively manufactured element (right) according to [55].

Four variables are chosen for the realization of the different geometries of the specimens: the diameter of the pins *D*, the distance between the pins measured from the centre *L*, the number of pins *NP* and the fillet radius *R* in the transition area between the sheet and the pins. The height of the pins is set to 5 mm. A representation of the geometric parameters can be seen in figure 4.3.

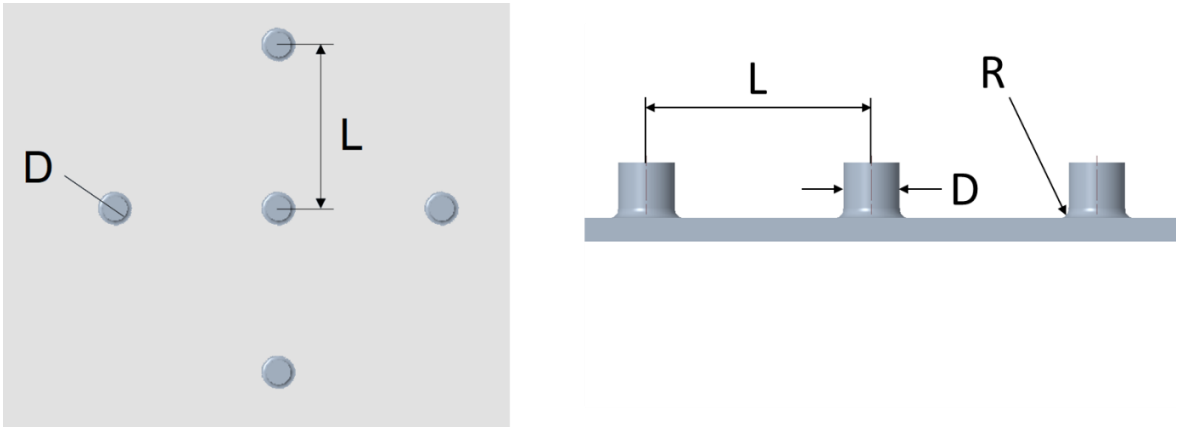

Figure 4.3: Representation of the geometric parameters of the specimens. Top view (left) and front view (right).

To analyse how the formability of the hybrid specimens is affected by the aforementioned parameters, different values of these parameters are chosen. The values chosen for these variables are shown in table 4.5.

Table 4.5: Investigated geometric factors and levels.

Diameter *D* in mm	Distance *L* in mm	Number of pins *NP*	Fillet radius *R* in mm
3	-	0	0.5
5	10	1	1
7	20	5	-

The specimen that has a single pin with a diameter of 5 mm, a height of 5 mm and a fillet radius of 0.5 mm is used as a hybrid reference component. The sheet metal forming process is performed at a drawing depth (*DD*) of 15 mm. Sheet specimens are also tested in order to compare them to hybrid components. Only specimens that do not have additively manufactured elements are tested at a drawing depth of 20 mm. To analyse the influence of temperature on the forming process three different testing temperatures are selected, that are 20 °C, 250 °C and 400 °C. Only the sheet metal specimens and the specimens in reference conditions are formed at a temperature of 250 °C. Among all the different, possible combinations, 43 combinations are chosen, which are listed in the appendix.

4.4.2 Creation of the CAD geometries

The geometries are created using PTC Creo Parametric software. Each geometry is

created twice in order to obtain two identical specimens, which will be subsequently formed at the two different temperatures 20 °C and 400 °C. For each building process, it is possible to create four different specimens, as seen in figure 4.4.

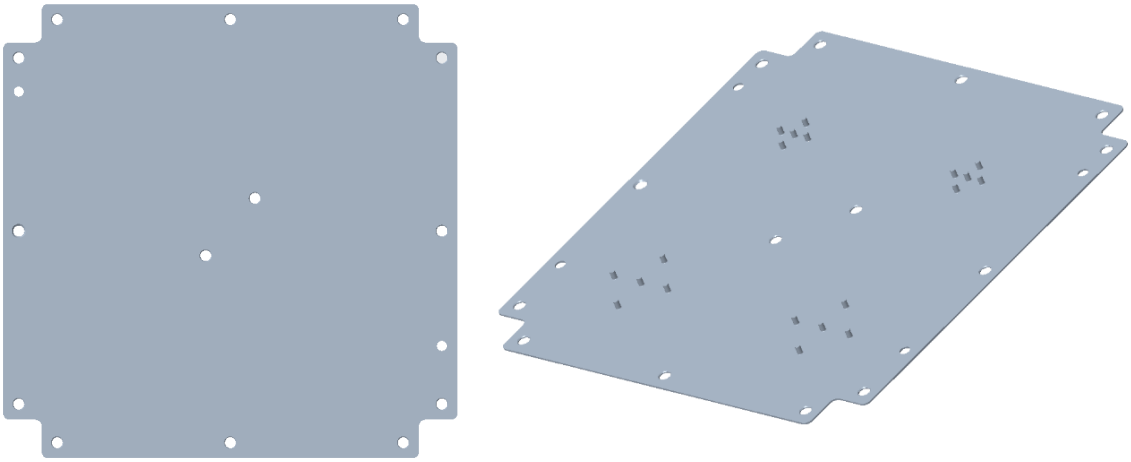

Figure 4.4: Starting sheet on which the pins are built (left). The same metal sheet after the building process (right).

Each sheet has two different types of specimens on the left side. On the right side these geometries are replicated. The geometries are saved in .stl format. This file is subsequently imported into the RDesigner software and it is sliced horizontally into 50 µm thick layers. The cross-section area of the component is built selectively, melting and re-solidifying metal powders in each layer. The file is then saved in .rea format and transferred into the additive manufacturing machine.

4.4.3 Additive Manufacturing building process

The starting sheet from which the different specimens are obtained is attached to a metal substrate plate, which is then inserted into the building chamber. The sheet is oriented on the substrate plate using dowel pins and fixed with screws using a torque of 7 Nm. Different process parameters were tested in order to identify the most suitable parameters to manufacture the specimens. The parameters analysed are the laser power, the focus position and the scan speed. For each of these parameters, three different values were considered. The values of the tested parameters are shown in table 4.6.

Table 4.6: Values of the tested Additive Manufacturing process parameters.

Laser power in W	Focus position	Scan speed in m/s
200	-0.5	0.5
350	-0.35	0.8
500	-0.2	1.1

The aim of this analysis is to identify the adequate set of values of the analysed parameters that allow to manufacture specimens with the highest possible relative density and that do not present a too deep heat affected zone.
First, weld seams on metal sheet made with the Additive Manufacturing technique were analysed. In figure 4.5 it is possible to see some examples of these specimens.

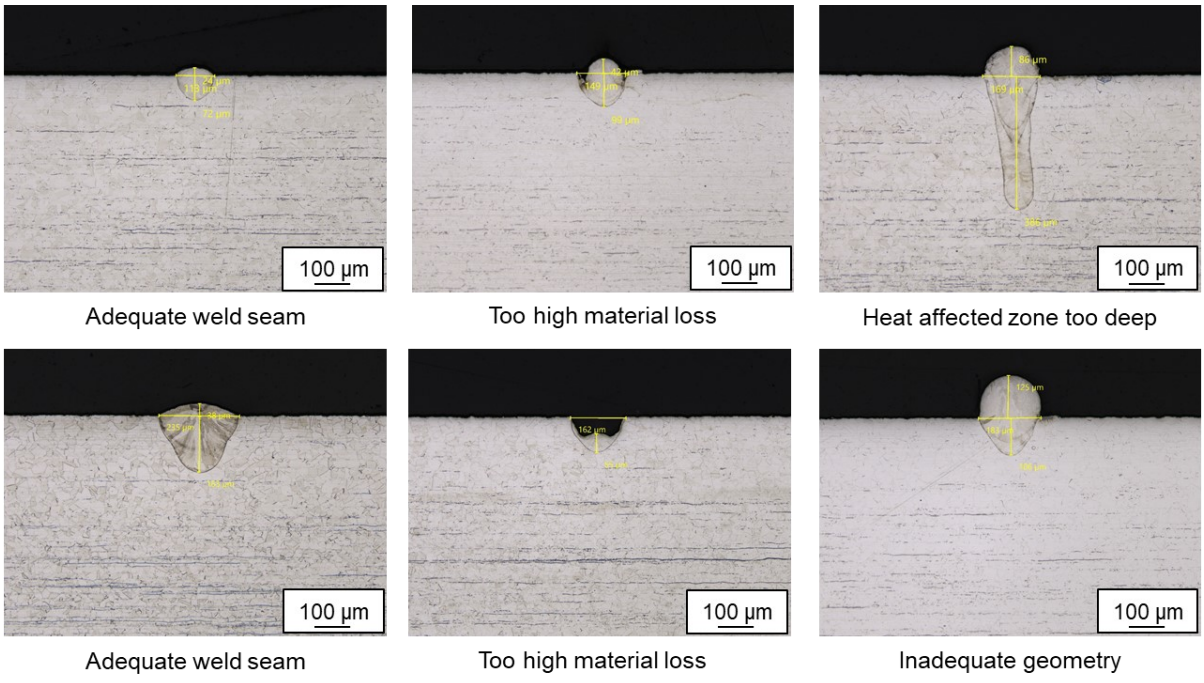

Figure 4.5: Investigations on weld seams made with the Additive Manufacturing technique.

On the left of figure 4.5 examples of suitable weld seams are shown. It is possible to notice that the heat affected zone is not too deep. In the centre it is possible to see examples of weld seams in which there is too much material loss. At the top right it can be noticed an example of a weld seam in which the heat affected zone is too deep, while at the bottom right it is shown an example of inadequate geometry of the weld seam.

Once the best parameters for weld seams were identified, these parameters were used to test additively manufactured elements realized on the metal sheets.
The specimens made with the different sets of values of the parameters were sectioned and analysed with an optical microscope. The relative density of the additively manufactured elements was calculated using a Matlab script.
In figure number 4.6 it is possible to see how the different combinations of values of the parameters adopted lead to obtain different relative density of the pin.

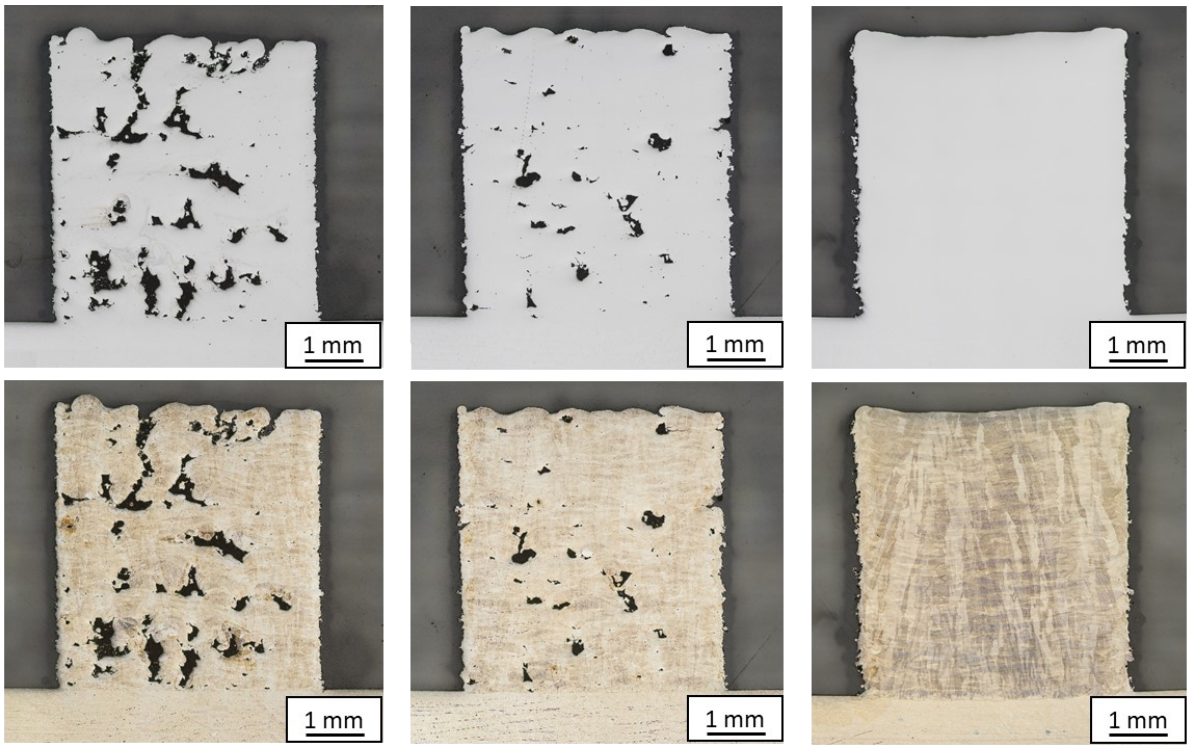

Figure 4.6: Microsections of etched and polished sections of additively manufactured elements built using different sets of process parameters.

On the left of the figure 4.6 there is an example of building parameters not adequate to manufacture the pins, as the relative density obtained is 89.91%.
On the right, instead, it is possible to see an example of suitable parameters for the Additive Manufacturing process, which leads to obtain a relative density of 99.97%.
The parameters used in the process are laser power = 350 W, focus position = -0.5, scan speed = 0.5 m/s. With these parameters it is possible to obtain a relative density of 99.97 %. In figure 4.7, the microsections of an additively manufactured element built with

the beforementioned settings can be seen.

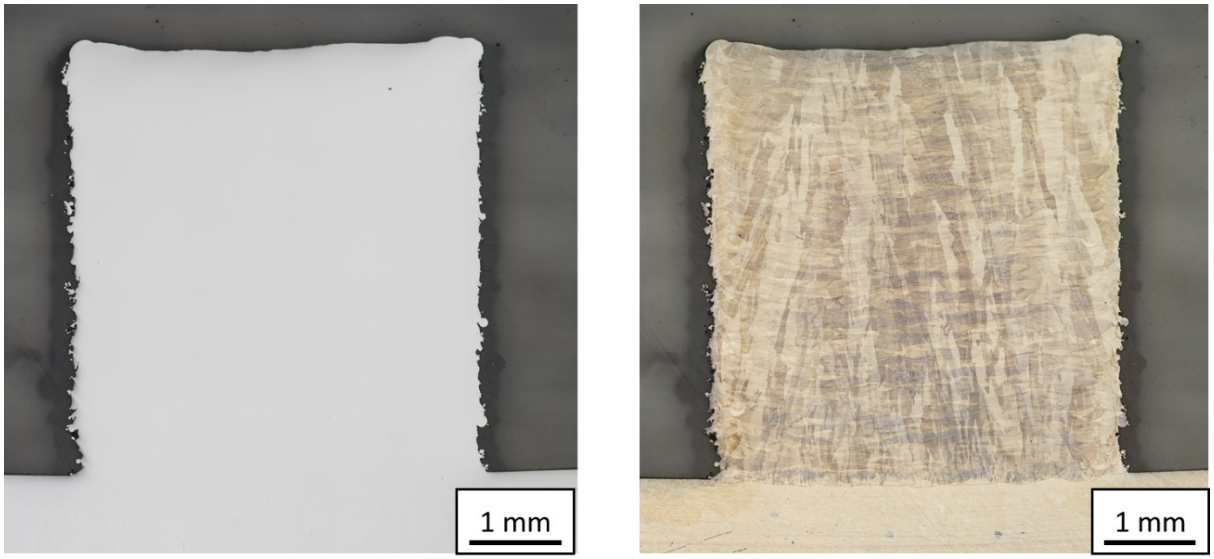

Figure 4.7: A microsection of an etched and polished section of an additively manufactured element built using abovementioned process parameter (left) with its granular microstructure (right).

4.4.4 Laser cut process

The square sheets containing the four different specimens are cut using a laser beam. A centering device is used to perform a circular cut with reference to the middle pin. The edges of the different specimens obtained are subsequently deburred using sandpaper.

4.4.5 Sheet metal forming process

The specimens obtained are then formed. As previously mentioned, the hybrid specimens are formed up to a drawing depth of 15 mm, while the sheet specimens are formed up to a drawing depth of 15 mm and 20 mm. The drawing depth is set using hard stops. To analyse the influence of temperature on the forming process, three different testing temperatures are chosen, that are 20 °C, 250 °C and 400 °C. To reach a certain forming temperature on the tools, higher temperatures are set on the heating element, as the temperature is controlled by temperature sensors inside the tools. To heat the specimens, it is necessary to use an oven, which is located near the press. A thermocouple is placed inside a round blank and this specimen is inserted inside the oven to determine its temperature. It is necessary to adopt some precautions so that the temperature of the specimen does not drop excessively on the way from the oven to the press. For this reason, the specimens are heated up to temperatures higher than the testing temperature. In fact, the temperature of the oven and the time spent inside it are selected so that the internal temperature of the specimen during forming is equal to the chosen testing temperature. The blank holder force of the press is set to 25 kN. The ram

speed on the working stroke is about 4.7 mm/s. The force-displacement curve is recorded for each experiment using a load cell and a displacement transducer.

4.4.6 Optical measurement process

In order to be able to take measurements with the ATOS optical measuring system, the specimens must be coated with a thin and equally distributed layer of white paint. It is necessary to clean the specimens with isopropanol to wash away any dust, before applying the coating. Subsequently, markers are attached to the specimens, as shown in figure 4.6.

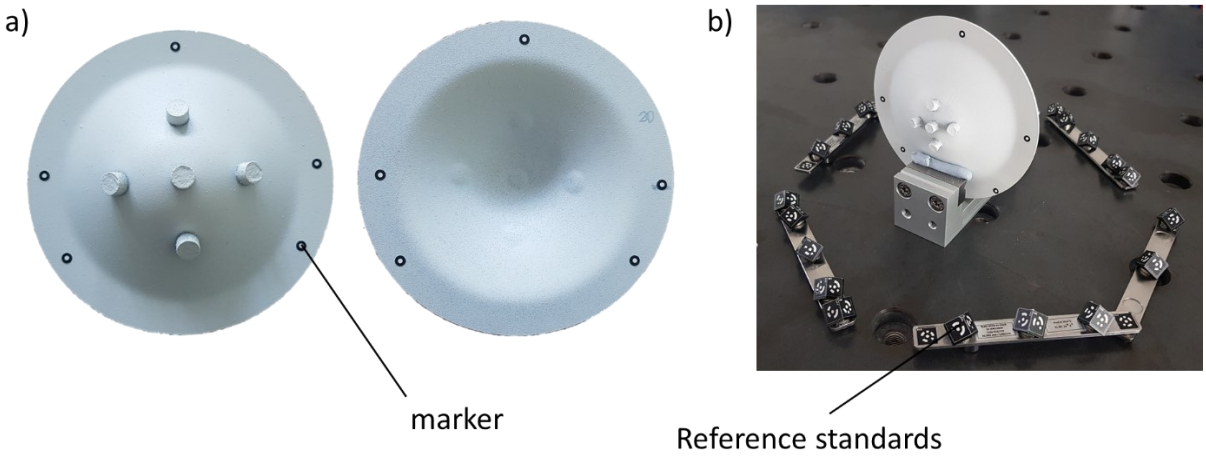

Figure 4.6: a) specimens with markers. b) reference standards used for the optical measurement.

The reference standards are then placed around the component. With the 3D coordinate measuring system TRITOP v.6.2 by GOM GmbH, the markers applied to the component are related to each other and to the reference standards. Finally, the ATOS scanner is used and the measurements of the components are carried out. Several measurements from different angles are required for a three-dimensional analysis of the component. The different measurements are then combined to obtain the final 3D mesh of the components.
The measurement results are analysed using the GOM Inspect Suite 2020 software by GOM GmbH Braunschweig to determine the thickness distribution of the specimens. A first alignment is needed. The X axis is chosen perpendicular to the rolling direction, while the Y axis is chosen parallel. The distribution of the thickness of the sheet is then determined and highlighted with different colours.

5 Results and discussion

The aim of this thesis is the analysis of the influence of the additively manufactured elements on the formability of hybrid components. Specifically, the influence of different geometric parameters of the additively manufactured elements and of the testing temperature are analysed. The thickness distribution of the hybrid specimens is calculated using optical measurements and it is used to analyse the influence of the considered variables on the formability of the components. In fact, an increased thickness reduction results in an earlier failure of the specimens and, thus, in a reduced formability of the components [55], as can be seen in figure 5.1. In this picture it is evident that the fractures arise at the base of the external pins, where the maximum thickness reduction occurs. From the comparison of the thickness distributions of the different manufactured specimens, it is possible to understand the influence of different parameters analysed on the thickness distributions and, thus, on the formability.

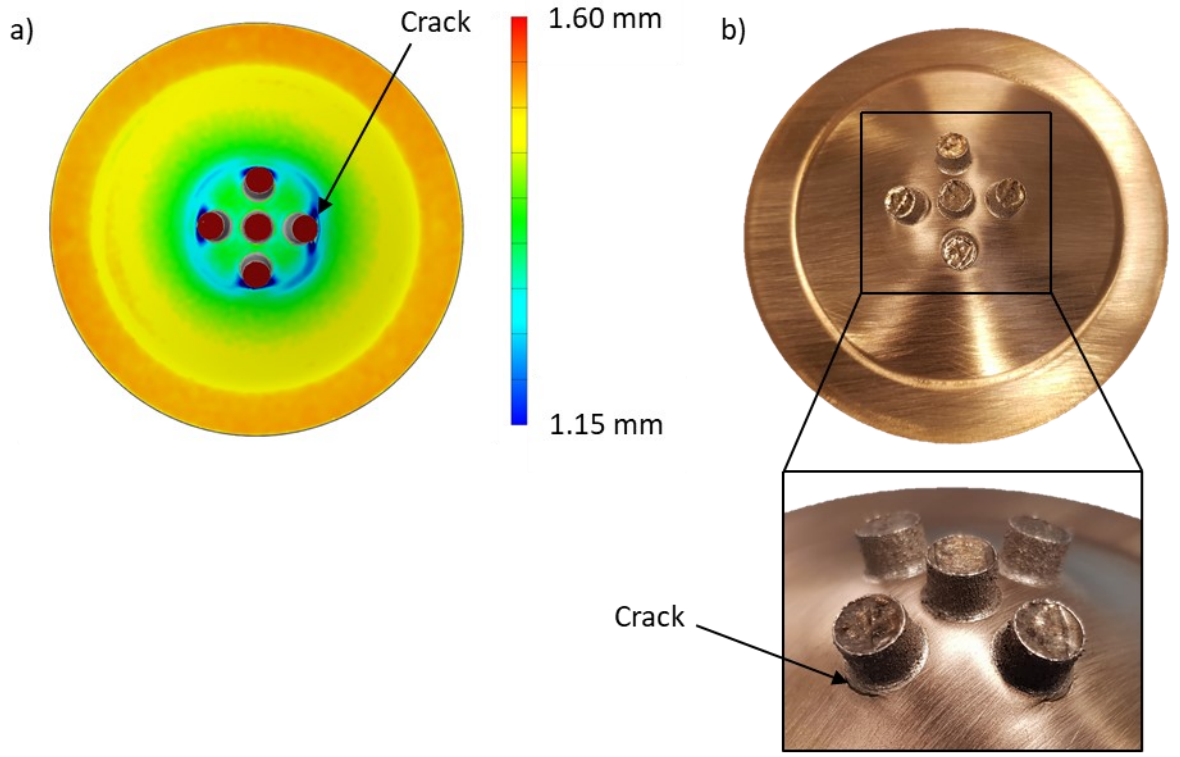

316L; D_0 = 105 mm; s_0 = 1.5 mm;
NP = 5; D = 7 mm; R = 1 mm; DD = 15 mm; T = 400°C; L = 10 mm

Figure 5.1: a) Sheet thickness distribution and b) picture of a failed hybrid specimen with magnification on the crack. Specimen: 316L; D_0 = 105 mm; s_0 = 1.5 mm; D = 7 mm; R = 1 mm; DD = 15 mm; T = 400 °C; L = 10 mm.

For each specimen the minimum thickness and the maximum thickness reduction are calculated for two sections of the specimens, that are section X and Y, respectively perpendicular to and parallel to the rolling direction, as it is shown in figure 5.2. From

the data collected, the graphs of the profile of the specimens and the graphs of their thickness distribution are made. It is possible to see an example of a hybrid component and exemplary graphs for the section X in figure 5.2.

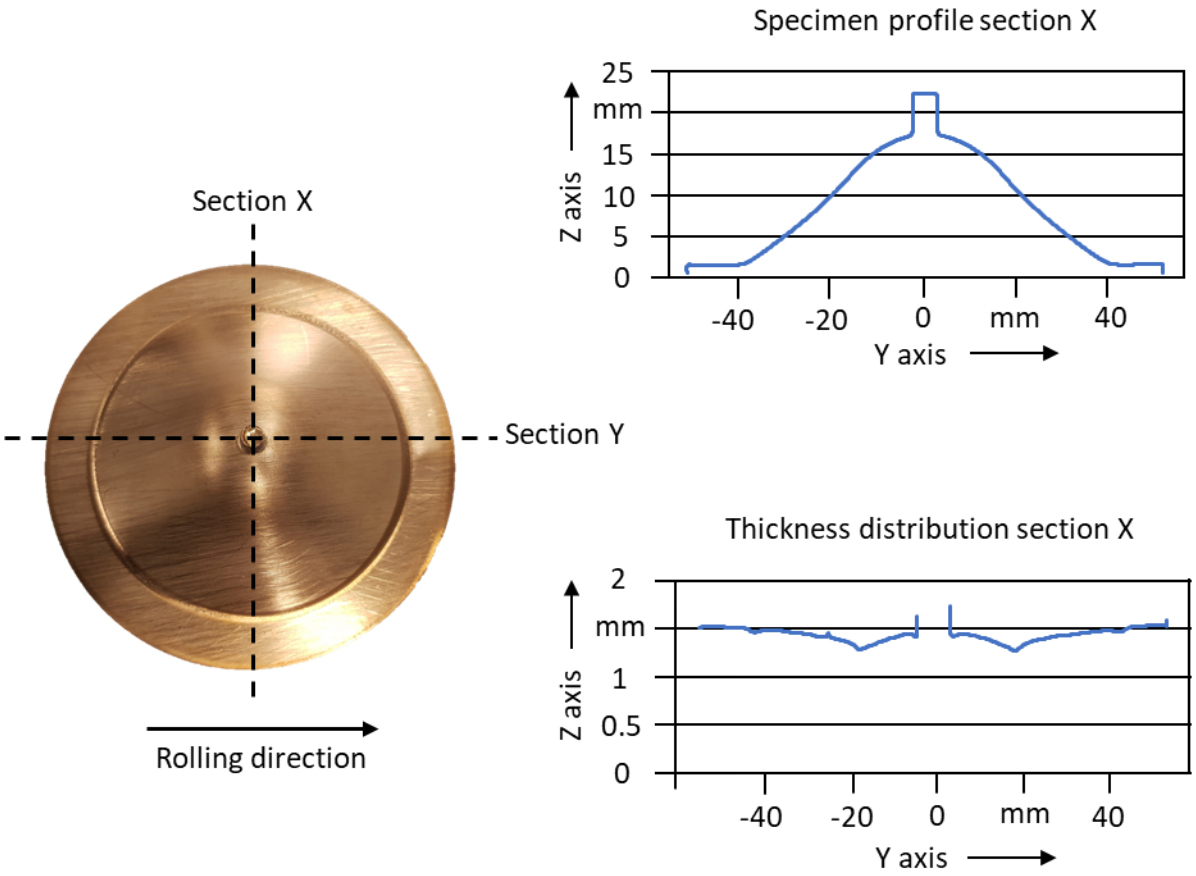

Figure 5.2: Example of a specimen in which the rolling direction, the section X and Y are highlighted (left). Graphs of the profile of section X of the specimen and of the thickness distribution (right).

Cracks occur in metal sheet specimens and hybrid components due to too high stresses that arise during the sheet metal forming process [51]. The failure of the specimens, when it occurs, takes place in different areas, depending on the geometrical configuration of the component analysed. To better understand how the different chosen parameters affect the sheet thickness distribution of the hybrid components, different zones are identified in the specimens, as shown in figure 5.3.

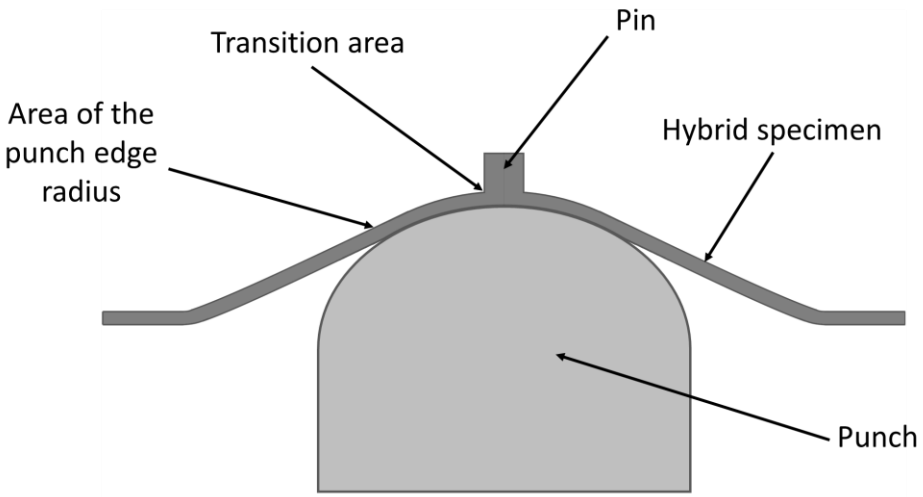

Figure 5.3: Representation of the areas of interest of a hybrid specimen for the further analyses.

The area of the punch edge radius is the area where the contact between the punch and the sheet ends, while the transition area is the area between the sheet and the pins. The area of the punch edge radius and the transition area, as will be explained below, are the areas where the higher thickness reductions are concentrated. For this reason, they are identified as the most critical areas for hybrid components.
In the following sections the influence of the chosen parameters on the thickness distribution of the specimens is analysed. In order to examine how the considered variables influence the formability of the specimens, the position and the value of the minimum thickness of the parts are analysed. To determine the thickness distribution of the formed components, the specimens are measured optically using GOM's ATOS measuring system (see chapter 4.4.6).

5.1 Influence of independent parameters

The influence of the geometric variables of the additively manufactured cylinders on the formability is examined in this section, i.e., the diameter of the pins *D*, the distance *L* between pins measured from centre, the number of pins *NP* and fillet radius *R* in the transition area between the sheet and the pins. The values of the geometric variables considered are shown in table 5.1.

Table 5.1: Investigated geometric factors and levels.

Diameter *D* in mm	Distance *L* in mm	Number of pins *NP*	Fillet radius *R* in mm
3	-	0	0.5
5	10	1	1
7	20	5	-

All hybrid components are formed up to a drawing depth of 15 mm, while the metal sheet specimens are formed up to a drawing depth of 15 mm and 20 mm. The testing temperatures considered are 20 °C, 250 °C and 400 °C. Only the sheet metal specimens and the specimens in reference conditions are formed at a temperature of 250 °C.
First, the force-displacement curves and the influence of the rolling direction on the thickness distribution are examined. Next, the influence of each geometric parameter of the pins and of the testing temperature is analysed. Finally, the effects of the combinations of the different parameters are considered.

5.1.1 Force-displacement curves

The force-displacement curve is recorded for each forming process using a load cell and a displacement transducer. The force of the blank holder is set to 25 kN. The graph in figure 5.4 shows the force-displacement curves of the hybrid specimens with only one pin in the reference conditions, i.e., with D = 5 mm and R = 0.5 mm, formed at the different testing temperatures.

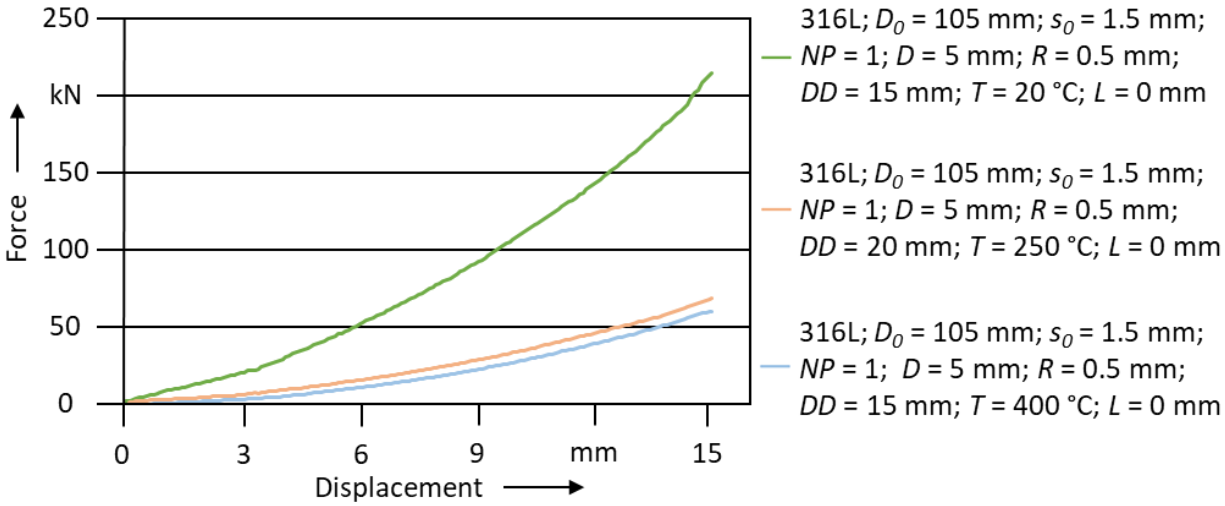

Figure 5.4: Force-displacement curves of hybrid specimens formed at different temperatures. Specimens: 316L; D_0 = 105 mm; s_0 = 1.5 mm; NP = 1; D = 7 mm; R = 1 mm; DD = 15 mm; L = 0 mm. Testing temperature: T = 20°C; T = 250°C; T = 400°C.

From the analysis of the data of the forming processes of the specimens, the required maximum forming forces are obtained. The specimens formed at a temperature T = 20 °C have a maximum forming force of 212.83 ± 5.11 kN, while the specimens formed at a temperature T = 250 °C have a maximum forming force of 67.77 ± 0.73 kN. The third set of specimens, formed at a temperature T = 400 °C, have a maximum forming force of 63.42 ± 1.52 kN. It can be noticed from the graph in figure 5.4 that there is a strong dependence between the maximum forming force and the testing temperature. This is due to the fact that as the testing temperature T rises, the yield strength of the material of the components decreases and, therefore, lower forming forces are required if the testing temperature rises [41].

5.1.2 Influence of the rolling direction

Before proceeding with the analysis of the influence of the geometric parameters of the pins on the formability of the hybrid components, it is necessary to determine the influence of the rolling direction, since the sheet presents anisotropic properties, due to the rolling process [55]. In figure 5.5 the sheet thickness distribution of a hybrid component, examined along the X direction (perpendicular to the rolling direction) and Y direction (parallel to the rolling direction) is shown. The process parameters of the specimen analysed are: 316L; D_0 = 105 mm; s_0 = 1.5 mm; NP = 1; D = 5 mm; R = 1 mm; DD = 15 mm; T = 400 °C; L = 0 mm.

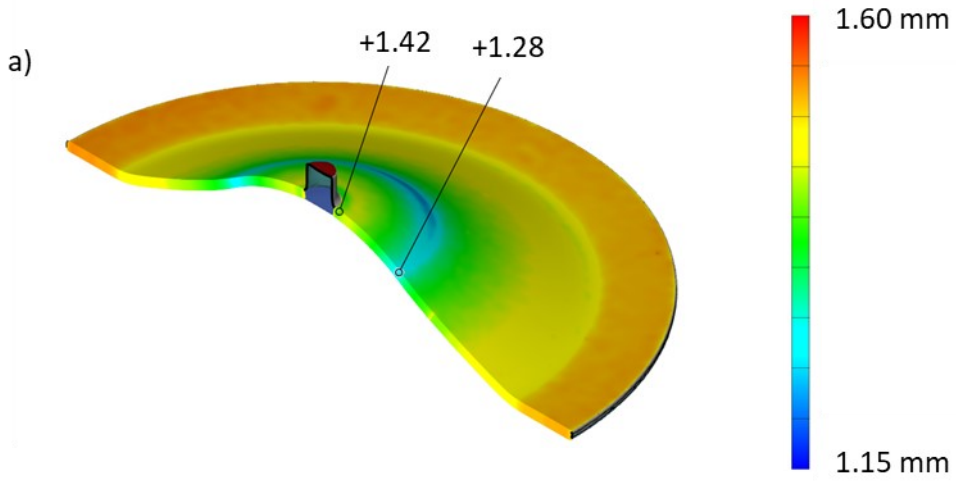

316L; D_0 = 105 mm; s_0 = 1.5 mm; NP = 1; D = 5 mm; R = 1 mm; DD = 15 mm; T = 400°C; L = 0 mm; section X

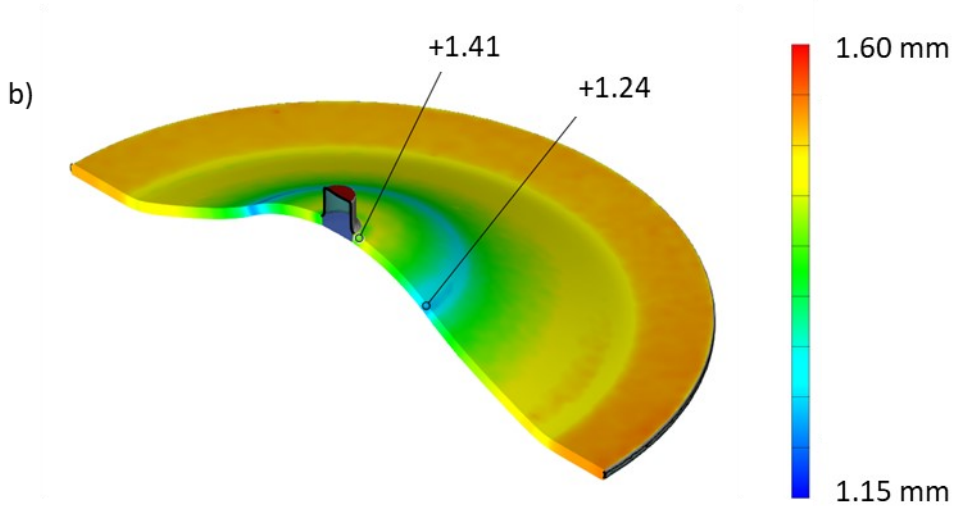

316L; D_0 = 105 mm; s_0 = 1.5 mm; NP = 1; D = 5 mm; R = 1 mm; DD = 15 mm; T = 400°C; L = 0 mm; section Y

Figure 5.5: Sheet thickness distribution of a) section X and b) Y of the specimen: 316L; D_0 = 105 mm; s_0 = 1.5 mm; NP = 1; D = 5 mm; R = 1 mm; DD = 15 mm; T = 400 °C; L = 0 mm.

By examining the thickness distributions of the specimen in the directions parallel and perpendicular to the rolling direction in figure 5.5, it can be noticed that they differ from each other. Regarding the section X in figure 5.5, the minimum thickness is 1.28 mm, while it is 1.24 mm in the section Y, both situated in the area of the punch edge radius. As well as in the area of the punch edge radius, there is also a thinning at the base of the pin in both sections. From the processing of the data obtained from the optical measurements of each specimen, the mean values of the minimum thickness for the sections X and Y of all the formed specimens are calculated. For the sections X the mean value of the minimum thickness is equal to 1.29 ± 0.07 mm, while for the sections Y it is equal to 1.26 ± 0.07 mm. It can be stated, therefore, that the formability of the specimens in the direction parallel to the rolling direction is lower than the one obtained in the perpendicular direction. The material, consequently, is stronger when it is perpendicular to the rolling direction. To get an overview of how the formability of the components can vary according to the rolling direction, the values of the thickness reduction of the sections X and Y of all the components are calculated, as well as the mean value of the thickness reduction. From this analysis the graph in figure 5.6 is obtained.

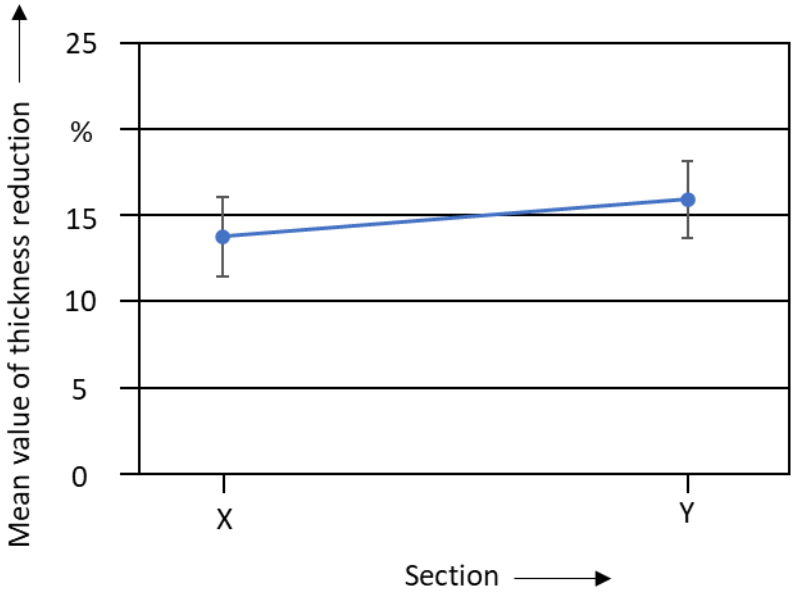

Figure 5.6: Influence of the rolling direction on the sheet thickness reduction of hybrid components and sheet specimens.

The influence of the rolling direction must be considered when manufacturing hybrid components. An explanation for the lower formability of the specimens in the section parallel to the rolling direction is the anisotropy of the material properties of the 316L sheet [55]. During the rolling process, in fact, directional properties are obtained in the resulting sheet, due to the flow of the grains during deformation, which creates a preferred direction of the atomic lattice of the grains [43]. Thus, the tensile strength along the rolling direction is lower than the one perpendicular to the rolling direction and,

consequently, the sheet is weaker in the direction parallel to the rolling direction [55]. For this reason, when manufacturing a hybrid component, it is advisable to place the additively manufactured elements perpendicular to the rolling direction, to avoid a decreasing of the formability of the specimens and not to incur an early failure of the specimens.

5.1.3 Influence of the diameter of the additively manufactured elements *D*

To analyse the influence of the diameter *D* of the additively manufactured elements on the formability of the hybrid components, specimens with different pin diameters are manufactured and formed. The considered diameters of the pins are 3 mm, 5 mm and 7 mm. Figure 5.7 shows examples of these specimens.

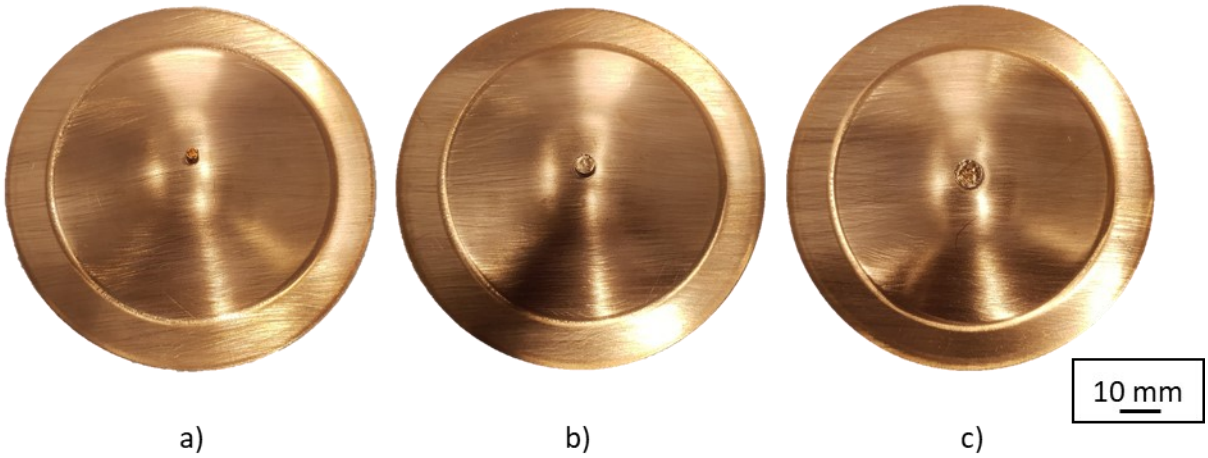

Figure 5.7: Examples of hybrid components with a single additively manufactured pin. a) D = 3 mm, b) D = 5 mm, c) D = 7 mm.

In figure 5.8 the sheet thickness distribution of three hybrid components with the same geometrical configuration but different diameters are shown. The configuration of the specimens is: 316L; D_0 = 105 mm; s_0 = 1.5 mm; NP = 1; R = 1 mm; DD = 15 mm; T = 400°C; L = 0 mm. To better highlight the influence of the diameter of the pins on the formability of the components, the sections Y of the specimens are taken as a reference, i.e., the ones where it is easier to see a clear influence on the thinning of the components when the values of the diameter vary.

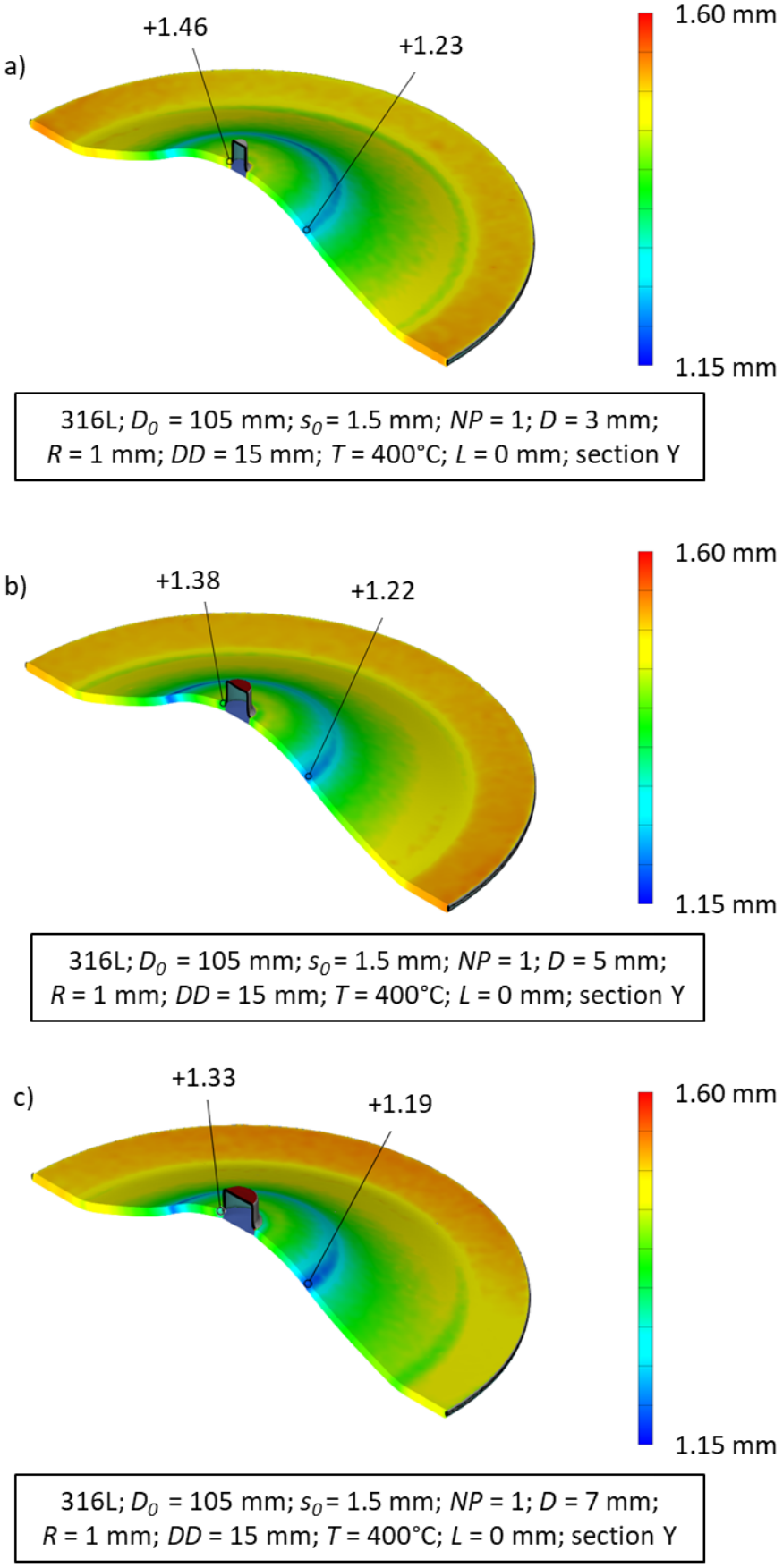

Figure 5.8: Sheet thickness distribution of three hybrid components in which only the diameter is varied: a) D = 3 mm, b) D = 5 mm, c) D = 7 mm. Specimens: 316L; D_0 = 105 mm; s_0 = 1.5 mm; NP = 1; R = 1 mm; DD = 15 mm; T = 400°C; L = 0 mm.

In figure 5.8 the areas of highest thinning are concentrated in the area of the punch edge radius and in the transition area. The component with D = 3 mm has a minimum thickness of 1.23 mm, the specimen with D = 5 mm has a minimum thickness of 1.22 mm, while the specimen with D = 7 mm has a minimum thickness of 1.19 mm. The minimum thickness occurs for all the components in figure 5.8 in the area of the punch edge radius. From the processing of the data obtained the mean values of the minimum thickness of the specimens with different diameters are calculated. For the specimens with D = 3 mm the mean value of the minimum thickness is equal to 1.29 ± 0.08 mm, for the specimens with D = 5 mm it is equal to 1.27 ± 0.06 mm and for the specimens with D = 7 mm it is equal to 1.26 ± 0.06. It is possible to affirm that the presence of the additively manufactured element has an influence on the sheet thickness distribution and, thus, on the formability of the components. As the diameter of the additively manufactured elements increases, a reduction in the formability of the component during the forming process is observed. To better understand the influence of the diameter on the thickness reduction of the parts, the graph in figure 5.9 is made.

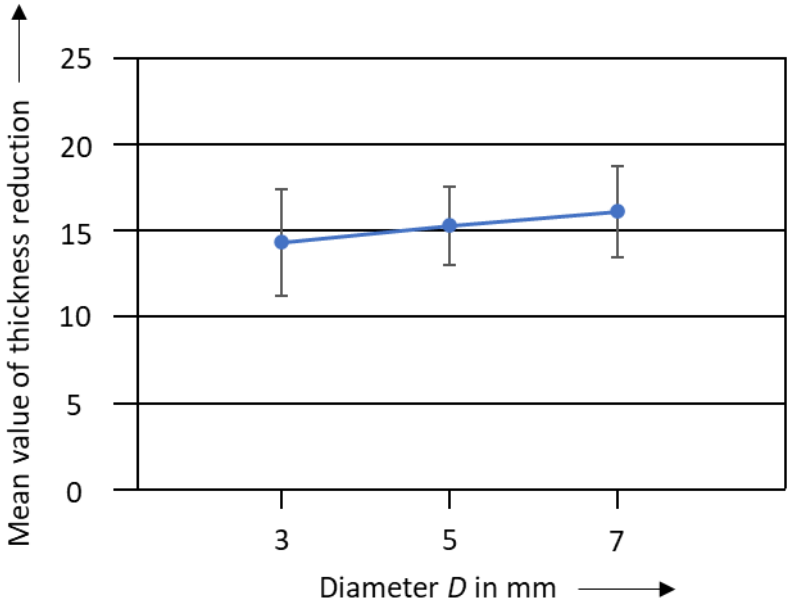

Figure 5.9: Influence of the diameter D on the sheet thickness reduction of hybrid components.

The two critical areas regarding the thinning of the components when the diameter D varies are the transition area and the area of the punch edge radius. One of the possible reasons for the higher thinning of the sheet of the hybrid components in the area of the punch edge radius is the loss of contact between punch and sheet [55]. As the displacement of the punch increases during the forming process, the component wraps around the punch when it is stretched [55]. The resulting friction between punch and sheet hampers the flow of the material and causes the thinning of the sheet at the edge of contact between punch and sheet [55]. The second critical area regarding the thinning of the hybrid component sheet is the transition area. One of the possible

reasons of the lower formability of hybrid components with larger pin diameter is the stiffened area under the cylinders increasing with increasing diameter [55]. As before mentioned, cracks are due to excessive stresses, which occur during the forming process and lead to the thinning of the sheet [51]. As can be seen in the schematic in figure 5.10, there is no full contact in the centre of the specimen during the forming process, because of the high stiffness of the pin [55].

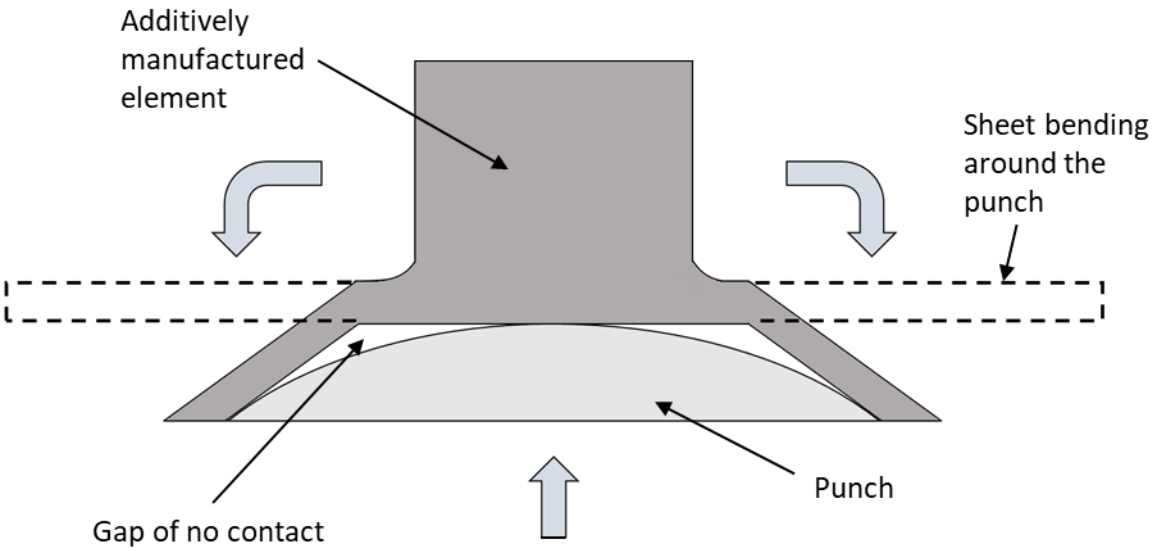

Figure 5.10: Schematic of the hybrid component bending around the punch. According to [55].

If the diameter of the additively manufactured element increases, a larger stiffened area and a bigger gap of no contact is obtained. In figure 5.11 the ring of the non-contact area around the centre of the additively manufactured element and the contact area of the specimens above analysed are shown.

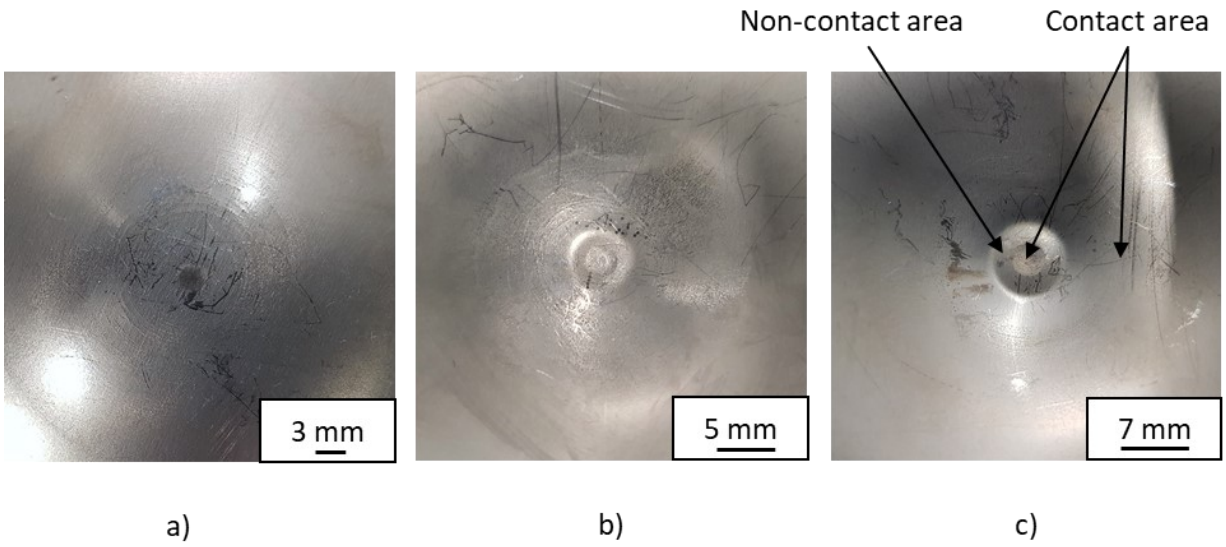

Figure 5.11: Backside of hybrid components with a single pin and a) D = 3 mm, b) D = 5 mm, c) D = 7 mm showing the non-contact area and the contact area between punch and component. Specimens: 316L; D_0 = 105 mm; s_0 = 1.5 mm; NP = 1; R = 1 mm; DD = 15 mm; T = 400°C; L = 0 mm.

The area of the component consisting only of metal sheet is more easily formable than the areas consisting of metal sheet plus cylinder, since the stiffness of the sheet is lower than the one of the sheet plus the pin [51]. As can be seen in figure 5.12, if the pin diameter increases there is a higher ratio of the component area with pin to the area without pin [51], and, consequently, a larger stiffened area.

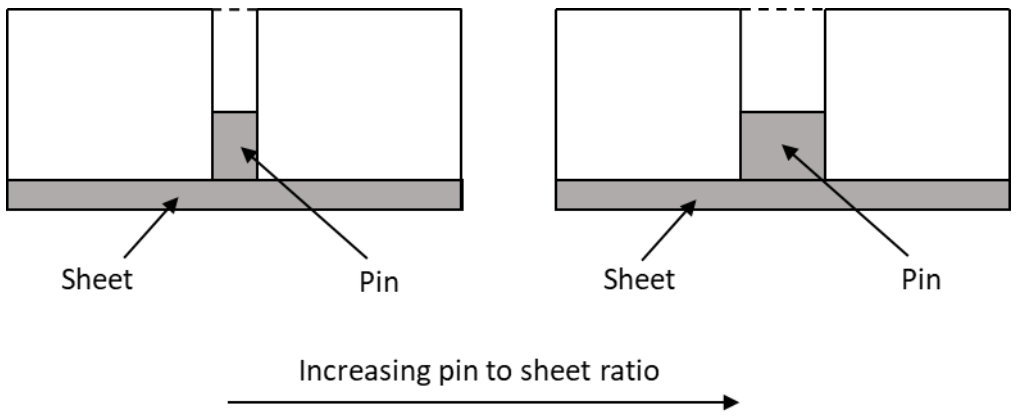

Figure 5.12: Explanation of the pin to sheet ratio, i.e., of the ratio of the component area with pin to that without pin, when the diameter D is varied. According to [51].

As the pin to sheet ratio increases, a concentration of the forming stresses on less material occurs, i.e., the area without pins, and, therefore, higher thickness reductions arise in this area [51]. The loss of contact between the punch and sheet during the forming process, due to the high stiffness of the pin, leads to bending stresses acting

on the sheet [55]. Consequently, tensile stresses arise in the transition area between the sheet and the pins, which can lead to necking and to the possible formation of cracks at the base of the pin [55]. The tensile stresses increase as the diameter of the pin increases, as larger non-contact gaps and, consequently, higher bending stresses arise. These observations are consistent with the results of [50], where sheet metal forming processes of single-pin hybrid components are modelled with numerical simulations to analyse the stress state occurring in the specimens. According to this research, the highest stresses are found in the transition area at the base of the pin [50]. It can be stated, thus, that additively manufactured elements have a stress concentrating effect, causing an increased necking and a decreased formability of the hybrid components [50]. Besides, the high surface roughness at the base of the pins, arising from the Additive Manufacturing process, too, has a stress concentrating effect and it is a starting point for crack initiation [50]. The presence of the additively manufactured element, however, causes an increased thinning also in the area of the punch edge radius. A possible explanation for this behaviour is that the tensile stresses that arise at the base of the cylinders also affect the state of stress that is created in the punch edge area, increasing the total tensile stress acting in this area and leading to greater thinning. Therefore, it is essential to select the most suitable value of the diameter of the pins when manufacturing hybrid components, in order to obtain the suitable formability and do not incur a premature failure of the specimens.

5.1.4 Influence of the fillet radius of the additively manufactured element *R*

Another relevant parameter to be analysed is the fillet radius *R* in the transition area between the metal sheet and the pins. The aim of this section is to analyse how the increase of the values of *R* affects the forming behaviour of the hybrid components. In figure 5.13 the sheet thickness distribution of two hybrid components with the same geometrical configuration, but different fillet radius *R*, are shown. The geometrical configuration of the specimens is: 316L; D_0 = 105 mm; s_0 = 1.5 mm; *NP* = 1; *D* = 5 mm; *DD* = 15 mm; *T* = 400°C; *L* = 0 mm. The section Y of the specimens is taken as a reference.

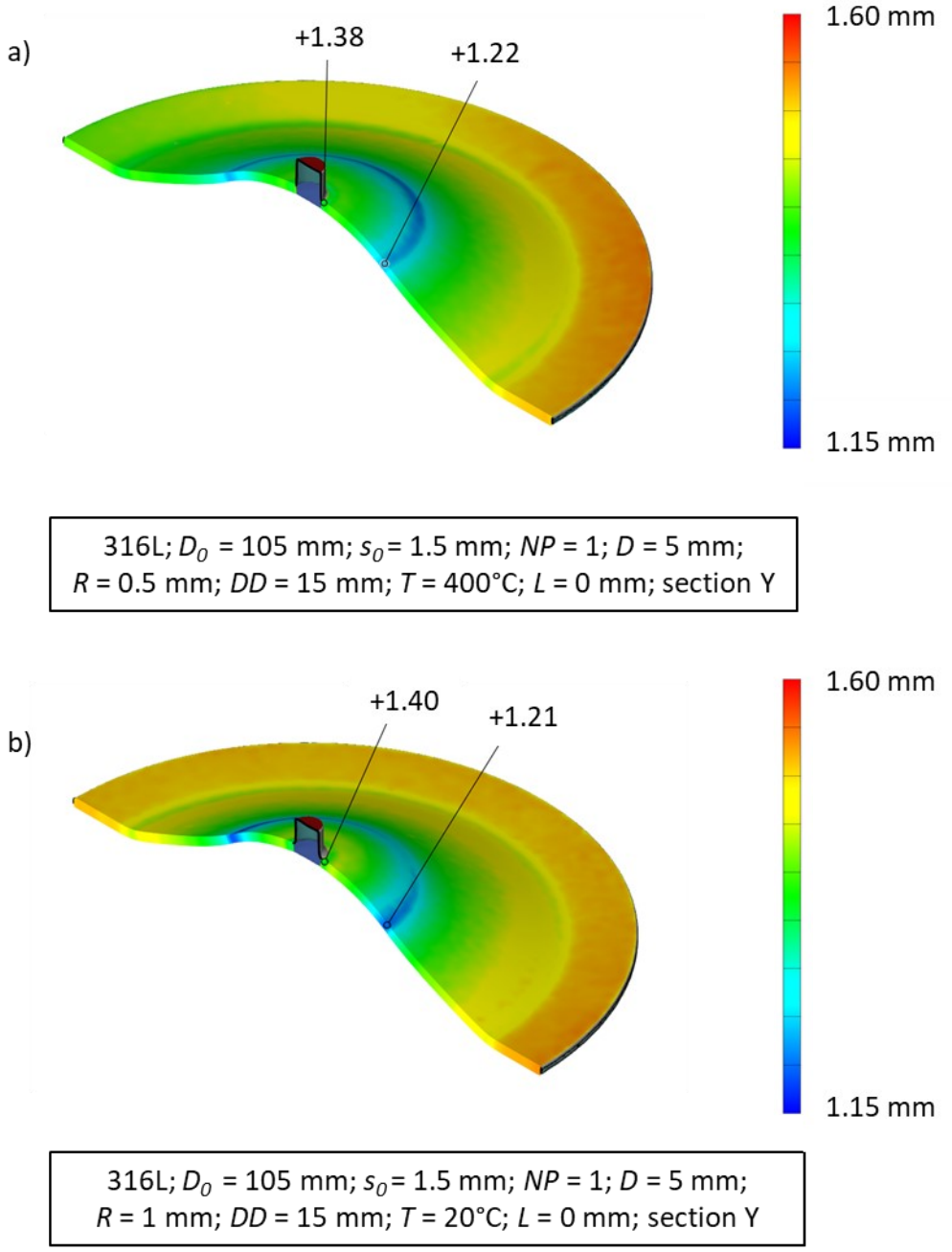

Figure 5.13: Sheet thickness distribution of two hybrid components in which only the fillet radius R is varied: a) R = 0.5 mm and b) R = 1 mm. Specimens: 316L; D_0 = 105 mm; s_0 = 1.5 mm; NP = 1; D = 5 mm; DD = 15 mm; T = 400°C; L = 0 mm.

In picture 5.13 the analysed specimens with R = 0.5 mm and R = 1 mm have respectively a minimum thickness of 1.22 mm and 1.21 mm. In both cases the minimum thickness for the analysed configuration lies in the area of the punch edge radius. To analyse how the parameter fillet radius R influences the formability of the manufactured hybrid component, the data of the minimum thicknesses reached by the specimens with R = 0.5 mm and R = 1 mm are processed. Specimens with R = 0.5 mm have a mean minimum thickness of 1.27 ± 0.06 mm, while those with R = 1 mm have a mean minimum thickness of 1.26 ± 0.07 mm. It is, therefore, possible to state that, as the fillet

radius increases, the formability of the manufactured components decreases. In the graph in figure 5.14 the influence of the fillet radius *R* on the sheet thickness reduction of hybrid components is shown.

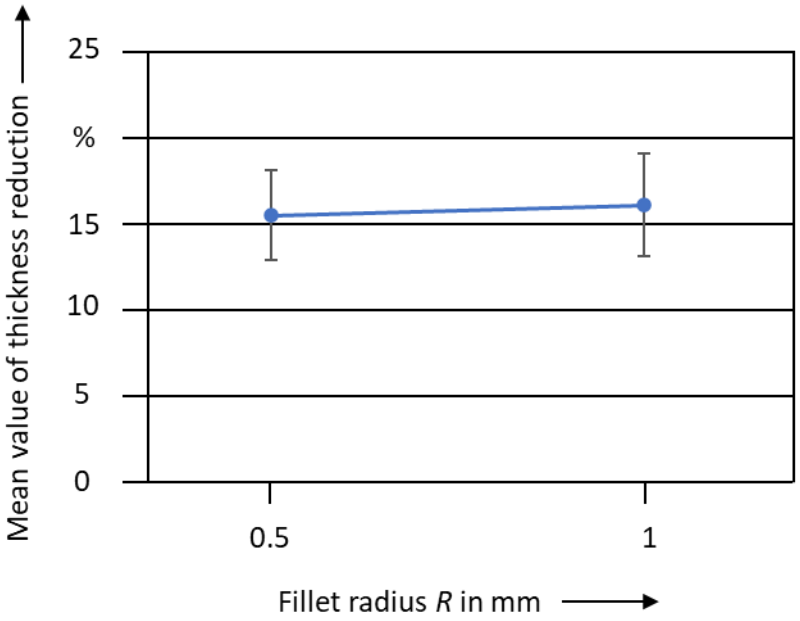

Figure 5.14: Influence of the fillet radius *R* on the sheet thickness reduction of hybrid components.

The reason for the decrease in formability with increasing *R* values could be that, by increasing the fillet radius, the stiffness of the component becomes higher in the area covered by the cylinders and their fillet radius. However, as can be seen in the graph in figure 5.14, the influence of the fillet radius on the formability is not as strong as the one occurring when the diameter varies. A possible reason for this behaviour can be that the increase in stiffness, due to a bigger fillet radius, is not as high as in the case of the increase in diameter. The effect of having a wider stiffened area, as explained before, is the reduction of the formability of the component during the forming process, because of the bigger non-contact area that occurs and, consequently, of the higher tensile stresses that occur at the base of the pins. The fillet radius, however, has the function of reducing the stress concentration effect in the transition area between the pins and the sheet and allows the component to withstand fatigue stresses [51]. It is necessary, therefore, to choose the suitable value of the fillet radius to be inserted, to reach a trade-off between the required formability of the components and the stress concentration effect. Another important aspect to consider is the high surface roughness of the fillet radius, that arises from the Additive Manufacturing process. The failure of the hybrid components at the base of the pins is enhanced by a high surface roughness, as it leads to a stress concentration effect and can be the cause of the initiation of cracks [50]. It is, therefore, necessary to adopt suitable parameters of the Additive Manufacturing process, which allow to reach a low surface roughness [50].

5.1.5 Influence of the number of the additively manufactured elements *NP*

In this section the influence of the number of pins *NP* on the formability of the hybrid components is examined. In figure 5.15 three components in which only the number of pins *NP* is varied are shown.

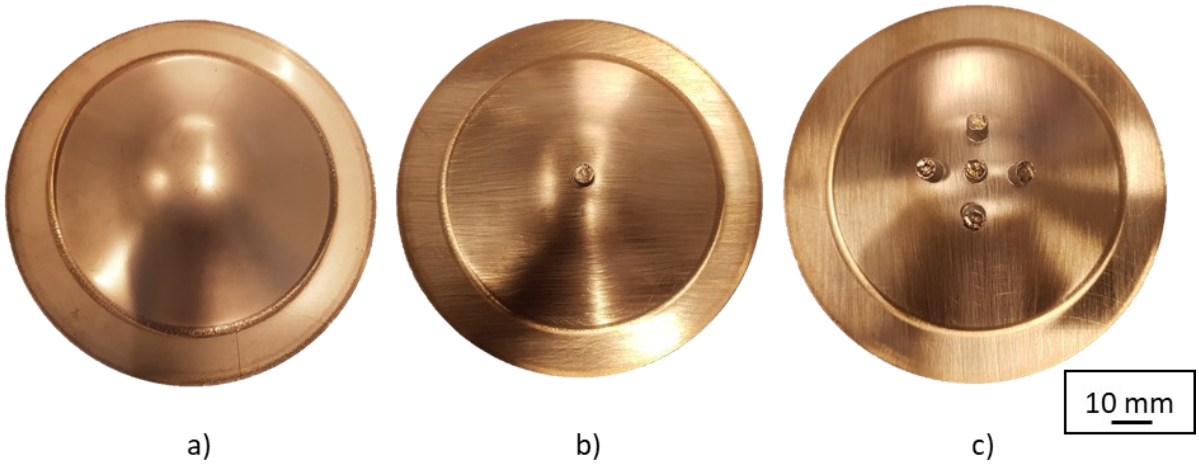

Figure 5.15: Example of hybrid components with a) no pins, b) one pin and c) five pins.

The section Y of the specimens is taken as a reference for the analysis of the thickness distributions. From the analysis of the results of the optical measurements, a strong influence of the testing temperature on the sheet thickness distribution of the specimens with different number of pins is noted. For this reason, in the following figures, the sheet thickness distribution of three specimens with different number of pins *NP*, formed at 20 °C and 400 °C, are shown. In figure 5.16 the thickness distributions of specimens formed at 20°C, are illustrated.

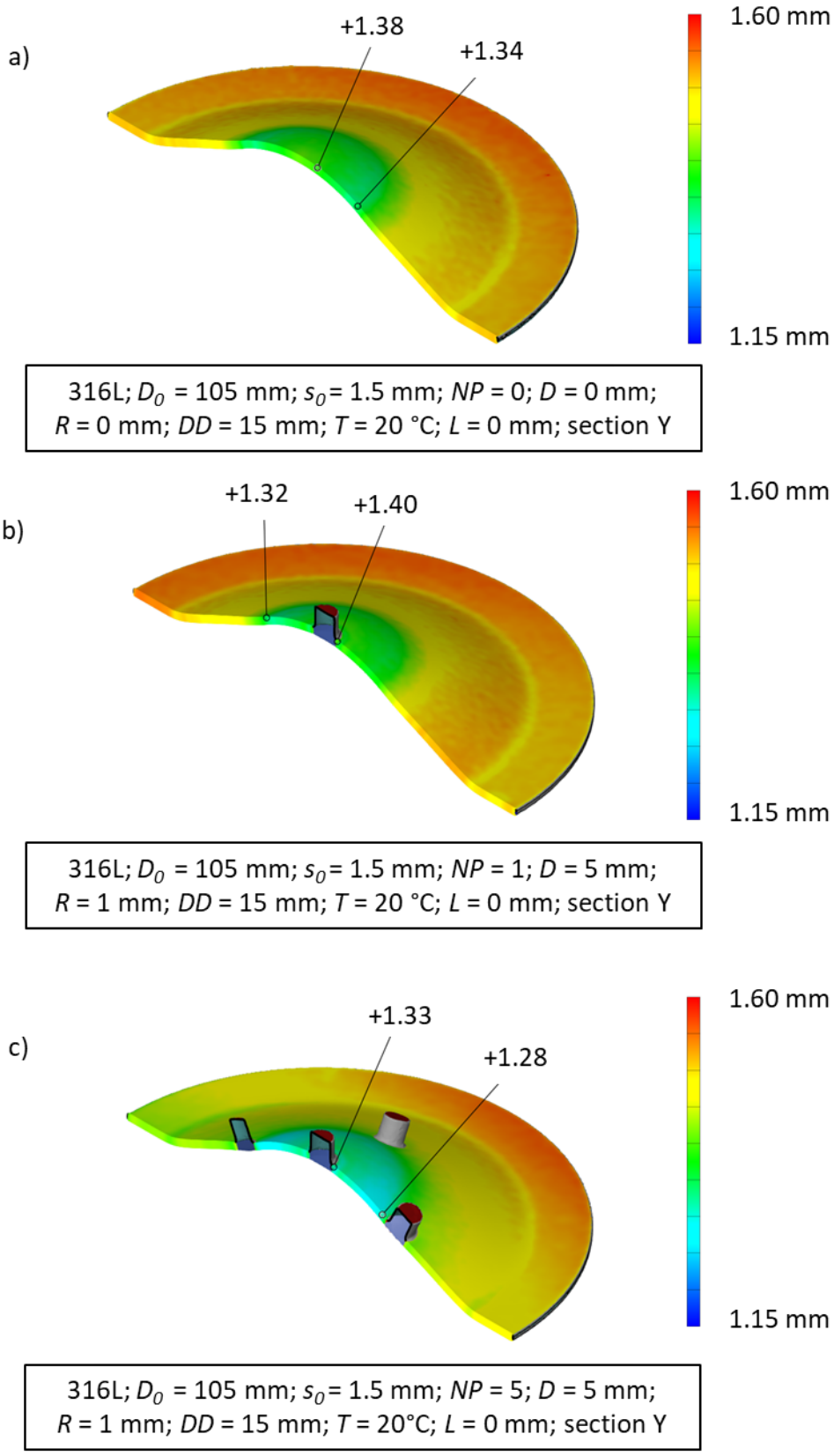

Figure 5.16: Sheet thickness distribution of three specimens in which only the number of pins NP is varied: a) NP = 0, b) NP = 1 and c) NP = 5. Specimens: 316L; D_0 = 105 mm; s_0 = 1.5 mm; D = 5 mm; R = 1 mm; DD = 15 mm; T = 20 °C.

In figure 5.16 it can be noticed that the minimum thickness reached for the specimen with no pin is 1.34 mm, with *NP* = 1 it is 1.32 mm and for the specimen with *NP* = 5 it is 1.28 mm. In the three components analysed the maximum thinning occurs in the area of the punch edge radius. Unlike the case of the specimen with one pin, in the case of the specimen with five additively manufactured elements it is noticed that the thickness reduction at the base of the external cylinders is not distributed evenly but it is concentrated on the side of the base closer to the area of the punch edge radius. From the analysis of the data obtained for all the formed components with different number of pins, the mean values of the minimum thickness are calculated. For sheet specimens the mean value of the minimum thickness is 1.27 ± 0.09, for hybrid specimens with one pin it is 1.29 ± 0.05, while for those with five pins it is 1.25 ± 0.06. It can be deduced that the formability of the components is influenced by the number of additively manufactured cylinders *NP*. In the graph in figure 5.17 the influence of the number of pins *NP* on the sheet thickness reduction of the components is shown.

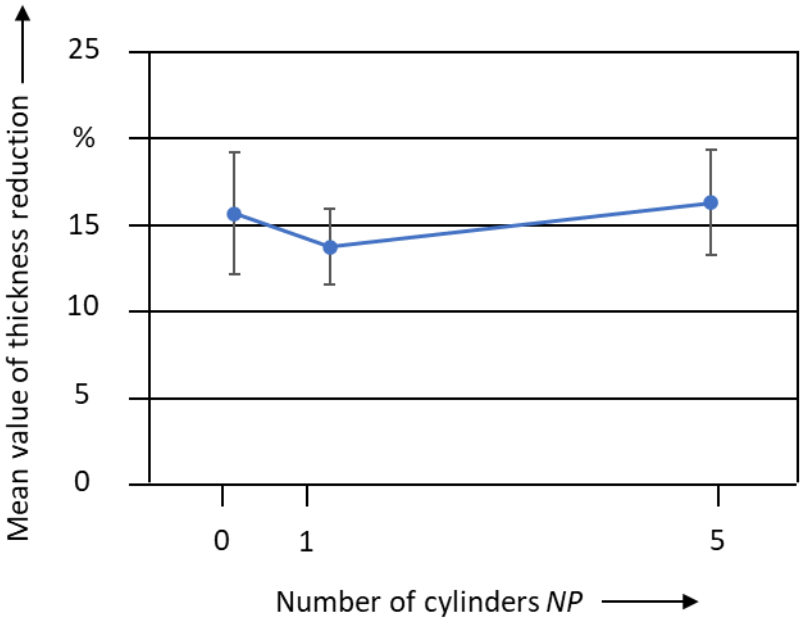

Figure 5.17: Influence of the number of pins *NP* on the sheet thickness reduction of the specimens.

As can be seen in the graph in figure 5.17, the sheet specimens have a mean value of the thickness reduction higher than the one of the specimens with one pin, but lower than the one of the specimens with five pins. To understand the reason for this behaviour, the thickness distribution of the specimens with the same geometrical configuration, but formed at a temperature of 400 °C, are shown in figure 5.18.

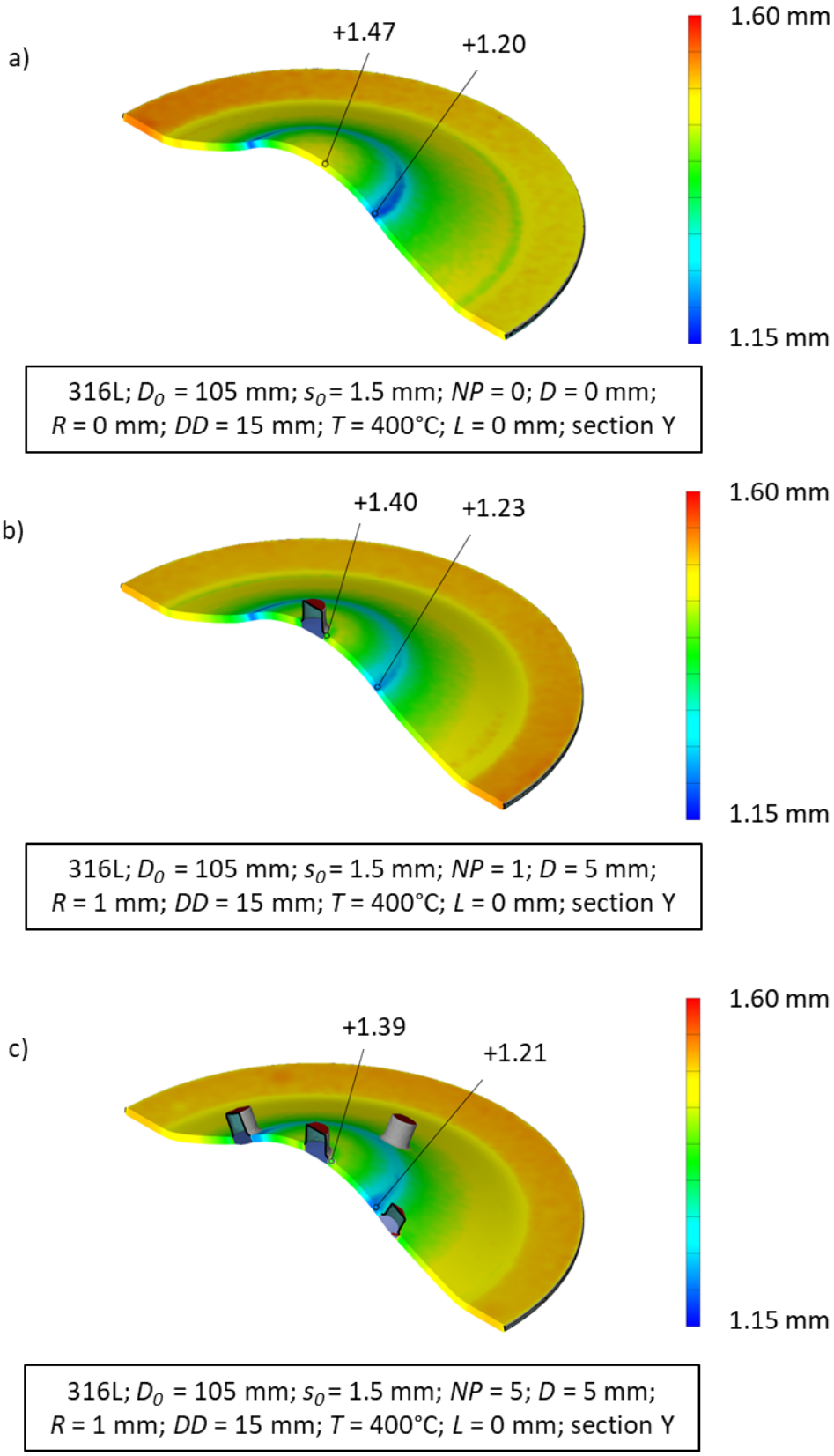

Figure 5.18: Sheet thickness distribution of specimens in which only the number of pins NP is varied: a) NP = 0, b) NP = 1 and c) NP = 5. Specimens: 316L; D_0 = 105 mm; s_0 = 1.5 mm; D = 5 mm; R = 1 mm; DD = 15 mm; T = 400 °C.

In the figure 5.18 the sheet specimen has a minimum thickness of 1.20 mm, in the specimen with *NP* = 1 the minimum thickness is 1.23 mm and in the specimen with *NP* = 5 it is 1.21 mm. As in the case of the above analysed specimens, formed at 20 °C, also in the specimens formed at 400 °C the maximum thinning occurs in the area of the punch edge radius.
It can be noticed that, when using low testing temperatures, the formability of sheet specimen is higher than the one of the specimens with one and five pins. In the case of high forming temperatures, on the other hand, the formability of the sheet specimen is lower than the one of the specimens with one and five pins.
One possible explanation for the lower formability of the specimens with more pins is the increased pin to sheet ratio. As can be seen in figure 5.19, as the number of pins increases, the area of the component which has a higher stiffness becomes wider and, consequently, a decrease in the formability of the hybrid components is obtained [51].

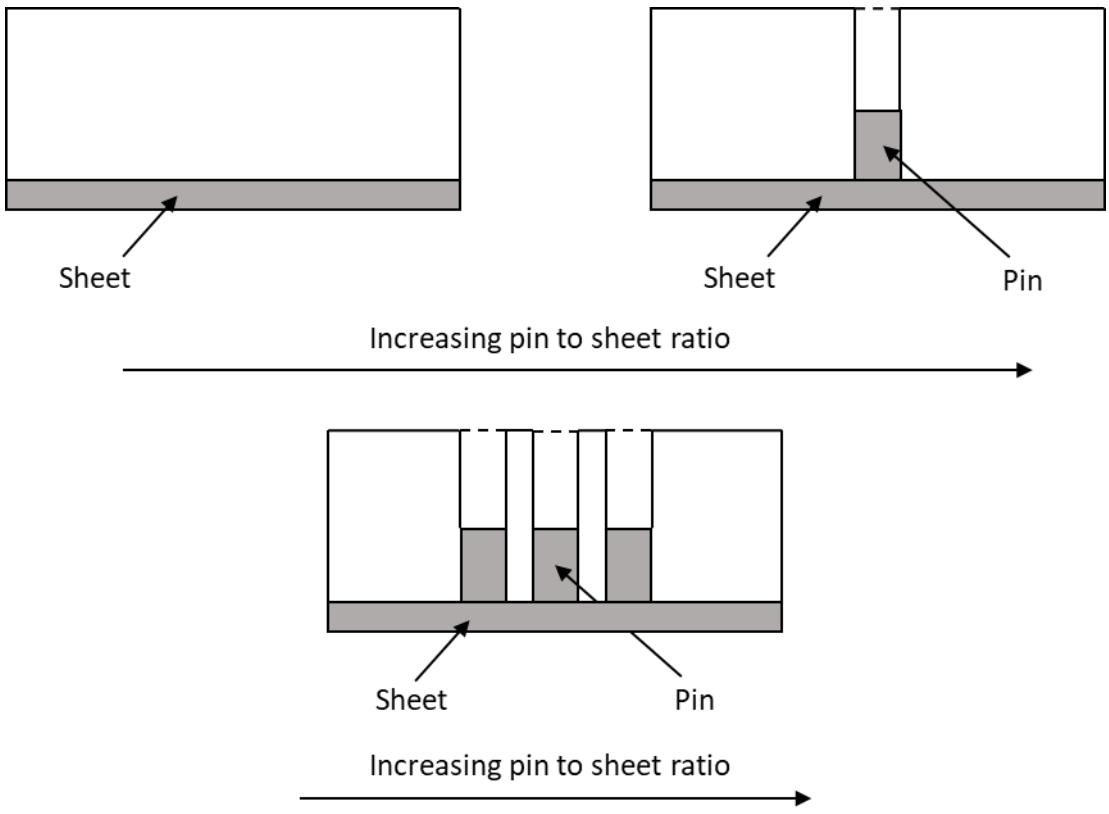

Figure 5.19: Explanation of the pin to sheet ratio, i.e., of the ratio of the component area with pin to that without pin, when the number of pins *NP* is varied. According to [51].

Thus, the effect of increasing the number of additive manufactured elements *NP* is similar to the effect of increasing the diameter *D*, when the testing temperature is low. The same effect can be seen in the specimens with one and five pins formed at high temperature. One explanation for the higher mean value of the thickness reduction of the sheet

specimens than the mean value of the thickness reduction of the specimens with one pin is the occurrence of residual stresses and microstructural changes due to the Additive Manufacturing process [51]. The combination of PBF-LB/M and sheet metal forming technologies to manufacture hybrid components leads to the production of parts with different microstructures and residual stresses [51]. As a consequence, a gradient of mechanical properties between the additively manufactured elements and the sheet arise, which lowers the formability of the components [51], as can be seen in the specimens tested at room temperature (figure 5.16). In figure 5.20 a microsection of an etched and polished section of an additively manufactured element with its granular microstructure is shown.

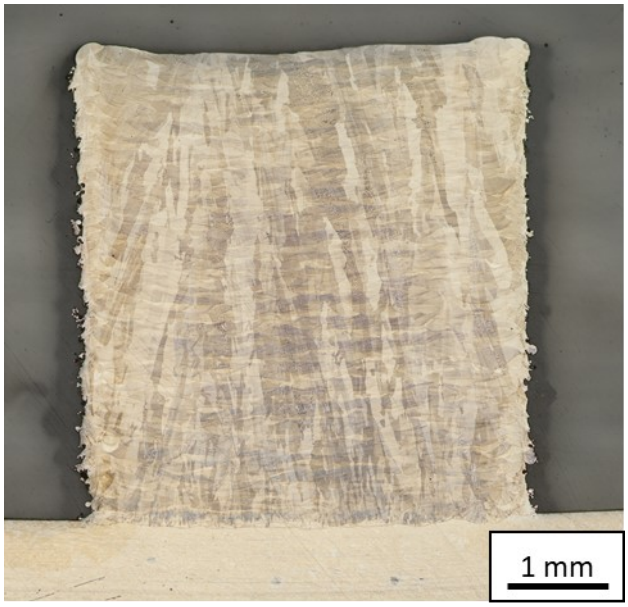

Figure 5.20: A microsection of an etched and polished section of an additively manufactured with its granular microstructure.

The residual stresses can be reduced and the gradient of mechanical properties can be smoothened by using adequate parameters for the Additive Manufacturing processes and adequate heat treatments [51]. If the testing temperature increases, it is possible to assume that the effect on the hybrid specimen is similar to that of a heat treatment, i.e., to reduce residual stresses and smoothen the gradient of mechanical properties, which leads to a higher formability.
In the case of the specimen with one pin, high stresses arise at the base of the additively manufactured element during the forming process. The total stress in the transition area, however, might be reduced due to the decrease of residual stresses. Consequently, also the state of stress occurring in the punch edge area might be reduced. Therefore, it is possible to assume that the stresses acting in the punch edge area when the specimens with one pin are formed at high temperatures, are lower than those occurring when the specimens are formed at room temperature. In the sheet specimens, on the other hand, higher stresses are concentrated in the punch edge area during the forming process,

since there is no pin that concentrates the stresses at its base. Due to this higher concentration of stresses and to the decrease in yield strength, because of the increased testing temperature, the specimens will show a greater thinning in this area and, therefore, a higher mean value of thickness reduction than the one of the specimens with one pin. For this reason, attention must be paid in choosing the suitable testing temperature. In conclusion, by increasing the number of pins it is possible to increase the geometrical complexity of the hybrid components, with the drawback of obtaining a lower formability.

5.1.6 Influence of the distance *L*

This section determines the influence of the distance *L* among the pins, measured from the centre. Figure 5.21 shows the images of two specimens with *L* = 10 mm and *L* = 20 mm.

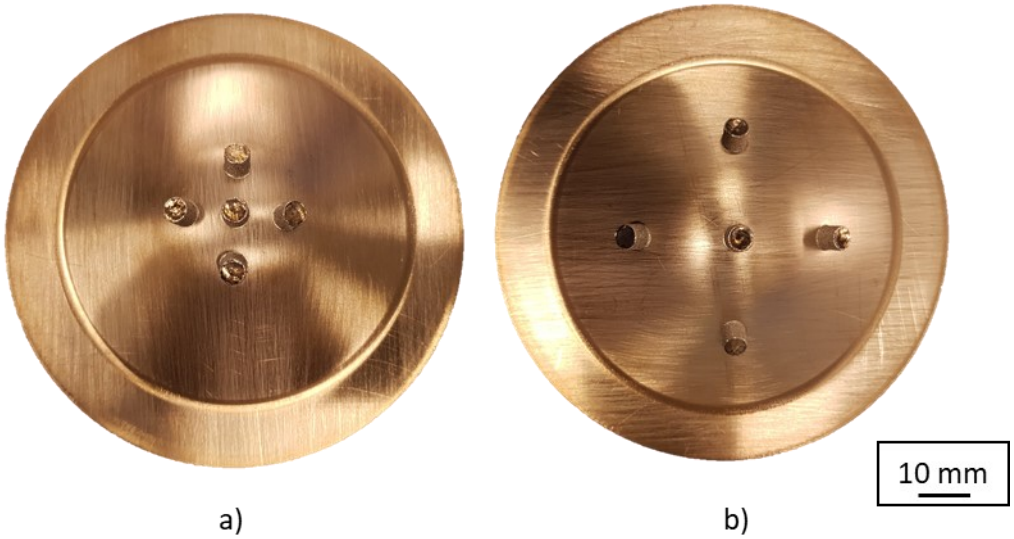

Figure 5.21: Example of hybrid components with a) *L* = 10 mm and b) *L* = 20 mm.

In figure 5.22 the thickness distributions of the sections Y of two hybrid components with the same geometrical configuration, but different values of *L* are shown. The geometrical configuration of the specimens is: 316L; D_0 = 105 mm; s_0 = 1.5 mm; *NP* = 5; *D* = 5 mm; *R* = 1 mm; *DD* = 15 mm; *T* = 400°C.

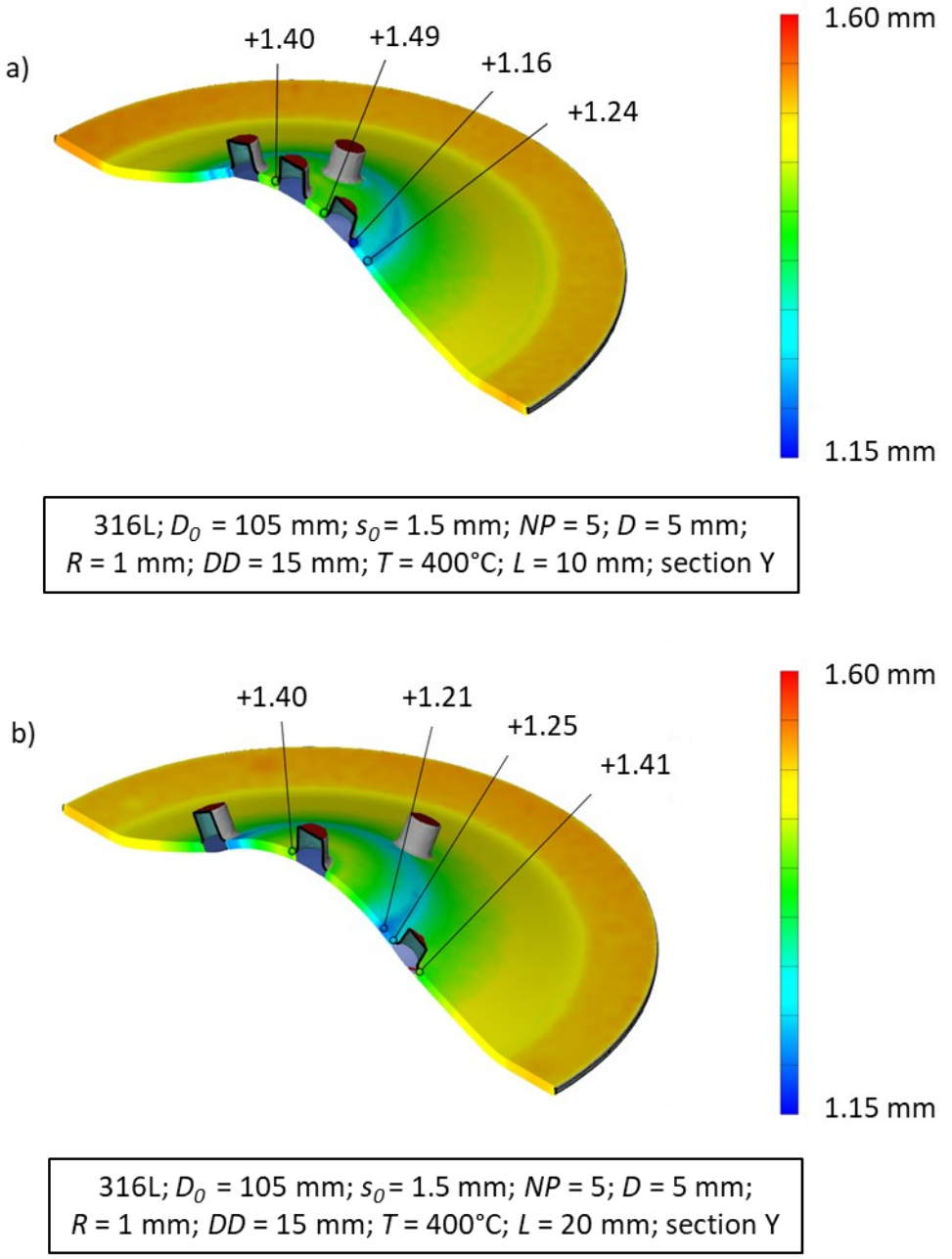

Figure 5.22: Sheet thickness distribution of two hybrid components in which only the length L is varied: a) L = 10 mm and b) L = 20 mm. Specimens: 316L; D_0 = 105 mm; s_0 = 1.5 mm; NP = 5; D = 5 mm; R = 1 mm; DD = 15 mm; T = 400°C.

In figure 5.22 it is possible to identify the minimum thickness of the two components examined, that is 1.16 mm for the specimen with L = 10 mm and 1.21 mm for the component with L = 20 mm. In the case of the specimen with L = 10 mm, the maximum thinning occurs in the transition area between the sheet and the external pins, specifically on the side of the base of the pins that is closer to the area of the punch edge radius. Regarding the specimen with L = 20 mm, the maximum thinning occurs in the transition area between the sheet and the external pins on the side of the base of the pins that is closer to the area of the punch edge radius, but this time in an opposite position to the

one of the specimen with *L* = 10 mm. From the processing of the data of the specimens with different values of *L*, the mean values of the minimum thicknesses are calculated. Hybrid components with *L* = 10 mm have a mean value of the minimum thickness of 1.25 ± 0.06, while those with *L* = 20 mm have a mean value of the minimum thickness of 1.27 ± 0.09. The position of the additively manufactured elements and their distance from the centre of the specimen influence the formability of the hybrid components. It can be deduced that the presence of additively manufactured elements is more critical for the components which have lower values of *L* rather than higher. For this reason, it can be stated that, increasing the distance *L*, a higher formability of the hybrid components can be achieved, as can be seen in the graph in figure 5.23.

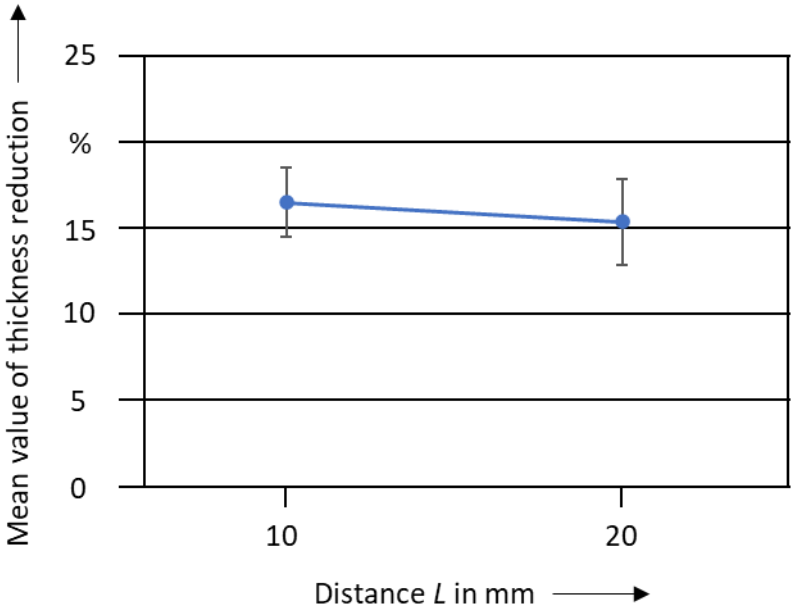

Figure 5.23: Influence of the length *L* on the sheet thickness reduction of hybrid components.

A possible explanation for the reduced formability of hybrid components with low *L* values is that a bigger gap of no contact between the sheet and the punch arises during the forming process [55]. This is due to the fact that the proximity of the pins does not allow the sheet to wrap completely around the punch during the process. If the *L* value is higher, the stiffened areas are not concentrated in the central part of the specimens but are more spaced, as can be seen in figure 5.24

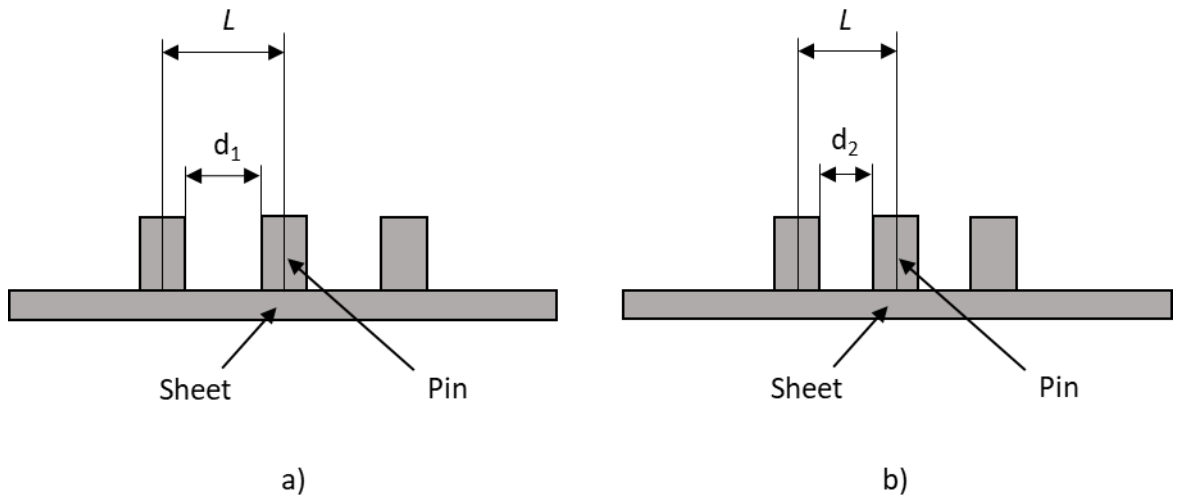

Figure 5.24: Influence of the length *L* on the distance between the bases of the additively manufactured elements d_1 and d_2. a) higher value of *L*, b) lower value of *L*.

As previously mentioned, within the area of no contact, bending forces act on the sheet and, therefore, tensile stresses arise in the transition area between the additively manufactured elements and the sheet [55]. Each pin has a stress concentration effect. If the additively manufactured elements are close, the total tensile stress arising in the area between the bases of the pins is higher than the total tensile stress which occurs in the case of more distant pins. Consequently, the increase in the total tensile stress leads to an increase in thickness reduction and a decrease in the formability of the components. Therefore, a suitable value of the distance *L* must be chosen when manufacturing a hybrid component, in order not to have too close stiffened areas and, consequently, too high tensile stresses in the area between the bases of the pins.

5.1.7 Influence of the testing temperature *T*

In this section the influence of the testing temperature *T* on the formability of the components is examined. In figure 5.25 the thickness distributions of two hybrid components with the same geometrical configuration but formed at different values of *T* are shown. The geometrical configuration of the specimens is: 316L; D_0 = 105 mm; s_0 = 1.5 mm; *NP* = 1; *D* = 5 mm; *R* = 1 mm; *DD* = 15 mm; *L* = 0 mm. The section Y of the specimens is taken as a reference.

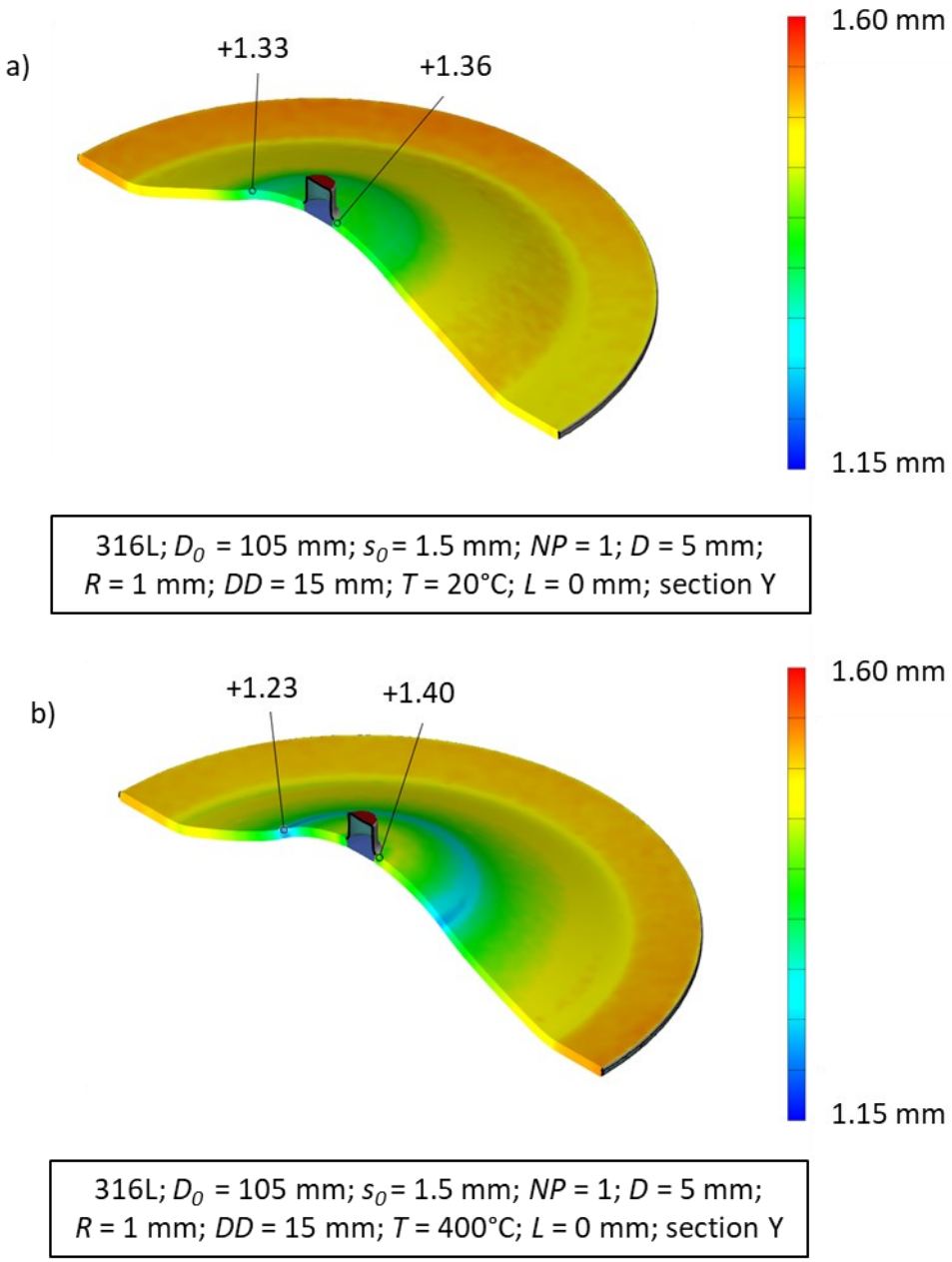

Figure 5.25: Sheet thickness distribution of two hybrid components in which only the temperature T is varied: a) T = 20 °C and b) T = 400 °C. Specimens: 316L; D_0 = 105 mm; s_0 = 1.5 mm; NP = 1; D = 5 mm; R = 1 mm; DD = 15 mm; L = 0 mm.

The minimum thicknesses are 1.33 mm for the specimen formed at T = 20 °C and 1.23 mm for the specimen formed at T = 400 °C. From the processing of the data obtained, the mean values of the minimum thicknesses of the specimens formed at different testing temperatures are calculated. For the specimens formed at a temperature of 20 °C the mean value of the minimum thickness is equal to 1.33 ± 0.03, while the specimens tested at a temperature of 400 °C have a mean value of the minimum thickness of 1.20 ± 0.03. Through the exam of the thickness distribution of the specimens it is evident that, as the temperature increases, a decrease in the formability of the component occurs. To better understand the influence of the testing temperature on the

thickness reduction of the components, the graph in figure 5.26 is made.

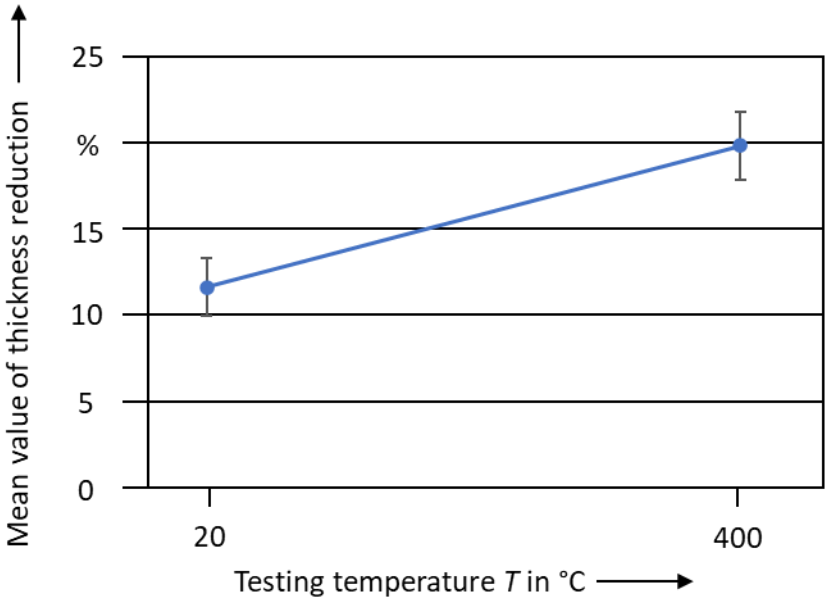

Figure 5.26: Influence of the testing temperature *T* on the sheet thickness reduction of the specimens.

As previously mentioned, the temperature *T* has a high influence on the maximum forming force. A material is easily formable if it has high ductility and low yield strength [41]. These two properties are related to the testing temperature at which the forming experiments are performed [41]. As the temperature rises, the ductility of the material increases, while the yield strength decreases [41]. As a consequence, if the ductility increases, the formability of the component becomes higher, while the formability decreases if the yield strength becomes too low. From the analysis of the data obtained, it can be deduced that the preponderant effect of the increasing temperature is to decrease the formability of the components, since the effect of the reduction in yield strength is stronger than the one of the enhancement in ductility. Thus, it is necessary to choose the suitable testing temperature, as the results on the formability can be contrasting. The main advantage of increasing the testing temperatures, however, is that lower loads on tools are needed in the forming process [41]. Because of the strong influence of the testing temperature on the thickness reduction of the specimens and, therefore, on the formability, care must be taken in choosing the adequate testing temperature in order not to incur the earlier failure of the specimens and to obtain lower loads on tools.

5.2 Influence of combination of parameters

In this section the influence of the combination of the parameters above analysed is examined. Interaction graphs are made from the analysis of the data obtained from the

optical measurements. From the analysis of the interaction graphs it is possible to evaluate how the interactions among the different factors influence the formability of the components. In figure 5.27 two examples of interaction graphs are shown.

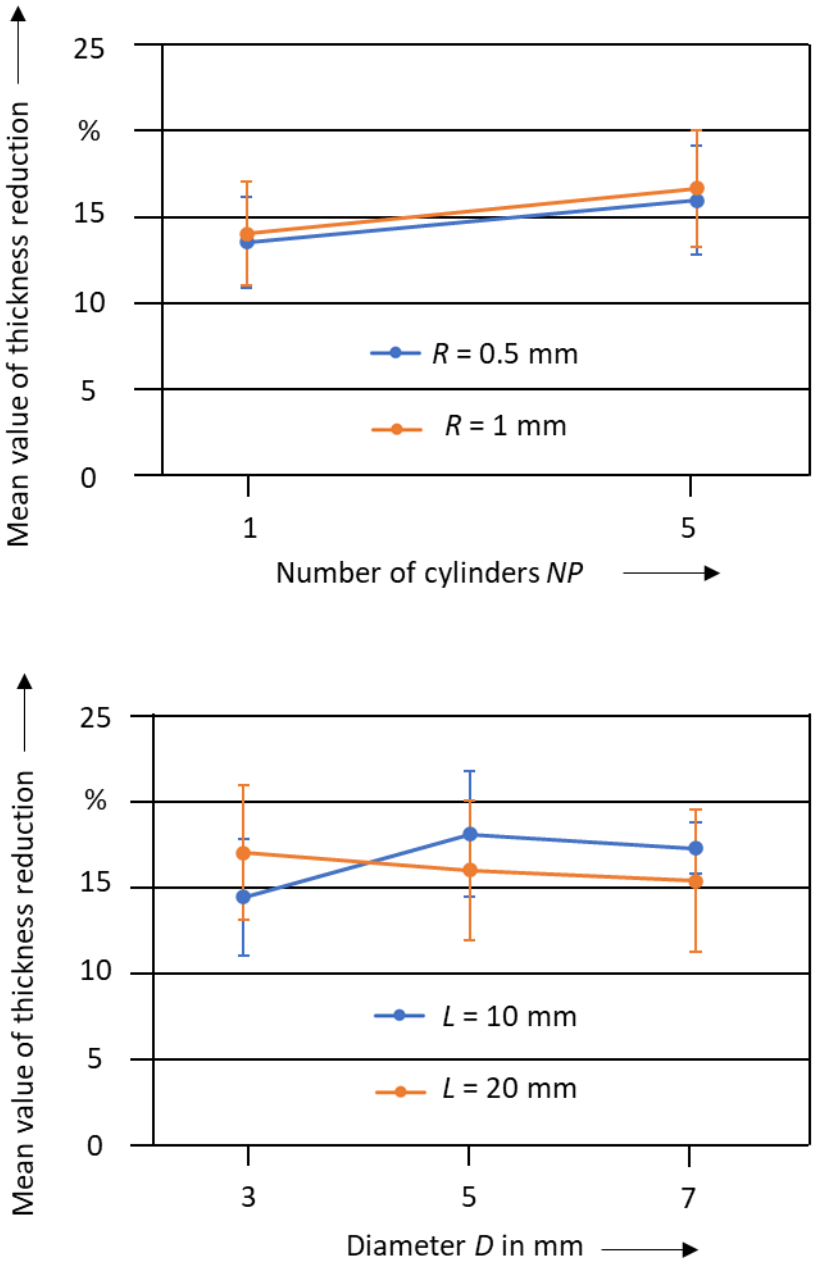

Figure 5.27: Interaction graphs for different combination of parameters: *R* and *NP* (top), *L* and *D* (bottom).

If the lines obtained from the interaction graphs are parallel, no interaction takes place between the analysed variables [60]. An example of this type of graph is shown at the top of the figure 5.27, where the interaction graph of the variables *R* and *NP* on the mean value of thickness reduction is illustrated. If, on the contrary, the lines obtained are not parallel, an interaction between the two variables occurs [60]. The more the

curves are non-parallel, the stronger the interaction [60]. An example of this type of graph is shown at the bottom of the figure 5.27, where the interaction graph of the variables *L* and *D* on the mean value of thickness reduction is illustrated. In the next sections the interaction graphs related only to the combinations of variables that highlight a high interaction are shown. The remaining interaction graphs are reported in the appendix.

5.2.1 Influence of combination of *D* and *NP*

From the analysis of the thickness distribution of the specimens with different values of the parameters *D* and *NP* the interaction graph in figure 5.28 is made.

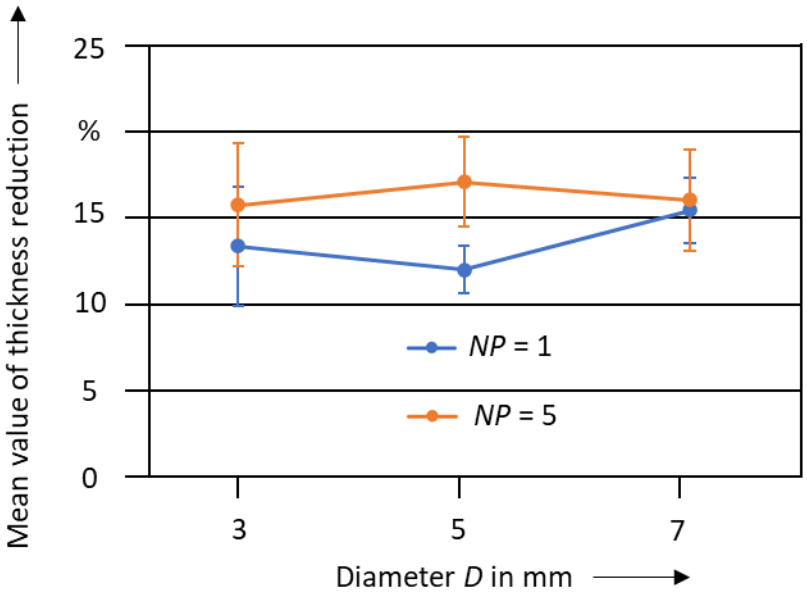

Figure 5.28: Combined influence of the diameter *D* and number of pins *NP* on the sheet thickness reduction of hybrid components.

In this graph the influence of the combination of the parameters *D* and *NP* on the mean value of the sheet thickness reduction is shown. It can be noticed that the curves represented in the graph are not parallel and tend to converge for the extreme values of the diameter, in a more marked way for the value of the diameter equal to 7 mm. Thus, it is possible to affirm that there is an interaction between the variables *D* and *NP* on the mean value of the sheet thickness reduction and, therefore, on the formability of the hybrid components. The relationship between the number of pins *NP* and the mean value of the thickness reduction depends on the value of the diameter *D* of the pins. As previously stated, both the increase in the diameter of the pins and the increase in their number have the same effect, i.e., to increase the stiffened area under the additively manufactured elements and, therefore, to increase the sheet to pin ratio [55]. For this reason, it can be deduced that there is an interaction between the parameters *D* and

NP, as can be seen in the graph in figure 5.28. In order to obtain a higher formability of the hybrid components and not to incur a premature failure of the parts, it is possible to find a trade-off between the values of these two parameters.

5.2.2 Influence of combination of *D* and *L*

It is examined below the influence of the combination of parameters *D* and *L* on the formability of the hybrid components. Figure 5.29 shows the interaction graph of the influence.

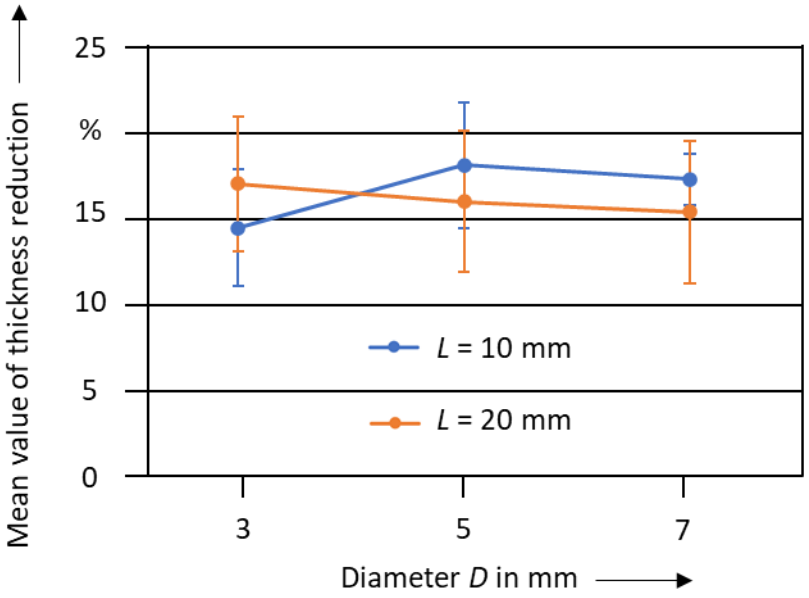

Figure 5.29: Combined influence of the diameter *D* and distance *L* on the sheet thickness reduction of hybrid components.

Unlike the case just examined, in the case of the analysis of the combination of parameters *D* and *L*, a marked interaction between the variables occurs on the left side of the graph, for low values of the diameter, as can be seen in figure 5.29. For high values of the diameter this interaction becomes less marked. The relationship between the distance *L* and the mean value of the thickness reduction depends on the value of the diameter *D* of the pins. The possible cause of the interaction between the two analysed variables is that, as the diameter of the additively manufactured elements increases, the distance between the base of the pins decreases, while the distance *L* is constant. For a better understanding of what just stated, figure 5.30 shows a diagram.

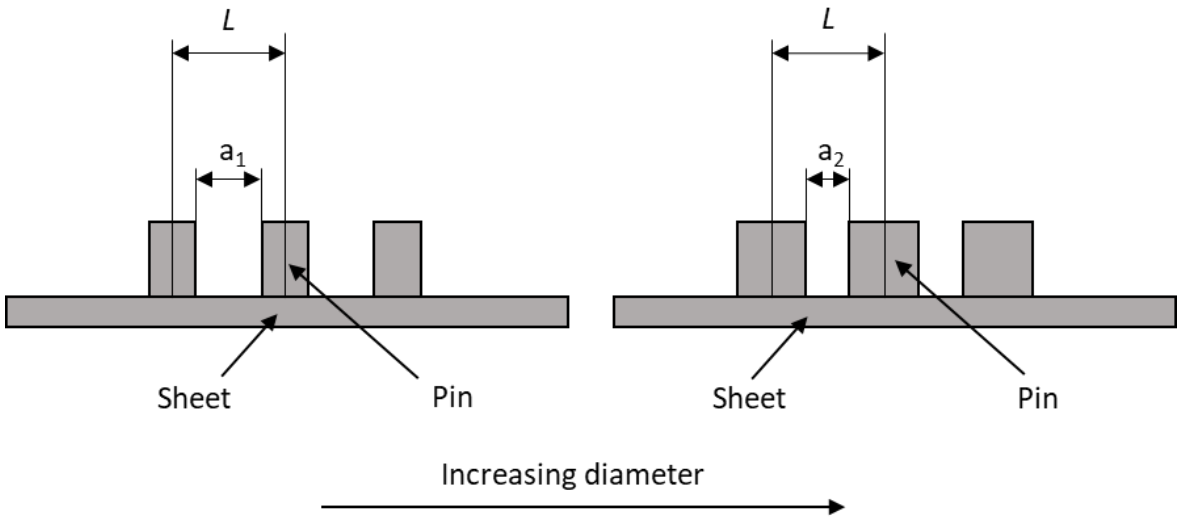

Figure 5.30: Influence of the diameter *D* on the distance between the base of the pins a_1 and a_2.

As can be seen in figure 5.30, the distance *L* remains constant, since it is the distance between the centres of the cylinders. The distance between the bases of two cylinders, on the other hand, depends on the diameter. In the case of a smaller diameter, there is a distance between the bases of the cylinders equal to a_1, while, if the diameter is increased, the distance between the bases of the cylinders decreases and is equal to a_2, that is lower than a_1. The greater proximity of the stiffened areas that is obtained by increasing the diameter leads to an effect similar to the one obtained by decreasing the distance *L*. As already mentioned, the closer the bases of the cylinders, the higher the total tensile stress that arises in the area between the bases of the pins, since each pin has a stress concentration effect. As the total tensile stress increases, an increase in thickness reduction and a decrease in the formability of the components occur. In order to obtain a higher formability it is possible to find a trade-off between the values of these two parameters, when manufacturing the hybrid components.

5.2.3 Influence of combination of *D* and *R*

In this section the influence of the combination of the parameter *D* and *R* is analysed. In figure 5.31 the interaction graph is shown.

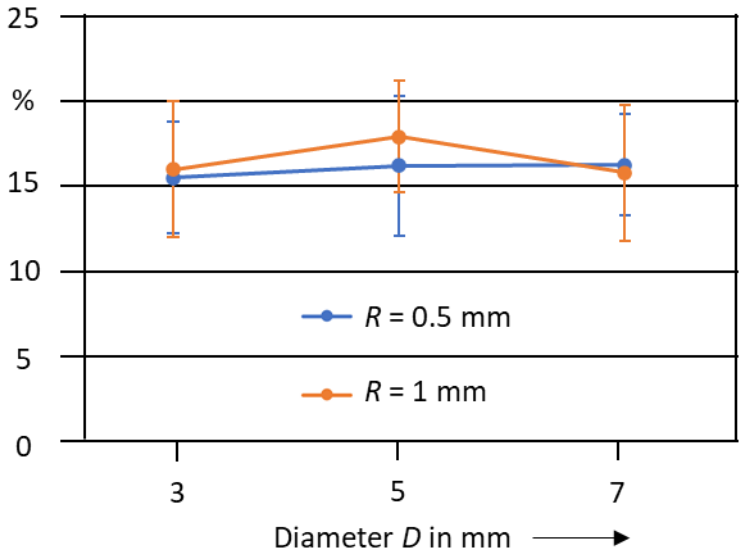

Figure 5.31: Combined influence of the diameter *D* and fillet radius *R* on the sheet thickness reduction of hybrid components.

As can be seen in the graph in figure 5.31, the relationship between the fillet radius *R* and the mean value of the thickness reduction depends on the value of the diameter *D* of the pins. This interaction graph shows that the curves tend to converge on the left and the right side of the graph. It can be stated, therefore, that an interaction between the two analysed variables occurs. A possible reason for the interaction between the two variables is, once again, the widening of the stiffened area under the additively manufactured elements. As explained previously, the effect of increasing the stiffened area is more marked when the diameter becomes bigger, while it is less marked when the fillet radius increases. In order to better understand the interaction that arise between the two variables analysed, the figure 5.32 is made.

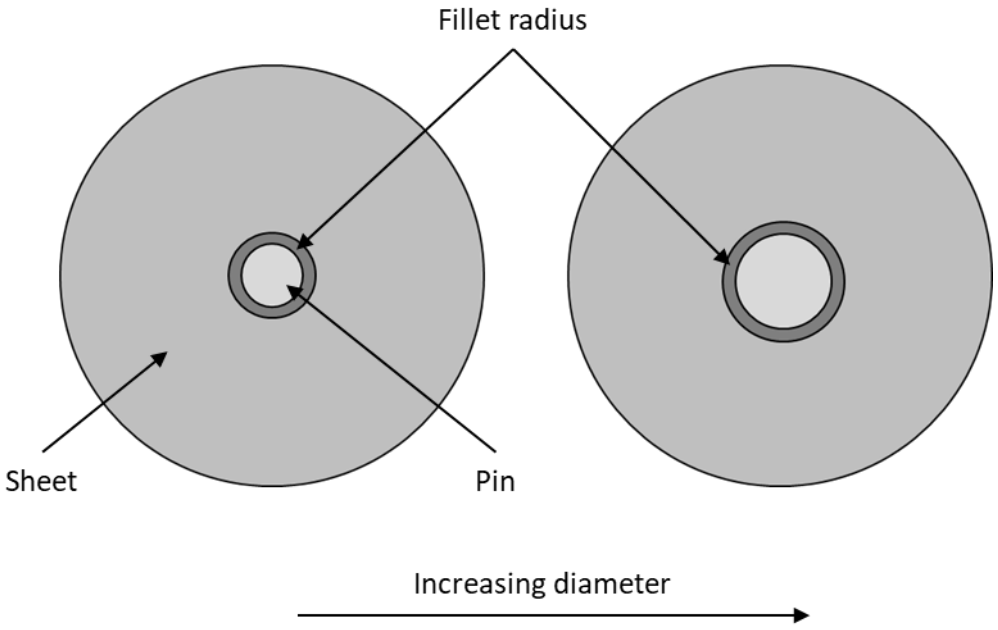

Figure 5.32: Influence of the increasing the value of the diameter *D* on the area covered by the fillet radius *R*.

As can be seen from figure 5.32, keeping the value of the fillet radius constant but increasing the diameter, the area stiffened by the fillet radius will be greater. It is, therefore, necessary to take into account this interaction between the variables *D* and *R* when manufacturing hybrid components, in order not to incur a premature failure of the components.

6 Summary and outlook

In this thesis the combination of PBF-LB/M with sheet metal forming technology to manufacture hybrid components is examined. The manufacturing of hybrid parts presents many challenges, as, during the manufacturing process, interactions occur between the technologies used [50], which lead to obtain a lower formability of the hybrid components. The aim of this thesis is to examine the influence of the testing temperature and the geometric parameters of the additively manufactured elements on the formability of the hybrid specimens. To analyse how the formability of the hybrid components is influenced by the presence of the additively manufactured elements, different hybrid specimens are manufactured, combining different values of the chosen parameters. The material used is 316L stainless steel. Together with the hybrid components, sheet metal specimens are formed. To manufacture the hybrid specimens, the additively manufactured elements are built on top of a circular blank, which has a diameter of 105 mm and a thickness of 1.5 mm. The specimens thus obtained are subsequently formed. To analyse the influence of the geometry of the pins on the formability of the hybrid components, the following geometric parameters are chosen and varied: the diameter of the pins *D*, the number of pins *NP*, the distance between the pins measured from the centre *L* and fillet radius *R* in the transition area between the sheet and the pins. The height of the pins is fixed and equal to 5 mm. The drawing depth chosen for the forming process is 15 mm. Sheet metal specimens are tested at a drawing depth of 15 mm and 20 mm. Three different testing temperatures are chosen, i.e., 20 °C, 250 °C and 400 °C. The formed components are measured with an optical measuring system to obtain their sheet thickness distribution. From the results of the optical measurements, it is possible to determine the position of maximum thinning on the specimens and, thus, identify the critical areas. An increased thickness reduction results in a reduced formability of the components and, consequently, in a possible earlier failure of the specimens [55].

Initially, the force-displacement curves of the forming processes of all the specimens are examined. As the testing temperature rises, the maximum force required for the forming process decreases. This is due to the fact that the increase in temperature leads to a reduction in yield strength of the material of the specimens [41].

To analyse how the formability of the hybrid components varies according to the rolling directions, two different sections of each manufactured specimen are examined, namely the section X and Y, respectively perpendicular to and parallel to the rolling direction. From the analysis of the results, it is noticed that the minimum thickness in the sections Y is lower than the one in the sections X. The difference between the thickness distribution of the analysed sections is due to the anisotropy of the material properties of the 316L sheet. The anisotropy arises from the rolling process, which creates directional properties in the metal sheet [43].

Subsequently, the influence of the geometric parameters of the additively manufactured elements on the formability of the hybrid components is evaluated. Sections Y are chosen as reference for the analysis of the influence of the different parameters, since

in the sections Y it is easier to observe a clear influence of the parameters on the thickness distribution.

The first geometric parameter to be analysed is the diameter of the pins *D.* It is noticed that if the diameter of the additively manufactured elements becomes bigger, the reached minimum thickness by the hybrid components decreases. One possible explanation is that the stiffened area that lies under the pins becomes wider as the value of the diameter increases [55]. Because of the high stiffness of this area, a bigger gap of no contact between the punch and the sheet occurs during the forming process and, therefore, bending stresses arise [55]. These bending stresses cause tensile stresses in the transition area between the pins and the sheet [55]. As the *D* increases, higher tensile stresses occur, leading to a higher thinning of the sheet and, thus, to a lower formability of the specimens [55].

The influence of the fillet radius *R* is subsequently determined. As *R* increases, a reduction in the formability of the components occurs. The possible reason for the lower formability of the specimens with high values of *R* is that, as in the case of the increasing of the diameter, there is an increment of the stiffened area, which comprises not only the area under the cylinders but also the one under the fillet radius. Furthermore, the fillet radius has a high surface roughness because of the Additive Manufacturing process [50]. The failure of the hybrid components at the base of the pins is enhanced by a high surface roughness, as it leads to a stress concentration effect and can be the cause of the initiation of cracks [51]. However, it is necessary to insert a fillet radius between the sheet and the additively manufactured elements because it allows the stress concentration effect at the base of the pins to decrease.

In the subsequent step, this thesis examines the variation of the number of pins *NP.* The increase of the value of *NP* corresponds to a proportional increment of the stiffened area and, for this reason, a consequent reduction of the formability of the hybrid components occurs [55].

Then, it is determined the influence of the distance *L* between the pins. From the analysis of the thickness distribution of the specimens with different values of *L*, it can be stated that the formability of the components increases when *L* increases. A possible reason for this behaviour is that, in case of low values of *L*, the proximity of the cylinders does not allow the sheet to wrap completely around the punch during the forming process and, thus, a bigger gap of no contact arises between the sheet and the punch. For this reason, the bending stresses that occur are higher, leading to a higher total tensile stress in the area between the bases of the pins, if compared to the case with high values of *L*.

The last parameter examined is the testing temperature *T*. As previously mentioned, if the temperature rises, the ductility of the material increases, while the yield strength decreases [41]. If the ductility increases, the formability of the component becomes higher, while the formability decreases if the yield strength becomes too low. Since from the analysis of the thickness distribution results that the formability of the hybrid specimens decreases as the testing temperature rises, it can be deduced that the effect of decreasing the yield strength is stronger than the one that regards the increasing of

ductility.

Finally, the various parameters analysed are combined together, to understand the influence of the combined parameters on the formability of the components. From this analysis interaction graphs are made, to identify which combinations of parameter present interaction between each other. The combination of parameters which present a relevant interaction are *D* and *NP*, *D* and *L*, *D* and *R*. The possible reason for the marked interaction of these variables is the stiffened area that is created when the values of these variables vary. It is, therefore, possible to reach a trade-off between the values of these variables, in order to achieve the desired formability. More research is needed on the influence of additively manufactured elements on the forming behaviour of hybrid specimens. Future research in this area should deal with the influence of other values of the analysed geometric parameters of the pins in order to understand if different ranges of values lead to different results in the formability of the specimens. Since the additively manufactured elements are the part of the hybrid components that adapts to the needs of consumers [51], it is necessary to investigate different combinations and values of parameters, as these have a strong influence on formability. For this reason, to increase the customization of the hybrid specimens, different heights and different geometries of the additively manufactured elements could be analysed, for example, testing triangular or rectangular geometries and increasing the height. Different values of the thickness of the sheet on which the additively manufactured elements are built and different values of drawing depth could be tested, to analyse if it is possible to obtain a higher formability of the components. Finally, a wider range of testing temperatures could be investigated, in order to find the most suitable range of temperatures that permits to obtain low forming forces but, at the same time, does not strongly decrease the formability of the hybrid components.

7 Literature

[1] B. Ahuja, A. Schaub, M. Karg, R. Schmidt, M. Merklein, and M. Schmidt, ‘High power laser beam melting of Ti 6 Al 4 V on formed sheet metal to achieve hybrid structures’, San Francisco, California, United States, 2015, p. 93530X. doi: 10.1117/12.2082919.

[2] T. Papke, D. Junker, M. Schmidt, T. Kolb, and M. Merklein, ‘Bulk Metal Forming of Additively Manufactured Elements’, *MATEC Web Conf.*, vol. 190, pp. 1–6, 2018, doi: 10.1051/matecconf/201819003002.

[3] M. D. Bambach, M. Bambach, A. Sviridov, and S. Weiss, ‘New process chains involving additive manufacturing and metal forming – a chance for saving energy?’, *Procedia Eng.*, vol. 207, pp. 1176–1181, 2017, doi: 10.1016/j.proeng.2017.10.1049.

[4] S. Y. Chin, V. Dikshit, B. Meera Priyadarshini, and Y. Zhang, ‘Powder-Based 3D Printing for the Fabrication of Device with Micro and Mesoscale Features’, *Micromachines*, vol. 11, no. 7, Art. no. 7, 2020, doi: 10.3390/mi11070658.

[5] B. Ahuja, A. Schaub, M. Karg, R. Schmidt, M. Merklein, and M. Schmidt, ‘High power laser beam melting of Ti 6 Al 4 V on formed sheet metal to achieve hybrid structures’, San Francisco, California, United States, 2015, vol. 9353. doi: 10.1117/12.2082919.

[6] K. S. Prakash, T. Nancharaih, and V. V. S. Rao, ‘Additive Manufacturing Techniques in Manufacturing -An Overview’, *Mater. Today Proc.*, vol. 5, no. 2, pp. 3873–3882, 2018, doi: 10.1016/j.matpr.2017.11.642.

[7] T. Papke and M. Merklein, ‘Characterization of Work Hardening Behavior of Additively Manufactured Stainless Steel 316L (1.4404) Using Bulk Metal Forming at Elevated Temperature’, pp. 1–10, 2019.

[8] L. Butzhammer *et al.*, ‘Experimental investigation of a process chain combining sheet metal bending and laser beam melting of Ti-6Al-4V’, pp. 1–10, 2017.

[9] N. T. Aboulkhair, M. Simonelli, L. Parry, I. Ashcroft, C. Tuck, and R. Hague, ‘3D printing of Aluminium alloys: Additive Manufacturing of Aluminium alloys using selective laser melting’, *Prog. Mater. Sci.*, vol. 106, pp. 1–19, 2019, doi: 10.1016/j.pmatsci.2019.100578.

[10] A. Schaub, B. Ahuja, L. Butzhammer, J. Osterziel, M. Schmidt, and M. Merklein, ‘Additive Manufacturing of Functional Elements on Sheet Metal’, *Phys. Procedia*, vol. 83, pp. 797–807, 2016, doi: 10.1016/j.phpro.2016.08.082.

[11] P.-J. Cunat, ‘Alloying Elements in Stainless Steel and Other Chromium-Containing Alloys’, pp. 1–24, 2004.

[12] ‘DIN EN 10088-1:2014-12, Nichtrostende Stähle_- Teil_1: Verzeichnis der nichtrostenden Stähle; Deutsche Fassung EN_10088-1:2014’, Beuth Verlag GmbH. doi: 10.31030/2102106.

[13] J. R. Davis, Ed., *Alloy digest sourcebook: stainless steels*. Materials Park, OH: ASM International, 2000.

[14] ‘Chemical compositions of AISI (ASTM/ASME) and UNS austenitic stainless steel grades – British Stainless Steel Association’. https://bssa.org.uk/bssa_articles/chemical-compositions-of-aisi-astm-asme-and-uns-austenitic-stainless-steel-grades/ (accessed May 18, 2021).

[15] C.-O. A. Olsson and D. Landolt, ‘Passive films on stainless steels—chemistry, structure and growth’, *Electrochimica Acta*, vol. 48, no. 9, pp. 1093–1104, 2003, doi: 10.1016/S0013-4686(02)00841-1.

[16] B. Leffler, ‘Stainless - stainless steels and their properties’, pp. 1–45.

[17] *Handbook of stainless steel by Outokumpu*. Outokumpu Oyj, Espoo, 2013.

[18] R. R. Maller, ‘Passivation of stainless steel’, pp. 28–32, 1998.

[19] G. Z. Liu, N. R. Tao, and K. Lu, ‘316L Austenite Stainless Steels Strengthened by Means of Nano-scale Twins’, *J. Mater. Sci. Technol.*, vol. 26, no. 4, pp. 289–292, Apr. 2010, doi: 10.1016/S1005-0302(10)60048-5.

[20] T. Papke and M. Merklein, ‘Characterization of Work Hardening Behavior of Additively Manufactured Stainless Steel 316L (1.4404) Using Bulk Metal Forming at Elevated Temperature’, p. 10, 2019.

[21] ‘Supra 316L/4404 EN 1.4404, ASTM TYPE 316L / UNS S31603 stainless steel grade details’. https://secure.outokumpu.com/steelfinder/properties/GradeDetail.aspx?OKGrade=4404&Category=Supra (accessed Jun. 09, 2021).

[22] P. J. Andersen, ‘Stainless Steels’, in *Biomaterials Science*, Elsevier, 2013, pp. 124–127. doi: 10.1016/B978-0-08-087780-8.00015-2.

[23] T. Papke and M. Merklein, ‘Characterization of Work Hardening Behavior of Additively Manufactured Stainless Steel 316L (1.4404) Using Bulk Metal Forming at Elevated Temperature’, p. 10, 2019.

[24] J. R. Davis, *Stainless Steels*. ASM International, 1994.

[25] P. J. Andersen, ‘Stainless Steels’, in *Biomaterials Science*, Elsevier, 2020, pp. 249–255. doi: 10.1016/B978-0-12-816137-1.00019-2.

[26] S. Tanhaei, Kh. Gheisari, and S. R. Alavi Zaree, ‘Effect of cold rolling on the microstructural, magnetic, mechanical, and corrosion properties of AISI 316L austenitic stainless steel’, *Int. J. Miner. Metall. Mater.*, vol. 25, no. 6, pp. 630–640, 2018, doi: 10.1007/s12613-018-1610-y.

[27] M. Merklein, D. Junker, A. Schaub, and F. Neubauer, ‘Hybrid Additive Manufacturing Technologies – An Analysis Regarding Potentials and Applications’, *Phys. Procedia*, vol. 83, pp. 549–559, 2016, doi: 10.1016/j.phpro.2016.08.057.

[28] F. Calignano *et al.*, ‘Overview on Additive Manufacturing Technologies’, *Proc. IEEE*, vol. 105, no. 4, pp. 593–612, 2017, doi: 10.1109/JPROC.2016.2625098.

[29] I. Gibson, D. Rosen, and B. Stucker, *Additive Manufacturing Technologies*. New York, NY: Springer New York, 2015. doi: 10.1007/978-1-4939-2113-3.

[30] E. M. Palmero and A. Bollero, '3D and 4D Printing of Functional and Smart Composite Materials', in *Encyclopedia of Materials: Composites*, D. Brabazon, Ed. Oxford: Elsevier, 2021, pp. 402–419. doi: 10.1016/B978-0-12-819724-0.00008-2.

[31] X. Song, W. Zhai, R. Huang, J. Fu, M. Fu, and F. Li, 'Metal-Based 3D-Printed Micro Parts & Structures', in *Reference Module in Materials Science and Materials Engineering*, Elsevier, 2020. doi: 10.1016/B978-0-12-819726-4.00009-0.

[32] J. Kruth, P. Mercelis, J. Van Vaerenbergh, L. Froyen, and M. Rombouts, 'Binding mechanisms in selective laser sintering and selective laser melting', *Rapid Prototyp. J.*, vol. 11, no. 1, pp. 26–36, 2005, doi: 10.1108/13552540510573365.

[33] Z. Quan *et al.*, 'Additive manufacturing of multi-directional preforms for composites: opportunities and challenges', *Mater. Today*, vol. 18, no. 9, pp. 503–512, 2015, doi: 10.1016/j.mattod.2015.05.001.

[34] T.-S. Jang, D. Kim, G. Han, C.-B. Yoon, and H.-D. Jung, 'Powder based additive manufacturing for biomedical application of titanium and its alloys: a review', *Biomed. Eng. Lett.*, vol. 10, no. 4, pp. 505–516, 2020, doi: 10.1007/s13534-020-00177-2.

[35] B. Ahuja, A. Schaub, M. Karg, M. Lechner, M. Merklein, and M. Schmidt, 'Developing LBM Process Parameters for Ti-6Al-4V Thin Wall Structures and Determining the Corresponding Mechanical Characteristics', *Phys. Procedia*, vol. 56, pp. 90–98, 2014, doi: 10.1016/j.phpro.2014.08.102.

[36] M. S. I. N. Kamariah, W. S. W. Harun, N. Z. Khalil, F. Ahmad, M. H. Ismail, and S. Sharif, 'Effect of heat treatment on mechanical properties and microstructure of selective laser melting 316L stainless steel', *IOP Conf. Ser. Mater. Sci. Eng.*, vol. 257, p. 012021, 2017, doi: 10.1088/1757-899X/257/1/012021.

[37] S. Dietrich, M. Wunderer, A. Huissel, and M. F. Zaeh, 'A New Approach for a Flexible Powder Production for Additive Manufacturing', *Procedia Manuf.*, vol. 6, pp. 88–95, 2016, doi: 10.1016/j.promfg.2016.11.012.

[38] T. Papke and M. Merklein, 'Processing of 316L hybrid parts consisting of sheet metal and additively manufactured element by Powder Bed Fusion using a laser beam', *Procedia CIRP*, vol. 94, pp. 35–40, 2020, doi: 10.1016/j.procir.2020.09.008.

[39] Z. Sun, X. Tan, S. B. Tor, and W. Y. Yeong, 'Selective laser melting of stainless steel 316L with low porosity and high build rates', *Mater. Des.*, vol. 104, pp. 197–204, 2016, doi: 10.1016/j.matdes.2016.05.035.

[40] 'BS EN ISO/ASTM 52911-1:2019 - Additive manufacturing. Design. Laser-based powder bed fusion of metals'. https://shop.bsigroup.com/ProductDetail?pid=000000000030404862 (accessed Jun. 04, 2021).

[41] M. P. Groover, *Fundamentals of Modern Manufacturing: Materials, Processes,*

and Systems, Fourth Edition. Hoboken, NJ: John Wiley & Sons Inc, 2010.

[42] B. Avitzur, ‘Metal Forming’, in *Encyclopedia of Physical Science and Technology (Third Edition)*, R. A. Meyers, Ed. New York: Academic Press, 2003, pp. 411–440. doi: 10.1016/B0-12-227410-5/00425-7.

[43] S. Kalpakjian and S. R. Schmid, *Manufacturing Engineering & Technology*. Pearson Education Centre, 2013.

[44] K. Chadha, D. Shahriari, and M. Jahazi, ‘An Approach to Develop Hansel–Spittel Constitutive Equation during Ingot Breakdown Operation of Low Alloy Steels’, in *Frontiers in Materials Processing, Applications, Research and Technology*, M. Muruganant, A. Chirazi, and B. Raj, Eds. Singapore: Springer Singapore, 2018, pp. 239–246. doi: 10.1007/978-981-10-4819-7_20.

[45] U. S. Dixit, ‘1 - Modeling of metal forming: a review’, in *Mechanics of Materials in Modern Manufacturing Methods and Processing Techniques*, V. V. Silberschmidt, Ed. Elsevier, 2020, pp. 1–30. doi: 10.1016/B978-0-12-818232-1.00001-1.

[46] K. H. J. Buschow, Ed., *Encyclopedia of materials: science and technology*. Amsterdam ; New York: Elsevier, 2001.

[47] V. L. Hattalli and S. R. Srivatsa, ‘Sheet Metal Forming Processes – Recent Technological Advances’, *Mater. Today Proc.*, vol. 5, no. 1, pp. 2564–2574, 2018, doi: 10.1016/j.matpr.2017.11.040.

[48] N. Saito, M. Fukahori, D. Hisano, H. Hamasaki, and F. Yoshida, ‘Effects of temperature, forming speed and stress relaxation on springback in warm forming of high strength steel sheet’, *Procedia Eng.*, vol. 207, pp. 2394–2398, 2017, doi: 10.1016/j.proeng.2017.10.1014.

[49] Z. Yang and Z.-Y. Cai, ‘Research on the process of stretch forming based on distributed displacement loading’, presented at the 5th International Conference on Advanced Design and Manufacturing Engineering, Shenzen, China, 2015. doi: 10.2991/icadme-15.2015.386.

[50] J. Hafenecker, T. Papke, and M. Merklein, ‘Influence of Stress States on Forming Hybrid Parts with Sheet Metal and Additively Manufactured Element’, *J. Mater. Eng. Perform.*, vol. 30, no. 7, pp. 5159–5169, 2021, doi: 10.1007/s11665-021-05674-8.

[51] J. Hafenecker, T. Papke, F. Huber, M. Schmidt, and M. Merklein, ‘Modelling of Hybrid Parts Made of Ti-6Al-4V Sheets and Additive Manufactured Structures’, in *Production at the leading edge of technology*, B.-A. Behrens, A. Brosius, W. Hintze, S. Ihlenfeldt, and J. P. Wulfsberg, Eds. Berlin, Heidelberg: Springer Berlin Heidelberg, 2021, pp. 13–22. doi: 10.1007/978-3-662-62138-7_2.

[52] ‘AM Powder – Stainless Steel (1.4404) | Spare Parts | DMG MORI Online Shop for business customers’. https://shop.dmgmori.com/b2b/en/Spare-Parts/AM-Powder-%E2%80%93-Stainless-Steel-%281-4404%29/p/3796836 (accessed Jun. 20, 2021).

[53] ‘LASERTEC 30 DUAL SLM - Additive Manufacturing machines by DMG MORI’. https://en.dmgmori.com/products/machines/additive-manufacturing/powder-bed/lasertec-30-slm (accessed Jun. 20, 2021).

[54] ‘Home - LASCO Umformtechnik GmbH’. https://www.lasco.com/ (accessed Sep. 15, 2021).

[55] J. Hafenecker, R. Rothfelder, M. Schmidt, and M. Merklein, ‘Stretch Forming of Ti-6Al-4V Hybrid Parts at Elevated Temperatures’, *Key Eng. Mater.*, vol. 883, pp. 135–142, 2021, doi: 10.4028/www.scientific.net/KEM.883.135.

[56] ‘High-precision 3D metrology | fast, precise’. https://www.gom.com/en/products/high-precision-3d-metrology (accessed Jun. 21, 2021).

[57] ‘Creo Parametric 3D Modeling Software | PTC’. https://www.ptc.com/en/products/creo/parametric (accessed Jun. 21, 2021).

[58] ‘CELOS Machine & Manufacturing’. https://it.dmgmori.com/prodotti/digitization/celos (accessed Jun. 21, 2021).

[59] ‘GOM Inspect Suite: Making quality easily visible | Software for 3D inspection’. https://www.gom.com/en/products/gom-inspect-suite (accessed Jun. 22, 2021).

[60] ‘Interpret the key results for Interaction Plot’. https://support.minitab.com/en-us/minitab-express/1/help-and-how-to/modeling-statistics/anova/how-to/interaction-plot/interpret-the-results/ (accessed Sep. 15, 2021).

8 Appendix

Table 8.1: List of the manufactured specimens.

Specimen n°	Diameter D in mm	Number of pins NP	Fillet radius R in mm	Distance L in mm	Testing temperature T in °C
1 (DD=15)	-	-	-	-	20
2 (DD=20)	-	-	-	-	20
3	3	1	0,5	-	20
4	3	1	1	-	20
5	3	5	0,5	10	20
6	3	5	0,5	20	20
7	3	5	1	10	20
8	3	5	1	20	20
9 (DD=15)	5	1	0,5	-	20
10 (DD=20)	5	1	0,5	-	20
11	5	1	1	-	20
12	5	5	0,5	10	20
13	5	5	0,5	20	20
14	5	5	1	10	20
15	5	5	1	20	20
16	7	1	0,5	-	20
17	7	1	1	-	20
18	7	5	0,5	10	20
19	7	5	0,5	20	20
20	7	5	1	10	20
21	7	5	1	20	20
22	-	-	-	-	250
23	1	5	0,5	-	250
24 (DD=15)	-	-	-	-	400
25 (DD=20)	-	-	-	-	400
26	3	1	0,5	-	400
27	3	1	1	-	400
28	3	5	0,5	10	400
29	3	5	0,5	20	400
30	3	5	1	10	400
31	3	5	1	20	400
32	5	1	0,5	-	400
33	5	1	1	-	400
34	5	5	0,5	10	400
35	5	5	0,5	20	400

36	5	5	1	10	400
37	5	5	1	20	400
38	7	1	0,5	-	400
39	7	1	1	-	400
40	7	5	0,5	10	400
41	7	5	0,5	20	400
42	7	5	1	10	400
43	7	5	1	20	400

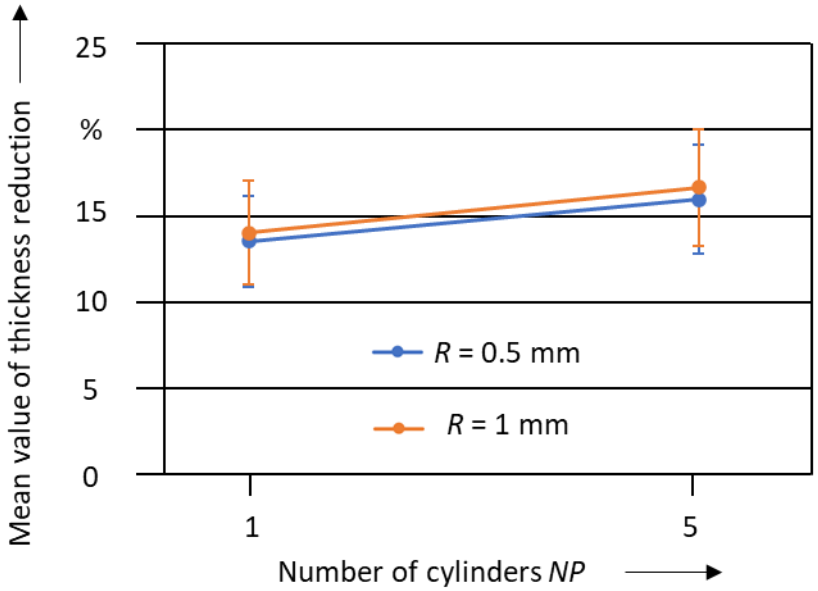

Figure 8.1: Combined influence of the number of cylinders *NP* and fillet radius *R* on the sheet thickness reduction of hybrid components.

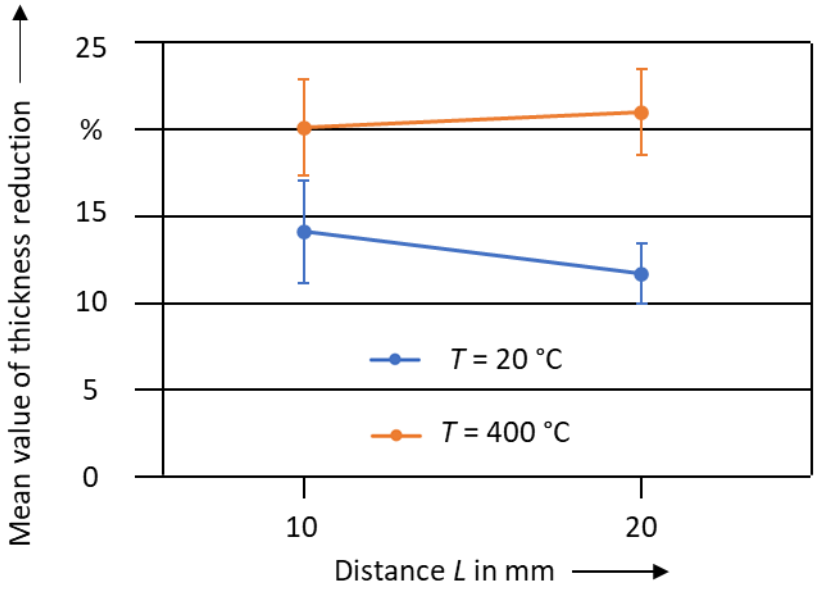

Figure 8.2: Combined influence of the distance *L* and the testing temperature *T* on the sheet thickness reduction of hybrid components.

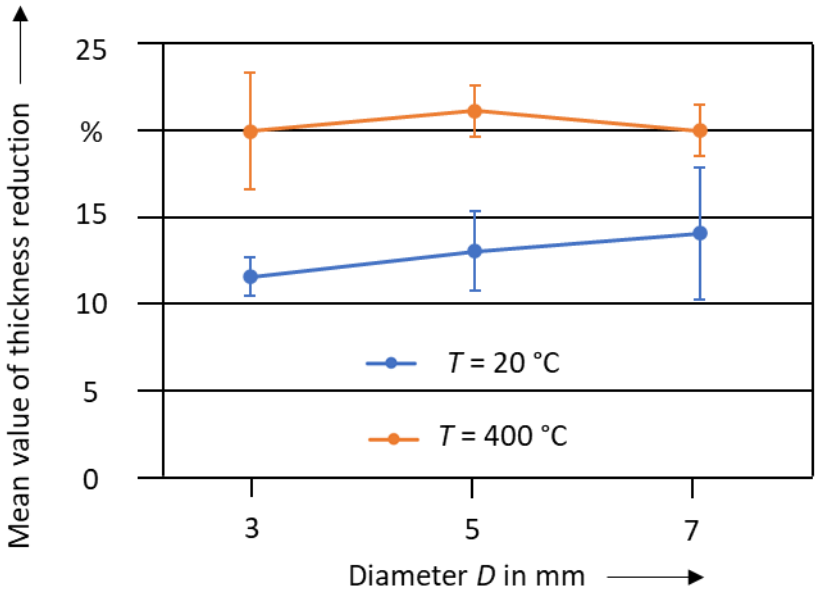

Figure 8.3: Combined influence of the diameter *D* and the testing temperature *T* on the sheet thickness reduction of hybrid components.

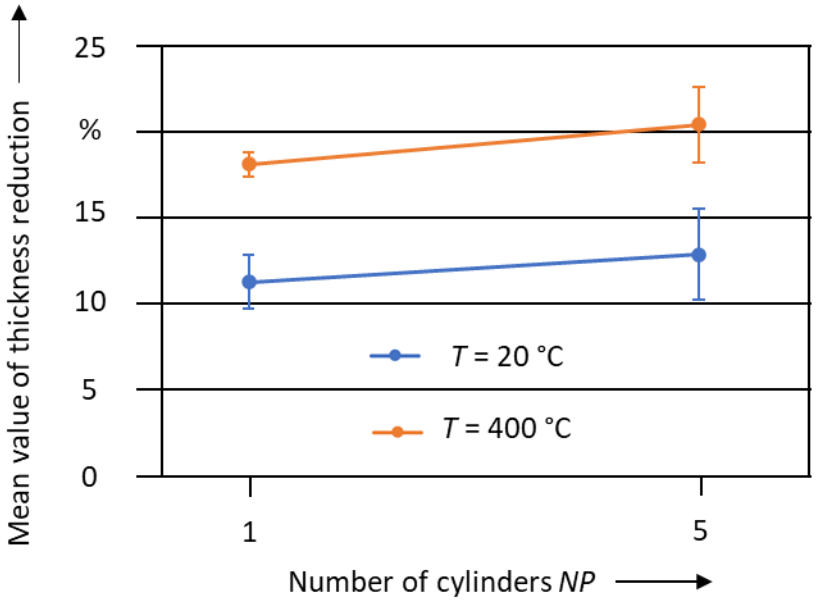

Figure 8.4: Combined influence of the number of cylinders *NP* and the testing temperature *T* on the sheet thickness reduction of hybrid components.